



High Data Rate Instrument Study

*Wayne Schober, Faiza Lansing, Keith Wilson
Jet Propulsion Laboratory, Pasadena, California*

*Evan Webb
Goddard Space Flight Center*

**National Aeronautics and
Space Administration**

**Jet Propulsion Laboratory
California Institute of Technology
Pasadena, California**



High Data Rate Instrument Study

*Wayne Schober, Faiza Lansing, Keith Wilson
Jet Propulsion Laboratory, Pasadena, California*

*Evan Webb
Goddard Space Flight Center*

**National Aeronautics and
Space Administration**

**Jet Propulsion Laboratory
California Institute of Technology
Pasadena, California**

The research described in this paper was carried out by the Jet Propulsion Laboratory, California Institute of Technology, under a contract with the National Aeronautics and Space Administration.

Reference herein to any specific commercial product, process, or service by trade name, trademark, manufacture, or otherwise, does not constitute or imply its endorsement by the United States Government or the Jet Propulsion Laboratory, California Institute of Technology.

ABSTRACT

The High Data Rate Instrument Study was a joint effort between the Jet Propulsion Laboratory (JPL) and the Goddard Space Flight Center (GSFC). The objectives were to assess the characteristics of future high data rate Earth observing science instruments and then to assess the feasibility of developing data processing systems and communications systems required to meet those data rates. Instruments and technology were assessed for technology readiness dates of 2000, 2003, and 2006. The highest data rate instruments are hyperspectral and synthetic aperture radar instruments which are capable of generating 3.2 Gigabits per second (Gbps) and 1.3 Gbps, respectively, with a technology readiness date of 2003. These instruments would require storage of 16.2 Terebits (Tb) of information (RF communications case of two orbits of data) or 40.5 Tb of information (optical communications case of five orbits of data) with a technology readiness date of 2003. Onboard storage capability in 2003 is estimated at 4 Tb; therefore, all the data created cannot be stored without processing or compression. Of the 4 Tb of stored data, RF communications can only send about one third of the data to the ground, while optical communications is estimated at 6.4 Tb across all three technology readiness dates of 2000, 2003, and 2006 which were used in the study. The study includes analysis of the onboard processing and communications technologies at these three dates and potential systems to meet the high data rate requirements. In the 2003 case, 7.8% of the data can be stored and downlinked by RF communications while 10% of the data can be stored and downlinked with optical communications. The study conclusion is that only 1 to 10% of the data generated by high data rate instruments will be sent to the ground from now through 2006 unless revolutionary changes in spacecraft design and operations such as intelligent data extraction are developed.

CONTENTS

	<u>Page</u>
1. Team Members.....	1-1
2. Executive Summary	2-1
3. Introduction.....	3-1
4. Science Requirements.....	4-1
4.1 Introduction	4-1
4.2 Study Guidelines	4-7
4.3 Technology Readiness Levels.....	4-9
5. Onboard Data Processing.....	5-1
5.1 Onboard Processing vs. High-bandwidth Downlinks.....	5-1
5.2 Comparison of Various Onboard Data Systems	5-11
5.3 Data Compression vs. Raw Data Downlink	5-25
6. Telecommunications	6-1
6.1 Introduction	6-1
6.2 LEO-to-Ground Downlink	6-5
6.3 Ground Station Data Management	6-21
6.4 Mass, Power and Cost	6-25
6.5 Conclusions and Recommendations	6-29
7. General Conclusions and Recommendations for Future Work	7-1
7.1 General Conclusions	7-1
7.2 Recommendations for Future Work.....	7-4
Appendix A. Breakthrough Technology – Intelligent Data Extraction.....	A-1
Appendix B. Acronym List.....	B-1

ILLUSTRATIONS

<u>Figure</u>	<u>Page</u>
4-1. Technology readiness levels for each phase	4-9
5-1. REE Project Overview	5-2
5-2. Intelligent coding of scientific requests reduces downlink size	5-3
5-3. Hierarchical organization of scientific data-extraction algorithms	5-4
5-4. Processing flow for hyperspectral instrument and Light SAR instrument	5-5
5-5. Mass memory capacity density vs. time	5-16
5-6. Mass memory power dissipation vs. time	5-17
5-7. CPU MIPs capability vs. time	5-18
5-8. CPU power dissipation vs. time	5-19
5-9. High data rate instrument – 2000	5-20
5-10. High data rate instrument – 2003	5-21
5-11. High data rate instrument – 2006	5-22
5-12. Rationale for choosing data compression	5-27
5-13. Experiments for scientists' evaluation	5-27
5-14. Two proposed compression modules – lossless and Lossy	5-28
5-15. Key metrics	5-29
6-1. Satellite ground track shows that a high latitude RF ground station affords downlink opportunities on every pass	6-2
6-2. The instruments gathered data at the full capacity over land	6-3
6-3. SSR data flow over 48 hours for RF downlink at 1 Gbps	6-4
6-4. 48 hour SSR loading profile for 10 Gbps downlink with three US ground stations	6-5
6-5. Ball Aerospace Quickbird Satellite can transmit up to 320 Mbps	6-8
6-6. Element-active phased array antenna built by Boeing for GSFC	6-9
6-7. Ka-band phased array antenna	6-10
6-8. Performance of Ka-band phased array antenna as a function of the off-axis beam-pointing angle	6-11
6-9. JPL's optical communications demonstrator	6-13
6-10. Schematic of basic design of optical communications terminal	6-14
6-11. Schematic block diagram for ground station	6-15
6-12. Relay satellite with 10 Gbps crosslink with 10 Gbps downlink	6-16
6-13. Schematic of transceiver for GEO relay satellite	6-18
6-14. Block diagram for transferring high rate data from optical communications receiver to bulk memory	6-22

ILLUSTRATIONS (Continued)

<u>Figure</u>	<u>Page</u>
6-15. High-speed data distribution network for stations with direct connectivity to the high speed WAN	6-24
6-16. High-speed WAN connectivity across CONUS	6-25

TABLES

<u>Table</u>	<u>Page</u>
4-1. Hyperspectral instrument configuration for the Year 2000 case.....	4-2
4-2. Hyperspectral instrument configuration for the Year 2003 case.....	4-3
4-3. Hyperspectral instrument configuration for the Year 2006 case.....	4-4
4-4.1. Instrument data rates and selected downlink rates for each option	4-6
4-5. Programmatic/Mission.....	4-7
4-6. Spacecraft	4-7
4-7. Costing	4-8
5-1. Hyperspectral imaging instrument. Extraction of 10 principal components and classification into 10 classes.....	5-6
5-2. Hyperspectral imaging instrument. Extraction of 50 principal components and classification into 40 classes.....	5-7
5-3. Light SAR imaging instrument. Extraction of 3 principal components and classification into 15 classes.....	5-8
5-4. Relevant mission parameters	5-12
5-5. Functional assignments to subsystems	5-13
5-6. Science data volume for 2000	5-15
5-7. Science data volume for 2003	5-15
5-8. Science data volume for 2006	5-15
5-9. Mass and power estimates for 2000 mission	5-24
6-1. Location, weather availability, and mean pass duration of ground stations with tracking capability to support laser communications experiments in 2000	6-3
6-2. Summary of X-band and Ka-band capabilities needed to meet required telecommunications data rates in 2000, 2003, and 2006	6-6
6-3. Summary of link budgets, mass, power consumption, and cost.....	6-7
6-4. Characteristics of InGaAs optical detectors to support 1550 nm downlink	6-16
6-5. Link analysis for 2.5 Gbps telecommunication data rate	6-19
6-6. Link summary for GEO-to-ground link for 10 Gbps data rate with 1-m receiver and 12 cm transmitter using year 2000 technology	6-20
6-7. Single wavelength channel LEO-to-GEO link with 30-cm receiver and 10-cm transmitter.....	6-21
6-8. Memory boards vs. high-speed SSR clip-ons needed to support data rates	6-23
6-9. RF system mass power consumption and cost.....	6-26
6-10. Estimated mass and power of GEO system for 10 Gbps GEO-to-ground multiplexed optical communications transceiver subsystem, year 2000 fiber technology	6-27

TABLES (Continued)

<u>Table</u>	<u>Page</u>
6-11. Estimated mass and power estimates for LEO terminal subsystems for 10 Gbps LEO-to-ground link based on year 2000 technology.....	6-27
6-12. Estimated mass and power for 10 Gbps LEO system for multiplexed optical communications transceiver subsystem.....	6-28
6-13. OCT mass, power, and costs for different terminals and data rates	6-28
6-14. Ground receiver, data storage system, and distribution system costs.....	6-29
7-1. Effective instrument data rate in Gbps for raw, uncompressed SAR and compressed hyperspectral imaging, and compressed hyperspectral imaging SAR imaging.....	7-1

1. TEAM MEMBERS

The following representatives comprised the study team (lead authors shown in bold):

Responsibility

Study Definition

Science Requirements

Hyperspectral

SAR

Lidar

System Guidelines

Technical Assessments & Trades

*On-board Processing vs.
High Bandwidth Downlinks*

*Data Compression vs.
Raw Data Downlink*

*Comparison of Various
Onboard Data Systems*

*Downlink Options and
Link Architecture*

Documentation

Team Members

***Wayne Schober, Jim Lesh,
Ed Danielson, James Andary,
Dennis Anducyk***

***Stephen Noland, Ed Danielson,
GSFC***

Jeff Simmonds

Stephen Noland

Robert Menzies

Faiza Lansing

Faiza Lansing

Victoria Gor, Ed Danielson



Fabrizio Pollara

Vince Randolph/Evan Webb

***Keith Wilson, Faiza Lansing,
Robert Lock, Matthew Griffin***

Edward Sewall

2. EXECUTIVE SUMMARY



High Data Rate Instrument Study

January 28, 1999

Wayne Schober	Evan Webb
Jet Propulsion Laboratory California Institute of Technology	Goddard Space Flight Center

Slide 1. High Data Rate Instrument Study *

The high data rate instrument study was funded by the Code Y Earth Science Technology Office in July of 1998. The study was a joint effort between the Jet Propulsion Laboratory (JPL) and the Goddard Space Flight Center (GSFC). The study was managed by Wayne Schober of JPL; Evan Webb led the study participation by GSFC. Faiza Lansing and Keith Wilson led the study at JPL.

* The Executive Summary slides were presented on January 28, 1999. The slides are printed with summary remarks provided for clarity.



JPL

High Data Rate Instrument Study - Objectives

- **Assess the characteristics of future high data rate Earth observing science instruments**
- **Assess the feasibility of developing data processing systems and communications technologies required to meet those data rates**

wn
1/24/99

Slide 2. High Data Rate Instrument Study - Objectives

The High Data Rate Instrument Study objectives were to assess the characteristics of future high data rate Earth observing science instruments and then to assess the feasibility of developing data processing systems and communications systems required to meet those data rates.



JPL

High Data Rate Instrument Study - Approach

- Identified lead individuals in the key technology areas of science, on-board data management, and telecommunications
- Science team reviewed the current and projected capabilities of high data rate instruments and provided projected data rates from instruments for the years 2000, 2003, and 2006
- Teams assessed the current state of technology and evaluated the technology required to downlink the high data rates projected by the science team. The teams were:
 - On-board Data Management
 - on-board storage and processing
 - image compression
 - intelligent data extraction
 - Telecommunications
 - x-band
 - Ka-band
 - optical
 - ground data distribution
- GSFC reviewed initial study information and provided corrections, changes, and inputs on their work on RF phased arrays. These inputs were incorporated into the study.

WRS
1/24/99

Slide 3. High Data Rate Instrument Study - Approach

The study manager identified lead individuals in the key areas of science, on-board data management and telecommunications. The science team developed a list of instruments with high data rates. These instruments and data rates were then projected to three technology readiness dates. The technology readiness dates selected were 2000, 2003, and 2006. Missions could be flown two to three years after these dates using those projected technologies.

Technology teams were formed to assess the current state of technology and evaluate the technology required to downlink the high data rates projected by the science team. The teams were:

On-board Data Management

- on-board storage and processing
- image compression
- intelligent data extraction

Telecommunications

- x-band
- Ka-band
- optical
- ground data distribution

Data rates of 0.1, 1, and 10 Gbps were used in the study to compare systems.

GSFC reviewed initial study information and provided corrections, changes, and inputs on their work on RF phased arrays. These inputs were incorporated into the study.



JPL

Need for High Data Rate Instruments

- **Improved monitoring and management of Earth's resources and environment require the high spatial and spectral resolution obtained by advanced space-borne hyperspectral, SAR and Lidar instruments**
- **Scientists ranging from geologists, volcanologists, agriculturists, urban planners and environmentalists use hyperspectral data to identify and locate mineral deposits, study atmospheric processes and dynamics, study lava's composition and flow, improve classification of land areas to optimize its use, and improve crop prediction and assess health of crops**

WTS
1/24/98

Slide 4. Need for High Data Rate Instruments

The current need for high data rate instruments and growing capability of those instruments is projected to continue until at least 2008.



JPL

High Data Rate Instrument Study - Assumptions

- Technology timeframe for this study is for Technology Readiness dates of 2000, 2003, and 2006. Launch dates are assumed to be at least two years after these dates.
- The orbit of the spacecraft is 700 km in a circular polar orbit and inclined at 98 degrees.
- Data is taken at the full instrument rate over land (approximately 1/3 of the time)
- RF ground stations in Alaska and Norway are assumed to be retrofitted to support high data rates at Ka-Band
- No unplanned new ground station construction is assumed
- RF communications in the V and W bands were not considered

WFO
1/2/99

Slide 5. High Data Rate Instrument Study - Assumptions

The choice of assumptions is very important to this and any system study since they bound the work performed in the study and therefore the results and conclusions. In particular, this study assumed that no unplanned ground stations would be constructed and that there would be no geosynchronous data transfer satellite for Ka-band or optical communications. However to have an even comparison between X-band and Ka-band RF communications, the RF ground stations in Alaska and Svalbard, Norway were assumed to be upgraded to Ka-band capability. This upgrade is not currently planned by SOMO.

In this study the number of optical ground stations has been limited to five (5) located at the mid-latitude locations of Hawaii, California, Massachusetts, and the Canary Islands. Increasing the number of these low-cost ground stations around the globe will significantly increase the data throughput at optical frequencies. Such stations would be baselined on Goddard's SLR 2000 autonomous stations.



JPL

High Data Rate Instruments/Data Rates

Technology Readiness Date	<u>2000</u>	<u>2003</u>	<u>2006</u>
Hyperspectral	1.6 Gbps	3.2 Gbps	40.3 Gbps
SAR	0.18 Gbps	1.3 Gbps	4.8 Gbps
LIDAR	5.0 Mbps	5.0 Mbps	5.0 Mbps

These high data rate instruments will be built; the question is what percentage of the data can be cost-effectively stored and transmitted.

WTS
1/24/99

Slide 6. High Data Rate Instruments/Data Rates

In the following group of charts, the data is displayed against the three technology readiness dates. Different instruments and technology are assumed for each date. Missions could be flown two or three years after the technology readiness dates.

Hyperspectral instruments will continue to have the highest data production of all the instruments with synthetic aperture radar (SAR) instruments coming in second. Lidar and other instruments were not considered further in this study to be drivers in high data rate requirements.

In the 2003 case, the SAR data rate represents a significant fraction of the hyperspectral data rate. Therefore, the data rates used to drive the technology in this study were from a satellite which had both instruments on it and used a combined data rate from those two instruments.



JPL

Science Data Storage Requirements/Capability

Technology Readiness Date	<u>2000</u>	<u>2003</u>	<u>2006</u>
Two Orbits (RF Cases)	6.5 Tb	16.2 Tb	162 Tb
Five Orbits (Optical Com Cases)	16.2 Tb	40.5 Tb	405 Tb
Estimated on-board Data Storage Capability	1 Tb	4 Tb	16 Tb
Ratio of Science Data Reduction to Storage Capability			
R F	6.5 (X-band)	4 (Ka-Band)	10 (Ka-Band)
Optical	16	10	25

WFB
1/24/99

Slide 7. Science Data Storage Requirements/Capability

A lot of new information is presented in this slide. First of all, the data is presented in Terabits (Tb) of data against the technology readiness dates. For fair comparison between RF and Optical communications technologies, total data produced by the instruments is calculated for the relevant number of orbits. For RF communications, high latitude ground stations are used since one of them is visible to the satellite on every orbital period. Two orbits of data are accumulated to account for a missed pass, other priorities for the ground station, and weather outage. In the Optical Communications case, data must be accumulated for five orbits even though five optical ground sites in Hawaii, California, Massachusetts, and the Canary Islands are participating. The lower latitude of these stations decreases visibility of these sites to the satellite on any given pass as shown on the next slide.

The data produced by the instruments is divided by the estimated on-board storage capability of the satellite by year. This results in a ratio showing that the amount of data produced by the instruments is about an order of magnitude greater than the ability of the satellite to store that data. This is the first bottleneck for getting data to the ground.

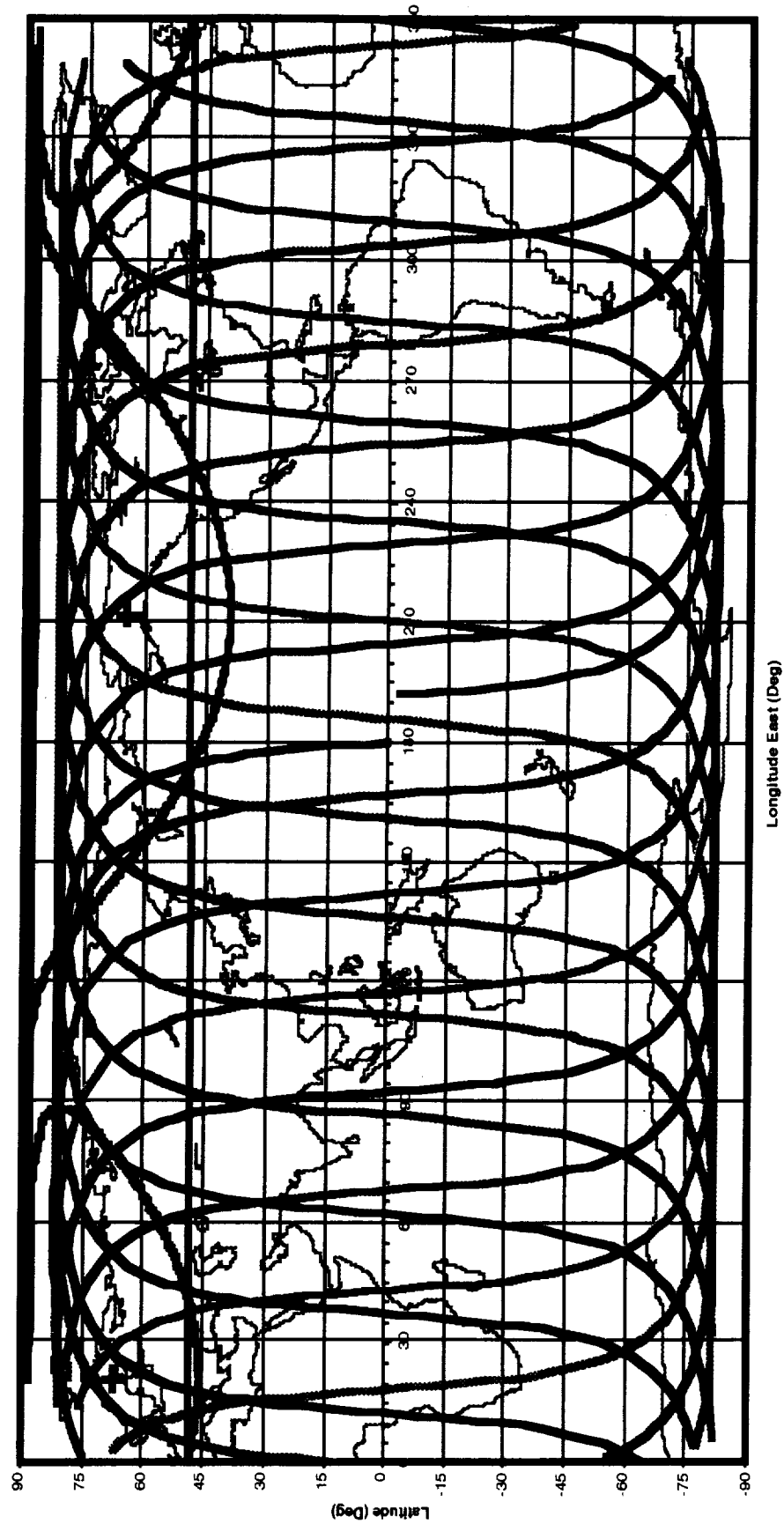


RF Systems Need to Store Two Orbits of Data JPL

RF Ground Stations:

Svalbard, Norway and ASF, Alaska

Satellite Ground Track

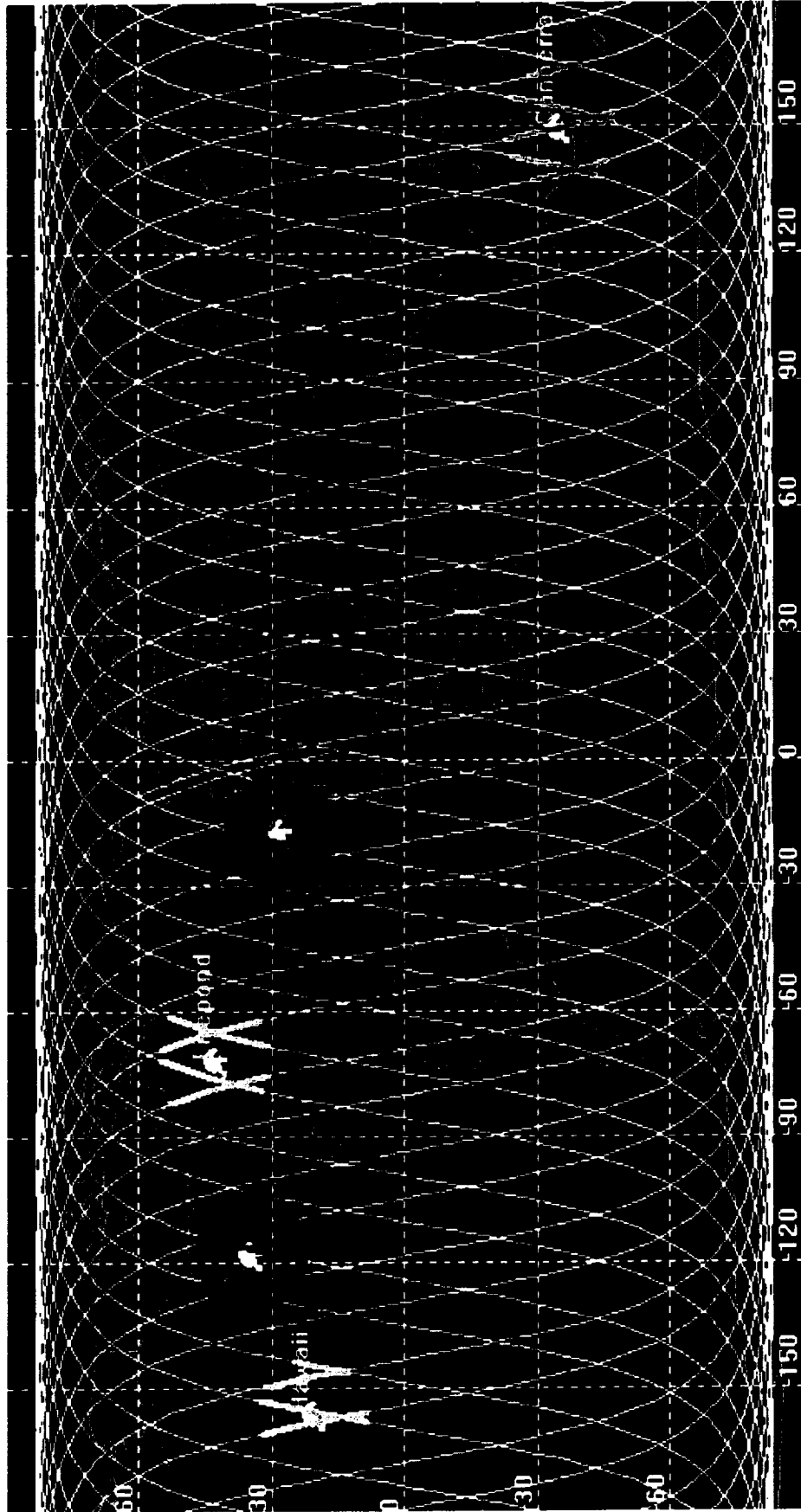




Optical Com Needs to Store 5 Orbits of Data JPL

Optical Comm. Ground Stations:

NASA/JPL TMF, OCTL, Canberra, Aus, AFRL AMOS Maui, HI,
ESA Tenerife, Canary Islands, and MIT Lincoln Labs Firepond



JPL

Storage Capability/ Telecom Capability

Technology Readiness Date	<u>2000</u>	<u>2003</u>	<u>2006</u>
Estimated On-Board Data Storage Capability	1 Tb	4 Tb	16 Tb
RF Cases	0.384 Tb	1.2 Tb	11.5 Tb
Optical Com Case	6.4 Tb	6.4 Tb	6.4 Tb
Ratio of Storage Capability to Telecom Capacity			
RF	2.6 (X-Band)	3.3 (Ka-Band)	1.4 (Ka-Band)
Optical	N/A (not limited)	N/A (not limited)	2.5

WFS
1/24/99

Slide 10. Storage Capability/ Telecom Capability

The estimated on-board data storage capability used in the previous comparison of the data produced vs the amount of data which can be stored is now used to show that the data which can be stored cannot be forwarded to the ground with RF communications systems and a projected optical system in 2006. The RF system used in the technology readiness year of 2000 is X-band. RF systems after that date assume that the ground stations in Alaska and Norway were retrofitted to Ka-band capability.

The Optical Communications downlink capability exceeds the on-board storage capability. The same Optical Communications system is used for all three technology readiness dates. The effect of the low number of ground stations where the RF telecom capability exceeds that of optical. Clearly, a LEO-to-GEO link would increase the throughput.

The ratio of storage capability to telecom capacity shows that for the RF cases, only about a third of the stored data can be transmitted to the ground.



JPL

Overall Gap between Instrument Data Generated and Storage/Downlink Capability*

Technology Readiness Date	<u>2000</u>	<u>2003</u>	<u>2006</u>
RF	27	13.2	14
% of Data Generated which can be Downlinked	(3.7%)	(7.8%)	(7.8%)
	X-Band Bandwidth Limited	Storage & Telecom Limited	Storage & Bandwidth Limited
Optical Com	16	10	63
% of Data Generated which can be Downlinked	(6.2%)	(10%)	(1.6%)
	Storage Limited	Storage Limited	Storage & Telecom Limited

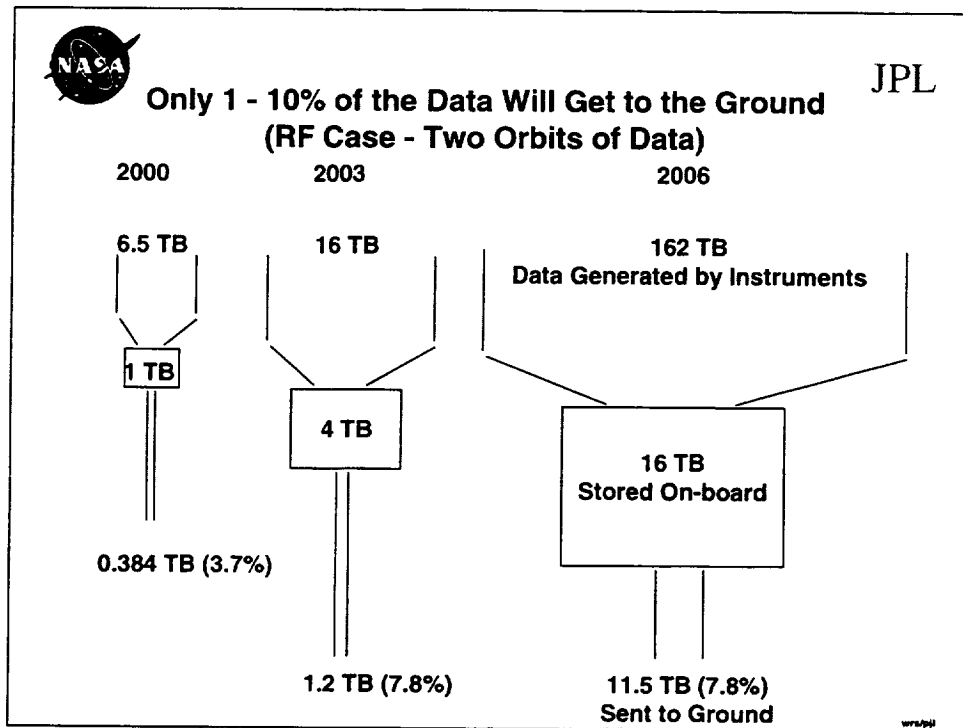
* Using current technology approaches projected to 2006 with no new ground stations, no geosynchronous communications transfer satellite but with upgrade of Alaska and Norway ground stations from X-Band to Ka-Band capability

WFS
1/24/99

Slide 11. Overall Gap Between Instrument Data Generated and Storage/Downlink Capability

The product of the ratios of the science data storage requirements to the on-board data storage capability and that of the on-board data storage capability to the downlink capacity gives the gap between the ability of the instruments to generate data and our ability to get that data to the ground. The percent of data generated that can be downlinked is just the inverse of this factor.

It should be noted that there is no single technology that is the bottleneck in getting data to the ground. In the year 2000 technology readiness case, the RF capability is limited by data storage and the bandwidth assigned to X-band communications. The 2003 RF case, the data is limited by on-board storage and telecommunications technology; in the 2006 RF case, data is limited by storage technology and the bandwidth assigned to Ka-band communications. Optical Communications are limited by the on-board data storage required and the overflight of ground stations.



Slide 12. Only 1-10% of the Data Will Get to the Ground

This slide is a depiction of the RF data only from the previous slide to graphically emphasize that the data storage and communications downlinking technology are increasing dramatically but that the data generated by instruments is also increasing dramatically.

On EO-1 only 90 seconds of data per orbit or less than 2% of the data will be downlinked. This situation of more data being generated than can be downlinked is not likely to improve in the foreseeable future without new breakthrough technologies.



JPL

Technology Breakthroughs Required

- Only 1 - 10% of instrument data can be downlinked to the ground now and for the foreseeable future
- Revolutionary changes in spacecraft design and operations required to increase downlinkable data
 - Intelligent Data Extraction
 - Optical Compression

WTS/JPL
1/24/99

Slide 13. Technology Breakthroughs Required

Instrument technology, data processing technology, on-board storage technology, and communications technology are all increasing at a rapid rate. However, it does not appear possible that the technologies required to store and downlink data will overtake the instrument's ability to produce data. Therefore, breakthrough technologies should be sought to narrow or close the gap.

Specifically, processing the data on-board the satellite and extracting the interesting data appears to be a viable solution. Lossless, optical compression of data should also be pursued pending the results of the proof-of-concept from the GSFC SBIR Program.



Intelligent Data Extraction

JPL

- Significantly interesting data are extracted and processed onboard the satellite at the instrument level to reduce the requirement for onboard data storage
- Data reduction rates on the orders of 10, 100, and 1000 are possible
- Low-level, mid-level and high-level features can be extracted from the data and reported according to bandwidth availability. For example, the data is collected in different filters or different sources provide multiple information for every pixel, so that each pixel of image data has an n-dimensional vector of values associated with it. The elementary feature-extractor will use mixture-modeling techniques to assign a unique label (can be 2 bits) for each pixel instead of a lengthy multi-dimensional vector (can be 80 bits, for example). This procedure alone can potentially achieve data reduction of one or two orders of magnitude.
- Mid-level information extraction algorithms will cluster low-level features into regions or other descriptive shapes using spatial information further decreasing required data rates by one - two orders of magnitude.
- High-level information extraction algorithms can report statistical information relevant to scientists
- Once the features of scientific interest for available instruments and data scenarios are identified and approved by the scientists, the appropriate algorithms for such feature extractions will be selected.

WPS
1/24/99

Slide 14. Intelligent Data Extraction

In intelligent data extraction, the data from each pixel is projected onto principal components (eigenspace), thereby reducing the original size of the spectrum to the size of eigenspace. The eigenspaces are derived from the multiple examples of each class and their principal axes point in the direction of maximum variance of the data. The size of the eigenspace can be chosen by scientists or dictated by system requirements to achieve the $O(10)$ reduction. $O(100)$ reduction, or mid-level information extraction is achieved by using spatial and spectral information to cluster low-level features into regions. The descriptors of these regions constitute the reduced data stream that is transmitted to Earth.



Optical Compression

JPL

- Up to 100:1 lossless data compression
- Format independent (not restricted to image data)
- Uses optical Fourier transform
 - Data is immediately written onto a Spatial Light Modulator, which is then transformed onto a detector - the transform is read out, and may be transformed several more times without data loss.
- Proof of concept demonstrated at OPTS Inc. with SBIR funding which ends in Feb 1999
- \$350K is required to validate the technology in a laboratory environment with Earth Science data

wra/pjl
1/24/99

Slide 15. Optical Compression

- Adaptive Network to implement well understood data processing algorithms using images and optics instead of electronics - Fourier transforms, data compression, pattern recognition.
- Data ingest at up to 8 Tbit/s is a 10,000 times faster input
- Processing rate of 500 Billion Operations/ Second for 50 watts power



Conclusions

JPL

- Technologies for increasing on-board data storage and downlink communications capabilities are increasing at about the same rate as the increase in data rate of high data rate instruments
- Only 1 to 10% of the data generated by high data rate instruments can be downlinked through the 2006 technology readiness timeframe using current technology approaches
- Current technology development programs in communications, data storage, data processing and data compression must be continued or the gap will increase
- Intelligent data extraction can fill the gap in the technology readiness cases of 2000 and 2003, but the power and mass requirements for a data processing system for the 2006 case becomes prohibitive
- Lossy data compression could fill the gap, but it generally encounters resistance from the science community

WTS
1/24/99

Slide 16. Conclusions



JPL

Recommendations

- Continue existing technology development programs for on-board data storage and downlink communications
- Develop Intelligent Data Extraction Technology
 - Technology under development in Cross Enterprise Technology Development Program
 - A specific program for Hyperspectral instruments is required
 - estimate 350K per year for three years; initial funding will show feasibility on existing hyperspectral data sets
- Develop Optical Compression - \$350K for Technology Validation
- Determine cost and schedule to upgrade ground station receivers and antenna in Alaska and Norway to support high data rates at Ka-band
- Study the feasibility of creating a geosynchronous optical data transfer capability which solves the downlink bottleneck

WTS
1/24/99

Slide 17. Recommendations

The existing technology programs in data storage, data processing, and communications must be continued or the gap between data produced and data downlinked to the ground will increase.

Breakthrough technologies should be pursued to close the gap. Specifically, Intelligent Data Extraction Technology being developed under the NASA Cross Enterprise Technology Development Program shows a lot of promise. A program needs to be initiated on hyperspectral data sets to confirm technical feasibility.

Another area to pursue is Optical Compression. The lossless data compression community should review the OPTS Inc. technology and pursue it as appropriate.

Upgrading the Alaskan SAR and Svalbard, Norway stations from X-band to include Ka-band should be planned. The cost and feasibility of geosynchronous optical and Ka-band satellites should also be studied as new high data rate missions evolve.



High Data Rate Instrument Study - Report Contents

JPL

- Executive Summary
- Introduction
- Instrument data rates needed to support the future high spectral and spatial resolution hyperspectral imaging instruments, the lidar and the synthetic aperture radar.
- Onboard processing of data and intelligent data extraction at the instrument level
- DRAM and disk-drive onboard data storage options that would support the instrument data rates and onboard processing
- Data compression of imaging data that will facilitate the recovery of higher data volumes using lower telecommunications data rates.
- General telecommunications architecture (X-band, Ka-band, and optical telecommunications spacecraft transceivers)
- Configuration of the optical ground station for the high-data-rate reception
- Data-distribution approaches that are expected to be available to stations located within the continental United States (CONUS)
- LEO-to-GEO and GEO-to-ground-relay optical link in section
- High-speed data storage and distribution from the ground stations
- Mass and power consumption for the spacecraft telecommunications system along with the estimated costs for the spacecraft RF and optical communications terminals; cost estimates for data delivery, i.e., for connecting the ground station to the WAN.
- Conclusions and recommendations

wrs
1/24/99

Slide 18. High Data Rate Instrument Study Report Contents

3. INTRODUCTION

NASA's imaging strategy for the 21st century calls for supporting the needs of the EOS missions with a suite of smaller and more capable satellites. These satellites will carry advanced hyperspectral imaging instruments and synthetic aperture radars which will generate several Gbps of data to meet the scientists' demand for higher spectral and spatial resolution. Returning these data to the ground and distributing them to the scientific community will require the use of several advanced technologies. In this report, we explore those technologies that comprise the end-to-end data delivery system.

The study approach was as follows:

1. The study manager identified the end-to-end mission needs and assembled lead individuals in the key technology areas of science, onboard data management, and telecommunications.
2. The science team reviewed the current and projected capabilities of high data rate instruments. The science team then provided projected data rates from instruments for the years 2000, 2003, and 2006.
3. Teams were assembled to assess the current state of technology and the technology required to downlink the high data rates projected by the science team. The teams were:
 - On-board data management
 - intelligent data extraction
 - on-board storage and processing
 - image compression
 - Telecommunications
 - x-band
 - Ka-band
 - optical
 - ground data distribution.
4. Preliminary study results were briefed to GSFC managers, who also provided inputs on the work being done by GSFC on RF phased arrays. These inputs were incorporated in the written report, and a draft was forwarded to GSFC for review. GSFC's comments were reviewed with E. Webb, appropriate modifications and expansions in scope were made, and the final report was prepared.

The final report below is broken into three major technical sections. In Section 4, we discuss the instrument data rates needed to support the future high spectral and spatial resolution hyperspectral imaging instruments, the lidar and the synthetic aperture radar. These rates are projected from the year 2000 to 2006 based on the expectation of a demand for more capable instruments with higher spatial and spectral resolution.

In Section 5.1 we discuss onboard processing of data and intelligent data extraction at the instrument level. In this approach, significantly interesting data are extracted and processed onboard the satellite at the instrument level to reduce the requirement for onboard data storage and to take advantage of the high-data-rate transmission. We describe data reduction rates on

the orders of 10, 100, and 1000 and discuss the required processing speeds, electrical power requirements, and general feasibility of meeting these target rates by the specified dates. The intelligent data extraction approach was deliberately selected to be aggressive since it had the potential of providing the greatest relief to the onboard storage and downlink telecommunications requirements. In section 5.2, we evaluate DRAM and disk-drive onboard data storage options that would support the instrument data rates and onboard processing. In section 5.3, we describe data compression of imaging data that will facilitate the recovery of higher data volumes using lower telecommunications data rates.

In section 6.1 we describe the general telecommunications architecture. We discuss the X-band, Ka-band, and optical telecommunications spacecraft transceivers for the 0.1, 1, and 10 Gbps telecommunications data rates in section 6.2. We present the configuration of the optical ground station for the high-data-rate reception in section 6.2.2.2, and explore the data-distribution approaches that are expected to be available to stations located within the continental United States (CONUS). We did not include details of the modifications to the RF ground stations to support these high data rates in this study. However, we do identify Svalbard, Norway, and the SAR facility in Alaska, two high-latitude stations that give visibility to the spacecraft on almost every pass, thus reducing the required onboard storage when these ground receiver sites are used.

We describe a LEO-to-GEO and GEO-to-ground-relay optical link in section 6.2.2.3. In this scenario, three ground stations located in the southwestern United States would provide 97% weather availability. Three stations located strategically in CONUS would support most of the mission requirements. This approach eliminates the need for a global network of ground stations.

In section 6.3 we describe strategies for high-speed data storage and distribution from the ground stations. We present the mass and power consumption for the spacecraft telecommunications system along with the estimated costs for the spacecraft RF and optical communications terminals in sections 6.4. We also provide cost estimates for data delivery, i.e., for connecting the ground station to the WAN. Our conclusions and recommendations for future work are in section 7.

4. SCIENCE REQUIREMENTS

4.1 Introduction

Improved monitoring and management of Earth's resources and environment will require the deployment of high spatial and spectral resolution onboard spacecraft. The spatial and spectral resolution obtained with advanced spaceborne hyperspectral imagers and synthetic aperture radars (SAR) will provide information on the changes in the Earth's dynamic processes. SAR instruments provide information on ocean dynamics, wave and surface wind speeds and directions, desertification and deforestation, and volcanism and tectonic activity. Interferometric SAR allow more accurate measurements of these changes.

Hyperspectral imaging instruments generate high spectral resolution images of surface features soil and vegetation that enable geologists, agriculturists and others to identify mineral deposits and to monitor crop health. Both instruments generate gigabits of data per second and the challenge is to get this information back to the principal investigator.

To set the basis for the study we have made certain key assumptions on instrument performance and on what would and would not be acceptable to the science principal investigator. These are elaborated in greater detail in section 4.1.1 below.

4.1.1 Assumptions

We were tasked to determine requirements for earth-pointing instrument scenarios that would provide stressful cases to drive a study of future high-data-rate downlink technology. In developing these requirements, our approach has been as follows:

- Survey the available earth science instrument community for examples of projected missions with instruments that would provide very high data rates.
- Project existing and proposed instrument technology to estimate scientifically useful instrument data rates for the epochs to be studied.
- Assess the feasibility of data rate reduction technologies such as compression and on-board data classification.
- Postulate reasonable acquisition scenarios involving orbit, acquisition times, instrument modes, etc.
- Distill the above information into downlink data-rate requirements for the study epochs.

Three instrument types were selected for inclusion in this study:

1. A hyperspectral imager, consisting of separate visible and SWIR channels, each producing its own data stream
2. Synthetic Aperture Radar (SAR) based on the projected capabilities of the lightSAR instrument.
3. A LIDAR, which provides a relatively low volume but constant data flow into the spacecraft data system.

Hyperspectral Imager

The hyperspectral imager selected for this investigation is based on a study of advanced LandSat concepts by Jeff Simmonds, JPL. The studied instrument concept was developed in response to the following science objectives:

1. Improve monitoring and management of Earth's resources and environment
2. Use hyperspectral data to:
 - Identify and locate mineral deposits
 - Study atmospheric processes and dynamics
 - Study lava composition and flow
 - Improve classification of land areas to optimize land use
 - Improve prediction of yields and assess health of crops
 - Develop better mapping strategies for disease containment
3. Maintain continuity of unenhanced Landsat data sufficiently consistent with previous Landsat data to enable comparisons for global and regional change detection and characterization.
4. Acquire and periodically refresh an archive of generally cloud-free images of all land surfaces.

Tables 4-1 through 4-3 provide the instrument design parameters that led to the estimates of data rate and volume for each study epoch. The data rates and volumes for the visible and SWIR channels were combined to provide an aggregate instantaneous instrument data rate that would provide complete emptying of the instrument data buffer during one frame time. This would permit no coverage gaps between adjacent frames.

Table 4-1. Hyperspectral instrument configuration for the Year 2000 case

Advanced Landsat Demo (2000)

Item	Value	Units/Spectrum Range
Orbit	700	km
GIFOV	43	m
Swath	61.45	km
Full FOV	7.18	degrees
# of x-track pixels	2048	
Spectral Channels	224	
VIS	64	0.4 - 1.0 μm
IR	160	0.9 - 2.5 μm
Integration Time	4.24	ms
Frame Time	8.68	s
Encoding	12	bits
VIS		
total data rate	30.9E+6	pixels/s
Frame volume	268.4E+6	pixels
IR		
total data rate	77.3E+6	pixels/s
Frame volume	671.1E+6	pixels
Total Scene	939.5E+6	pixels
Raw Rate (w/o overhead)	11.3E+9	bits
Data Rate	1.3E+9	bits/s

2 identical spectrometer modules behind a 15 degree TMA

FPA's = CCD for VIS and HgCdTe for SWIR (1024x160) at 18.5 micron pitch

Table 4-2. Hyperspectral instrument configuration for the Year 2003 case

Advanced LandSat 2003

Item	Value	Units/Spectrum Range
Orbit	705	km
GIFOV	30	m
Swath	185	km
Full FOV	14.95	degrees
# of x-track pixels	6166	
Spectral Channels	224	
VIS	64	0.4 - 1.0 μm
IR	160	0.9 - 2.5 μm
Integration Time	4.44	ms
Frame Time	27.37	s
Encoding	12	bits
VIS		
total data rate	88.9E+6	pixels/s
Frame volume	2.4E+9	pixels
IR		
total data rate	77.3E+6	pixels/s
Frame volume	671.1E+6	pixels
Total Scene	8.5E+9	pixels
Raw Rate (w/o overhead)	102.2E+9	bits
Data Rate	3.7E+9	bits/s

6 identical spectrometer modules behind a 15 degree TMA

FPA's = CCD for VIS and HgCdTe for SWIR (1024x160) at 18.5 micron pitch

Table 4-3. Hyperspectral instrument configuration for the Year 2006 case

Advanced LandSat 2006 Hi Res

Item	Value	Units/Spectrum Range
Orbit	705	km
GIFOV	10	m
Swath	185	km
Full FOV	14.95	degrees
# of x-track pixels	18500	
Spectral Channels	224	
VIS	64	0.4 - 1.0 μm
IR	160	0.9 - 2.5 μm
Integration Time	1.48	ms
Frame Time	27.38	s
Encoding	12	bits
VIS		
total data rate	800.1E+6	pixels/s
Frame volume	21.9E+9	pixels
IR		
total data rate	2.0E+9	pixels/s
Frame volume	54.8E+9	pixels
Total Scene	76.7E+9	pixels
Raw Rate (w/o overhead)	920.0E+9	bits
Data Rate	33.6E+9	bits/s
w / IMC=8	1.15E+11	bits
Data Rate	4.20E+09	bits/s

6 identical spectrometer modules behind a 15 degree TMA

FPA's = CCD for VIS and HgCdTe for SWIR (1024x160) at 6 micron pitch

The amount of data compression that can be effectively used for hyperspectral instrument data is determined primarily by the desired quality and utility of the returned imagery. Lossless compression techniques can achieve, at best, approximately 2:1 reduction. By 2006 the lossless performance may be up to 3 or 4:1. Various types of lossy compression can achieve larger savings at the expense of the utility of the imagery and the loss of some science data. The selection of compression rate can be a parameter of the overall collection strategy. For this study we estimated that the average compression achieved would be 10:1. We assumed that the majority of the Science users would accept this level of quality from the compression.

Another data volume reduction technique that could be applied to this data involves applying processing techniques (to the image data onboard the spacecraft) that perform selection and/or classification of image features and only return the results of these processes. These techniques have the potential for dramatic savings in transmitted data volume at the expense of not having the original image data available for purposes of discovery. This subject is discussed in detail below, but was not included in the requirements for data-link capacity.

The total volume of data returned from the spacecraft is driven both by the instantaneous instrument data rate and by the strategy applied to data collection. For this study we assumed that the hyperspectral instrument would be operated mostly in daylight, and only over continental land masses and their adjoining coastal waters. We also assumed that the instruments would not be operated at their highest resolution all the time, but would be used in both survey (low resolution) and investigation (high-resolution) modes.

We applied the above assumptions to the instantaneous hyperspectral instrument data as a contribution to the selected study rates shown in the summary table below.

Synthetic Aperture Radar (SAR)

The SAR instruments selected for this study are the Shuttle Radar Topographic Mission (SRTM) interferometric SAR instrument and the LightSAR mission concept from JPL. These instruments will help satisfy the following science objectives:

- Provide information on the changes in the Earth's dynamic processes
 - Changes in vegetation type, extent
 - Desertification and deforestation
 - Volcanism and tectonic activity
 - Soil moisture content and soil erosion measurements
- Data on ocean dynamics, wave and surface wind speeds and directions
- Terrain elevation and contour information.

Multi-wavelength multi-polarization Synthetic Aperture Radar instruments such as SIR-C/X expand our understanding of the physics behind these phenomena. Interferometric SAR allows more accurate measurements of these changes

The data generated by SAR instruments is not in image form but is a digitized representation of the radar echoes returned from the area illuminated by the radar beam. SAR data is usually digitized at fairly coarse resolution, 4-5 bits being common. As the SAR scans along its path, the digital radar data forms a two-dimensional time record of the amplitudes of the echoes that is commonly called the "Radar Phase History". The information about the target scene is distributed in this two-dimensional record in a form similar to a one- or two-dimensional hologram, depending on the SAR mode in use. The phase history is converted into an image by a process that involves correcting the data for the position of the antenna, correcting for other known phase perturbations in the signals, and then often application of a Fourier transform in one or two dimensions.

Because the image information is dispersed throughout the phase history, SAR data does not contain the redundant information that compression algorithms commonly remove to achieve their benefit. Also, image formation processing on board is considered infeasible for the foreseeable future because a) it is very computationally intensive, and b) the position of the antenna phase center must be known to a fraction of the SAR wavelength at all times. This information is usually not available without substantial post-processing of tracking data. For these reasons, we have elected to not include any data volume reduction in the SAR data in selecting the study downlink data rates.

The SAR peak instrument data rates are shown in the summary table below. For the 2000 case, the actual SRTM data rate is used. For 2003, the LightSAR operating at 1 m resolution is used, and for 2006, LightSAR operating at .25 m resolution is used.

LIDAR

A LIDAR instrument is included in the study as an example of an instrument that, while not providing a very high data rate, operates continuously throughout the mission, and thus provides a constant non-trivial data volume that must be accommodated.

Requirements Summary

The estimated instrument data rates and the selected downlink rate requirements for this study are given in Table 4-4.

Table 4-4. Instrument data rates and selected downlink rates for each option

Instrument/Year	2000	2003	2006
Hyperspectral	1.6 Gbps	3.2 Gbps	40.3 Gbps
SRTM/LightSAR	180 Mbps	1.3 Gbps	4.8 Gbps
LIDAR	5 Mbps	5 Mbps	5 Mbps
Note: instrument rates include 20% overhead			
Selected Study Link Rates	0.1 Gbps	1 Gbps	10 Gbps

The Link Rate requirements were selected after consideration of:

1. Instrument peak/worst-case data rates.
2. Average compression rate.
3. Operational scenarios and collection strategies.

Please note also that the instruments selected could produce much higher data volumes if operated in a more aggressive manner, or if the users demanded higher performance and no loss from the data compression or classification.

4.2 Study Guidelines

Programmatics/Mission (Table 4-5), a spacecraft description (Table 4-6), and costing data (Table 4-7) are described below.

Table 4-5. Programmatics/Mission

Customer	Wayne Schober
Study Lead	Faiza Lansing
Mission	High Data Rate Trades Study
Target Body	Earth
Trajectory	700 km Circular Orbit, 98 deg Inclination
Science Instruments	Hyperspectral, SAR, Lidar
Technology cut-off Date	2000, 2003, 2006
Mission Duration	2 years
Mission Class	C
Hardware Model	Protoflight S/C, EM instruments

Table 4-6. Spacecraft

Redundancy	Selected
Stabilization	3-Axis
Heritage	Commercial Spacecraft
Radiation Total Dose	20 krad behind 0.1 cm (100 mils) thick Aluminum
Payload Data Rate	1 Mbps - 45 Gbps
Tracking Network	ASF, Svalbard, Norway, and Others

Table 4-7. Costing

Cost Target	TBD
FY \$ (year)	98
Phase A Duration (months)	3
Phase B Duration (months)	6
Phase C/D Duration (months)	24
Phase E Duration (months)	TBD
Spare Approach	Selected
Parts Class	Commercial + Military 883B
S/C Supplier	Industry
Instrument Supplier	Industry / University
I&T Site	S/C Contractor
Launch Site	ETR
Burdens - JPL Program Office	TAP
Reserves	20%

4.3 Technology Readiness Levels

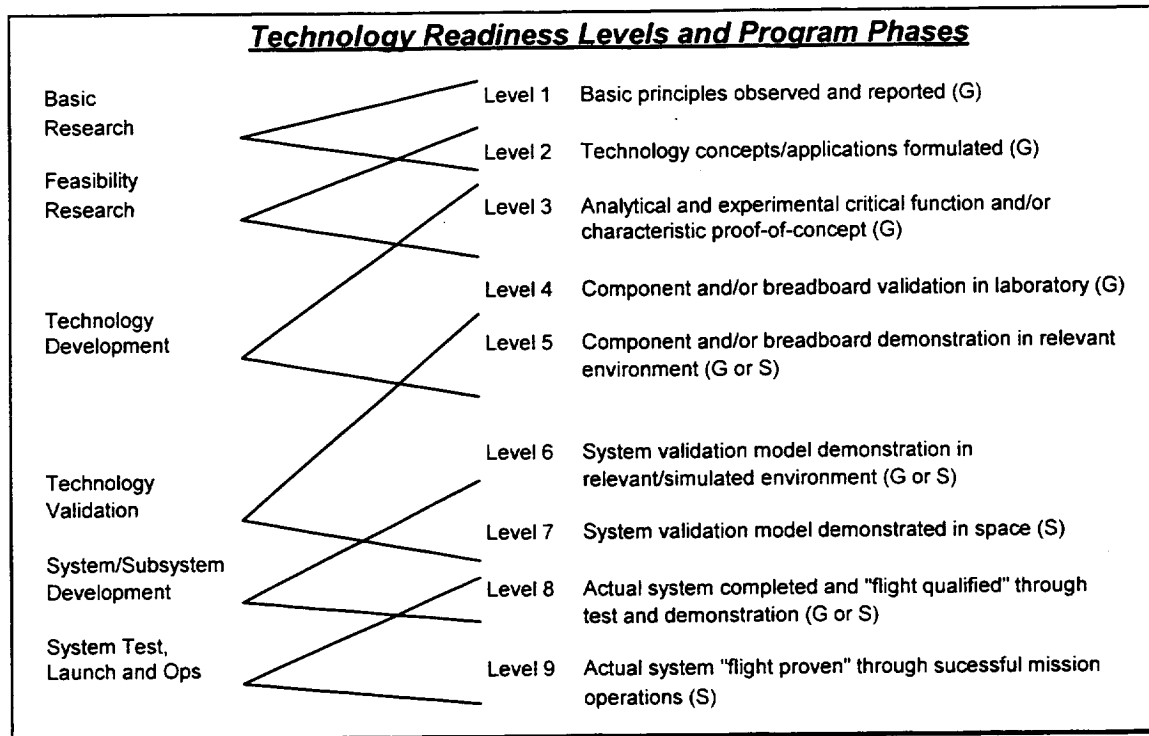


Figure 4-1. Technology readiness levels for each phase

5. ONBOARD DATA PROCESSING

5.1 Onboard Processing vs. High-bandwidth Downlinks

5.1.1 Introduction

Recent developments in technology continue to maintain or increase the gap between the ability of instruments to collect data and the capacity of data downlink. Currently, we are capable of collecting much more data than we are able to send to Earth. Moreover, the rate at which scientists analyze data is significantly slower than the rate of data acquisition. These two gaps can be reduced if scientifically important information content per bit of data is maximized.

To achieve this, scientists will have to specify the goals or data that are of scientific interest. For example, a scientist might prefer to receive a composite of scientifically interesting image fragments collected from thousands of images of a terrain, rather than 100 raw consecutive images. Or the scientist might prefer to obtain 3 images of a geologically active region and disregard 10 images of a desert. While the scientist specifies the task, the computer system will perform the selection process. Current machine-learning technologies allow the translation of such tasks into computer programs, which, when installed on board the spacecraft will perform the role of data selectors and data analyzers for the scientific goals specified. Scientists' requests and the reasoning behind scientific data analysis will be coded and computer programs will interpret the data in ways defined by scientists. As a result, the required downlink bandwidth will go down tremendously and the work with the acquired data will take on a different format, allowing scientists to spend much less time on extracting scientifically interesting information from large image data sets and much more time analyzing and studying scientifically relevant information, selected by the onboard computer.

This study identifies appropriate algorithms for extracting scientifically-interesting information from images collected by Earth-orbiting instruments in order to reduce the bandwidth of the downlink while preserving the scientifically interesting content of the image. The approach will be scientifically driven and hierarchical, achieving different levels of data reduction. The study will be conducted for three different data reduction rates: $O(10)$, $O(100)$, and $O(1000)$ and for two different instruments: hyperspectral and SAR. The costs of onboard implementation and autonomous execution of such algorithms will be explored and the feasibility of the entire process will be evaluated.

5.1.1.1 Assumptions

In addition to the general assumptions of this report, the onboard processing section has one specific assumption reflecting a novel autonomous approach to scientific data extraction. It is a known fact that image-processing algorithms are heavy consumers of computational resources. In order for data processing and analysis to be feasible on board the spacecraft, sufficient computational resources have to be available on board. The remote exploration and experimentation (REE) project (626-30) is used in this study for estimation of computational resources available on board the spacecraft in future years. Therefore, this study of onboard data rates assumes the success and on-time accomplishment of REE milestones depicted in Figure 5-1.

The REE project leverages NASA's high performance computing and communication program experience and uses scalable reconfigurable parallel architectures to bring state-of-the-art commercial computing capabilities into space. It will use hardware units developed by Seeker engineering (hardware based on CRAY/SGI design) and Lockheed Martin Sanders (custom design). Such architectures will enable the implementation of an onboard parallel computer operating at 300-1000 MOPS/watt (32-bit mixed integer & floating point Ops) without the use of high-cost radiation hardened processors or special purpose architectures. An overview of the REE project is presented in Figure 5-1).

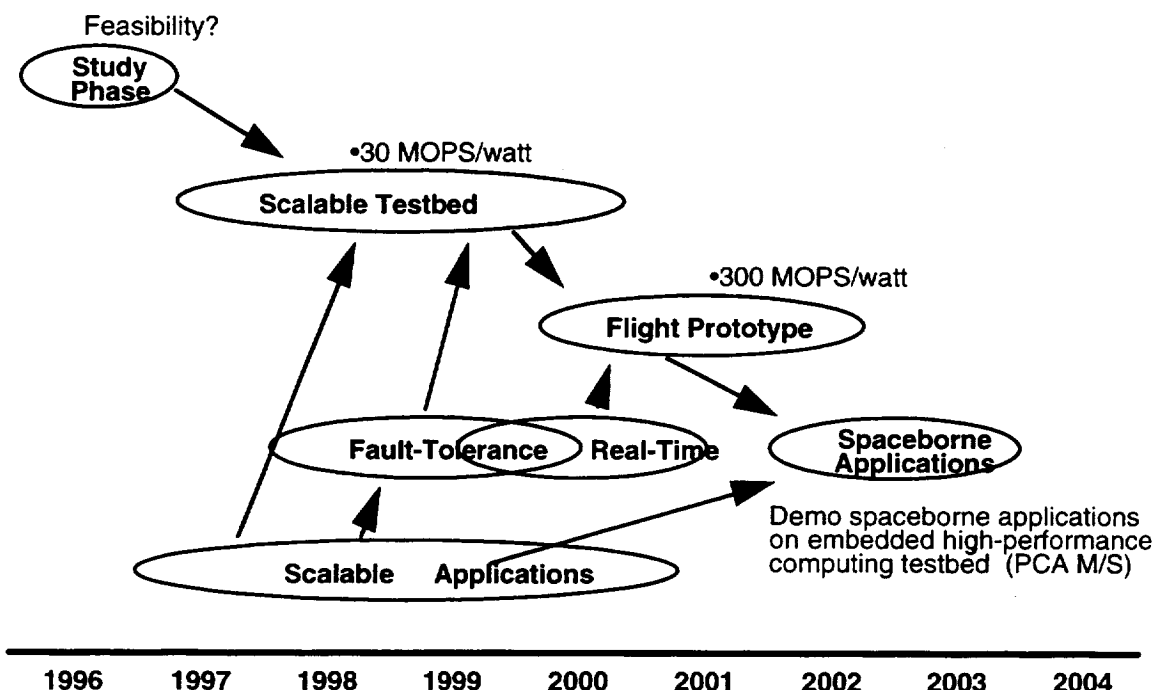


Figure 5-1. REE project overview

According to this project, a first-generation, scaleable, embedded computing testbed operating at 30-200 MOPS/watt will be installed in 1999 and the flight prototype embedded scaleable computer operating at 300-1000 MOPS/watt will be demonstrated in 2002. Assuming a processing power of 100 Watts by the year 1999, a 20 GFLOPS/second processing capability will be demonstrated for onboard processing and, by 2002, a capability of 100 GFLOPS/second will be within reach. The success of this project will open the door for computationally expensive processing on board the spacecraft and will allow a significant reduction in downlink bandwidth and data rates, therefore minimizing the overall cost of the mission. This report relies on the overall success of this project, and assumes its on-time delivery.

5.1.2. System Description

The primary scientific goal of the specified mission is to classify existing ground cover into groups that are interesting to scientists. They might be interested in Earth

resources (various minerals), types of crops, presence of crop diseases, ocean contamination levels, various types of vegetation, or amount of snow cover.

In the proposed system, a science-driven onboard feature-extraction procedure automates the loop between scientific request and data delivery, while significantly minimizing downlink bandwidth. To generate a request, scientists might wish to point to examples of data types of interest. These examples are automatically extracted from images and fed through machine-learning software, which codes scientific requests into compact, efficient recognizers and uploads them to the spacecraft (see Figure 5-2). The onboard computational process extracts features of scientific interest from image data and downlinks them to Earth.

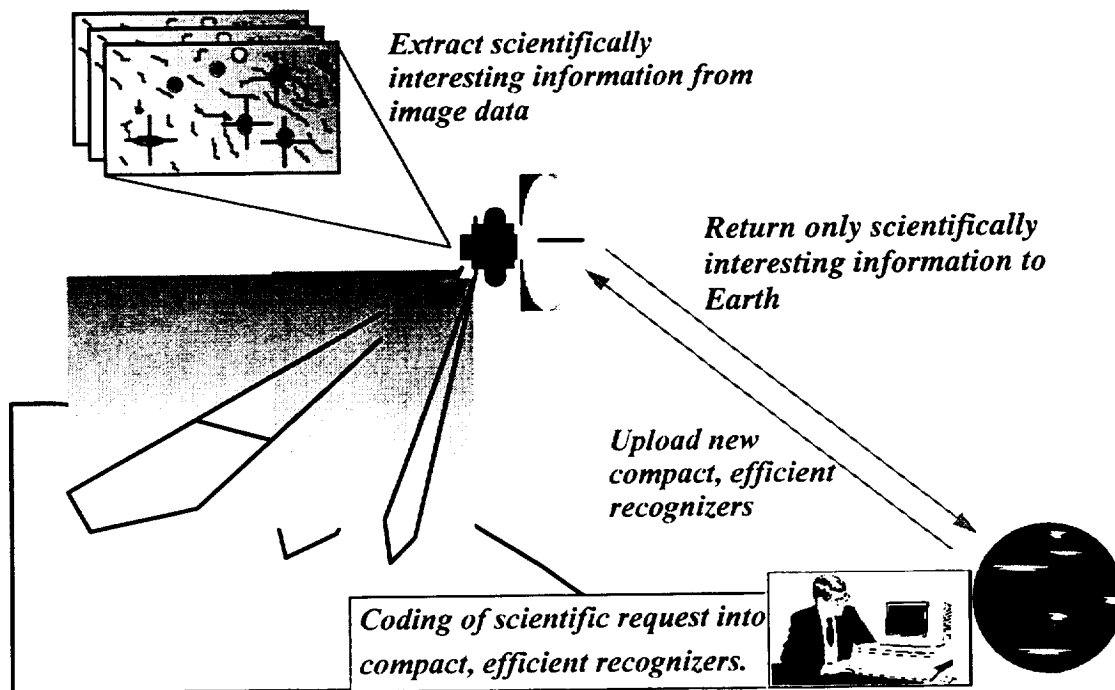


Figure 5-2. Intelligent coding of scientific requests reduces downlink size

Depending on available bandwidth, different levels of information extraction are applied in order to preserve as much detail as possible for direct scientific analysis. Low-level ($O(10)$ data reduction), mid-level ($O(100)$ data reduction) and high-level ($O(1000)$ data reduction) features are extracted from data and reported according to bandwidth availability.

Machine-learning algorithms are employed to achieve this goal. The typical machine-learning problem can be divided into two parts: training or learning the model for interesting classes; and, given the model, new data classification. In this study, we evaluated the cases when a model is learned from class examples provided by scientists (such examples can be easily obtained for Earth-observing missions). We also addressed the case when no examples are present and the model has to be learned concurrently with data acquisition and classification (see Appendix A).

Three algorithms were chosen for scientific data extraction: principal component extraction, iterated conditional modes, and statistical data representation. These algorithms can be organized hierarchically, where the input for higher-order data reduction algorithm is the output from the lower-order data reduction algorithm as shown in Figure 5-3.

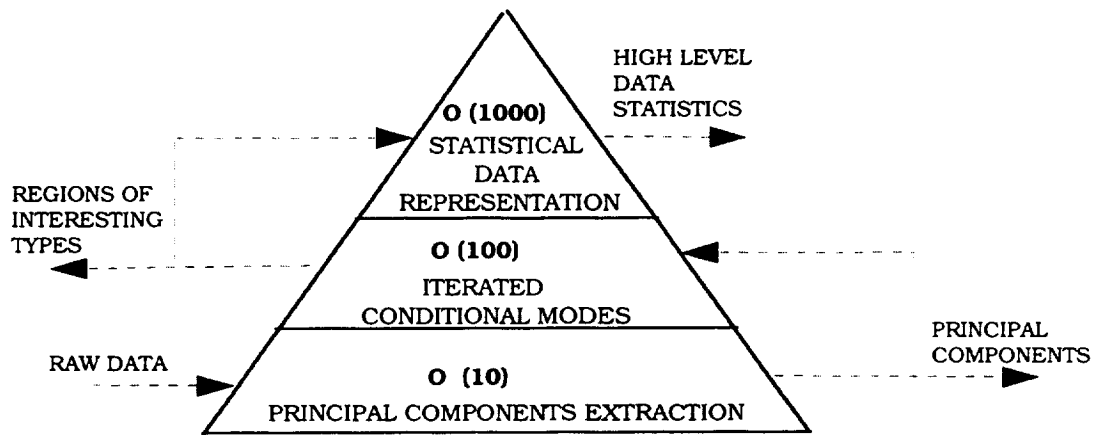


Figure 5-3. Hierarchical organization of scientific data-extraction algorithms

Algorithms were selected to maximize scientifically interesting content per bit of data.

In this study, the following formulas were obtained for a number of floating point operations (see Appendix A for details).

Hyperspectral imaging instrument:

O(10) feature extraction algorithms:

$$\text{OPS} = 2 \cdot M^2 \cdot P^2; \quad (\text{Eq. 1})$$

$$\text{Bytes} = M^2 \cdot (P + K); \quad (\text{Eq. 2})$$

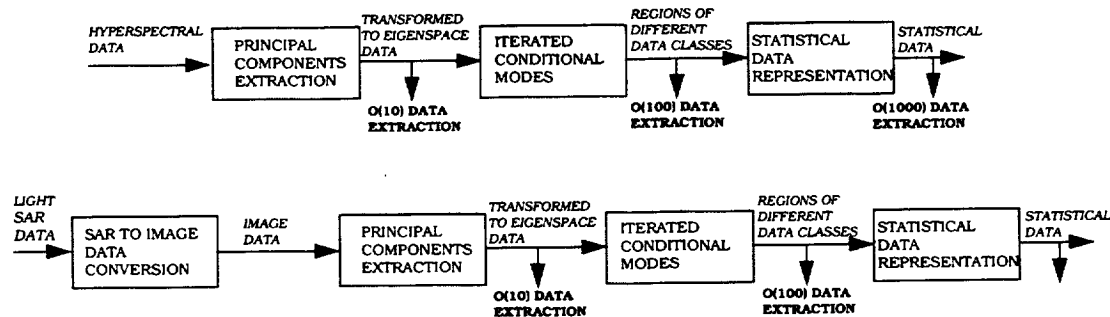


Figure 5-4. Processing flow for hyperspectral instrument and Light SAR instrument

5.1.3 Requirements: Mass, Power, and Cost (Case Study)

In this section, a case study is presented that summarizes power and computational requirements for specific cases of science parameters' settings. These cases were selected for demonstration of the requirement derivation process and are representative of possible scientific goals. Scientific parameters are mission-specific and no absolute numbers can be given that would be applicable to every mission. Instead, Eq.1-Eq.4 can be used to derive requirements for any mission, given parameters defined by the scientists. The REE technology used in this study is a new technology and no numbers for costs or masses are currently available. Therefore, cost and mass derivations are not included in this case study.

Proposed algorithms are currently implemented on SUN platforms and are being evaluated on various scientific data sets. Versions of such algorithms are used to solve a variety of problems. For example, principal component extraction methods are used to search for small-scale geological features such as volcanoes in Magellan CD-ROM databases of Venus; various classifiers are used as intelligent, trainable image-analysis tools for automating the analysis of over 3 Terabytes of image data for a sky survey; and iterative conditional modes are used in developing tools for recognizing features on the solar disk from images, mostly taken by ground-based solar observatories. Most of these algorithms are stand-alone applications driven by a GUI to tackle corresponding problems. The issues of parallelizing such algorithms were addressed and versions running in-parallel on multiple platforms currently exist. The technology readiness levels of 2-3 may be assigned to current processes, emphasizing their application to real data

sets, and their implementation in integrated demos, though not in a real-time environment, and not on board spacecraft designed for real missions.

Hyperspectral Imaging Instrument

Case 1: Extraction of 10 principal components ($O(10)$, $O(100)$, $O(1000)$) and classification into 10 classes ($O(100)$, $O(1000)$). 224 spectral bands, 12-bit encoding. Reflects on 1998 algorithmic capabilities. Formulas from the previous section are used for calculations. Parameter estimates/year from Table 5-1 are used for a representative case study. Real-time processing is assumed. $O(10)$ uses principal components only, the others use both principal components and ICM. Assume real-time processing. Assume 900 MOPS/node.

Table 5-1. Hyperspectral imaging instrument. Extraction of 10 principal components and classification into 10 classes

EXTRACTION OF 10 PRINCIPAL COMPONENTS AND CLASSIFICATION INTO 10 CLASSES EXAMPLE

	O(10)	O(100)	O(1000)
Data Rate (in Bits/sec)	100 M	1 G	40 Gbps
Image size (rwsxcls)/sec	193 x 193	610 x 610	4092 x 4092
OPS rqrd by process	3772 M	43420 M	2 T
Bytes rqrd by process	13 M	142 M	6.4 G
# of nodes	4	48	2222
Power drawn by proc. unit	19 Watt	43 Watt	2000 Watt
Mass	TBD	TBD	TBD
Hardware capability (year)	2000	2003	2003
Feasibility (yes or no)	yes	yes	no

Case 2: Extraction of 50 principal components (O(10), O(100), O(1000)) and classification into 40 classes (O(10), O(100), O(1000)). Two hundred and twenty-four spectral bands, 12-bit encoding. Reflects on 2002 algorithmic capabilities. Formulas from the previous section are used for calculations and parameter estimates/year from Table 5-2 are used for representative case study. Real-time processing is assumed. O(10) uses principal components only, the others use both principal components and ICM.

Table 5-2. Hyperspectral imaging instrument. Extraction of 50 principal components and classification into 40 classes

EXTRACTION OF 50 PRINCIPAL COMPONENTS AND CLASSIFICATION INTO 40 CLASSES EXAMPLE

	O(10)	O(100)	O(1000)
Data Rate (in Bits/sec)	100 M	1 G	40 Gbps
Image size (rwsxcls)/sec	193 x 193	610 x 610	4092 x 4092
OPS rqrd by process	7.06G	70.5 G	3.2 T
Bytes rqrd by process	20.34 M	203.2 M	6 G
# of nodes	8	78	3525
Power drawn by proc. unit	35 Watt	70.5 Watt	3172 Watt
Mass	TBD	TBD	TBD
Hardware capability (year)	2000	2003	2003
Feasibility (yes or no)	yes	yes	no

Light SAR Instrument

Case 3: Unlike the hyperspectral instrument, Light SAR has only 9 values per pixel (3x3 scattering matrix) and requires an additional 5G OPS for processing (this is an approximate number) and 64M bytes of memory (this is an approximate number). In this example, 3 principal components will be extracted from image data and classified into 15 classes. 8-bit encoding is assumed. The resolution of the image data after SAR-to-image conversion is assumed to be such that the total volume of data remains the same. Even though raw Light SAR instrument rates are slower than hyperspectral instrument rates, the size of the image produced per one second of data is larger (the hyperspectral instrument has 224 bands per pixel, while the Light SAR instrument has 9 polarizations per pixel), resulting in higher consumption of power as depicted in the following table. It is useful to note that despite the fact that absolute power for the SAR instrument is higher than hyperspectral, its rate of growth as a function of algorithm parameters is slower (since only 9 polarizations per pixel are assumed).

Table 5-3. Light SAR imaging instrument. Extraction of 3 principal components and classification into 15 classes

EXTRACTION OF 3 PRINCIPAL COMPONENTS AND CLASSIFICATION INTO 15 CLASSES EXAMPLE

	O(10)	O(100)	O(1000)
Data Rate (in Bits/sec)	100 M	1 G	5 Gbps
Image size (rwsxcls)/sec	1178x1178	3726x3726	8333x8333
OPS rqrd by process	325G + 5G = 37G	320G + 5G = 325G	1.6T + 5G = 1.6T
Bytes rqrd by process	42M + 64M = 106M	417M + 64M = 481M	2.1G + 64M = 2.1G
# of nodes	42	362	1777
Power drawn by proc. unit	185 Watt	325 Watt	1600 Watt
Mass	TBD	TBD	TBD
Hardware capability (year)	2000	2003	2003
Feasability (yes or no)	yes?	yes?	no

The given case study indicates that data extraction algorithms can handle near-real time data rates for years 2000 and 2003. Data rates for 2006 are problematic and can be addressed through non-real time processing, custom hardware design, and optimal loss of scientific information.

5.1.4. Conclusions and Recommendations for Future Work

This section of the study indicates that intelligent data extraction, driven by scientific requests, can be implemented to run autonomously on board the spacecraft within a context of realistic and useful mission. The autonomous algorithms, utilizing state-of-the-art machine-learning and data-classification techniques, exist and currently serve the purposes of data mining and classification of large scientific data sets. These algorithms can be used to interpret scientific requests to allow downlink data selection and prioritization. New REE technology described in this report allows implementation of these algorithms on board the spacecraft for real-time data processing and analysis. Such implementation enables a useful compromise between the preservation of scientific data, downlink reduction, and power consumption for years 2000 and 2003. For 2006, projected instrument data rates are too high to be processed with 2003 hardware, and the prognoses for state-of-the-art hardware in 2006 which will support 2006 instrument data rates cannot be made currently. On the other hand, the algorithms for such processing are available now.

The next step in the task of reducing the size of the downlink by intelligent autonomous data selection is the demonstration of such processes on the real data set (for example, EOS hyperspectral data set) and proving that downlink bandwidth can be significantly reduced, while satisfying the scientific constraints of the mission. When the algorithms are optimized for specific mission and scientific requests, and the results are acceptable to the mission scientists, the hardware implementation issue can be addressed. The parallel architecture can be constructed from reconfigurable units, and the prototype can be built, allowing an accurate estimate of power and mass requirements. The entire process should encourage close interaction between mission scientists and science-processing unit developers, ensuring the sufficiency of scientifically interesting information extracted from the images.

The proposed tasks and data set description for future work on autonomous scientific data extraction are listed below.

Data set:

EOS hyperspectral data set. Part of the images should be labeled by scientists and will make up the training set for the algorithm and ground truth used in the evaluation of results.

Task 1.

Prepare the data set and label a portion of the images for algorithm training and ground truth.

Task 2.

1) Apply the combination of proposed tasks and data set descriptions in the study algorithms: principal component extraction and iterative conditional modes to new data sets of hyperspectral (224 spectral bands) imagery of Earth ground cover.

Experimentally determine optimal interaction between two algorithms and modes of operation.

2) Investigate the effects of parameter settings on algorithm performance and obtain the optimal parameter setting. Make necessary modifications and further developments to existing algorithms to accommodate new data.

Task 3.

1) Conduct experiments to understand the structure of the data, and select the most appropriate model for data representation and feature extraction. Concentrate on extracting the most scientifically-meaningful features from the data for pixel representation.

2) Run algorithms from Task 2 on new data features. Add necessary modifications and developments to existing algorithms to accommodate new data.

Task 4.

1) Search for new data classes through applications and development of different clustering techniques.

Task 5.

1) Propose a parallel architecture for the best technique and implement this technique on parallel platform.

5.2 Comparison of Various Onboard Data Systems

5.2.1 Background

Some future missions will require very high data rates for their science instruments. Intelligent data extraction techniques will be provided in the science instrument to reduce the overall data volume. The arrays of processors needed to achieve each instrument's throughput requirements do not exist today. The following outline or wish list provides a description of some the challenges that lay ahead regarding advanced avionics performance needs. A separate spacecraft onboard processing system provides the advantage of allowing a less complex and slower Command and Data System (CDS) requirement for the high-speed science data collection and processing. This study evaluates spacecraft and instrument onboard data systems. Architectural options for accommodating these data rates will be evaluated. The goal is maximal science data return realized at the lowest cost.

5.2.2 Approach

The relevant mission parameters are listed in Table 5-4. It is assumed that both the science instrument avionics and the spacecraft avionics will have dual-string architectures for mission reliability at high data rates.

Table 5-4. Relevant mission parameters

Mission Parameter Guidelines and Requirements	2000 Technology Description	2003 Technology Description	2006 Technology Description
Launch Year	2002	2005	2008
Primary Mission Duration	2 years	2 years	2 years
Additional Extended Mission	TBD	TBD	TBD
Redundancy	Block Redundant	Block Redundant	Block Redundant
Technology Cutoff Date	2000	2003	2006
Number of Instruments	Hyperspectral SAR LIDAR	Hyperspectral SAR LIDAR	Hyperspectral SAR LIDAR
Science Data Input Rate(s)	0.2-1.6 Gbps	1.3-4.5 Gbps	4.5 -45 Gbps
Science Data Volume (Memory)	5800 Gbits	7200 Gbits	8640 Gbits
Intelligent Data Extraction	10:1	10:1; 100:1	10:1; 100:1; 1000:1
Instr./CDS Data Rate	100 Mbps	1 Gbps	10 Gbps
CDS Data Compression	1:1, 2:1	1:1; 2:1	1:1; 2:1; 20:1
CDS Data Volume (Memory)	400 Gbit Downlink Blocks	600 Gbit Downlink Blocks	6000 Gbit Downlink Blocks
Telecom uplink rate	2 kbps	2 kbps	2 kbps
Telecom downlink rate	100 Mbps	1 Gbps	10 Gbps
Radiation (Total Ionizing Dose) Behind 0.25 cm (100 mils) Al	6 krads	6 krads	6 krads
Power Source	Batteries and Solar Panels	Batteries and Solar Panels	Batteries and Solar Panels
Mission Class	B/C	B/C	B/C
Parts Class (See References 1, 2, and 3)	Commercial screened	Commercial screened	Commercial screened

5.2.3 Science Instrument and SPACECRAFT Avionics Functional Assignments

Instrument and S/C subsystem elements will perform the following functions defined in Table 5-5. All phases of the science data flow within the S/C are covered.

Table 5-5. Functional assignments to subsystems

Function(s)	Instrument(s)	CDS	Telecom
Raw Science Data Gathering	x		
Intelligent Data Extraction	x		
Initial Data Compression	x		
Science Data Packets	x		
Science Data Storage	x		
Instr./ CDS Data Transfer	x	x	
Data Compression(s)		x	
Downlink Data Storage Blocks		x	
Packet Headers		x	
Frame Headers		x	
Reed Solomon Encoding		TBD	
CDS/Telecom Data Transfer		x	x
Convolutional Encoding			x
Downlink Transmit			x

5.2.4 Spacecraft Command and Data Subsystem (CDS)

The Spacecraft CDS is required to perform many critical spacecraft functions, including the following:

- Uplink command processing and distribution
- Sequence storage and control
- Maintenance and distribution of spacecraft time
- Collection and formatting of engineering spacecraft sensor data
- Bulk storage of science and engineering data
- Subsystem control and services
- Spacecraft system control services (non-attitude control)
- Spacecraft fault protection

Instrument and Spacecraft CDS Software

The S/C CDS will be able to use a commercially available operating system and will be programmable in a high-level language such as C or C++.

5.2.5 Science Instrument Collection Schemes for 2000, 2003, and 2006

The following rate group tables define various worst-case mission scenarios that put the most demand on processing and memory capacity capability.

Science Data Volume for 2000 Mission (see Table 5-6)

The instrument raw science data rate will be as high as 1.6 Gbps. The instrument will collect 28.8 Tbits of science and state-of-health (SOH) data during a maximum 5-hour period. Real time data will be extracted by the array of instrument processors to reduce the data volume by a factor of 10. The real-time intelligent data-extraction process reduces the overall size of the instrument mass storage element. The instrument will not perform data compression algorithms on the science data. Intelligent data extraction of the science data will reduce the science and engineering data volume to 5.8 Tbits. Packetization, and encoding overhead will increase the overall science data volume. The science instrument will have the capability to store two cycles of science data in case a downlink encounter is missed.

Science Data Volume for 2003 Mission (see Table 5-7)

The instrument raw science data rate will be as high as 5.0 Gbps. The instrument will collect 90 Tbits of science and SOH data during a maximum 5-hour period. Real time data will be extracted by the array of instrument processors to reduce the data volume by a factor of 10. The real time intelligent data extraction process reduces the overall size of the instrument's mass storage element. The instrument will perform real time lossless 2.5:1 data-compression algorithms on the science data. Intelligent data extraction of the science data will reduce the science and engineering data volume to 7.2 Tbits. Packetization and encoding overhead will increase the overall science data volume. The science instrument will have the capability to store two cycles of science data in case a downlink encounter is missed.

Science Data Volume for 2006 Mission (see Table 5-8)

The instrument raw science data rate will be as high as 45 Gbps. The instrument will collect 864 Tbits of science and SOH data during a maximum 5-hour period. Real time data will be extracted by the array of instrument processors to reduce the data volume by a factor of 10. The real time intelligent data-extraction process reduces the overall size of the instrument mass storage element. The instrument will perform real time lossy 20:1 data compress algorithms on the science data. Intelligent data extraction of the science data will reduce the science and engineering data volume to 8.6 Tbits. Packetization and encoding overhead will increase the overall science data volume. The science instrument will have the capability to store two cycles of science data in case a downlink encounter is missed.

Table 5-6. Science data volume for 2000

Mission: Hyperspectral or SAR or LIDAR Study Name: High Data Rate Instrument 2000

Instrument Processing Rate Group Table

Science & Engineering Data Collection Time Slots

Subtotal Mass Memory Required (Gbits) 5760

Subsystem Totals 1600.0 28800 5760

Science Instrument or Engineering Interface	Data Rate (Mbps)	Collection Time (seconds or events)	Raw Data Storage (Gbits)	Intelligent Data Extraction Factor	Compression Factor	# of Cycles Before Downlink	Compressed Data Storage (Gbits)	Description/Comments
Instrument channel A	800	18000	14400	10	1.0	2	2880	Assume first downlink encounter is missed. Ten hours of data downlinked optical in TBD minutes.
Instrument channel B	800	18000	14400	10	1.0	2	2880	Assume first downlink encounter is missed. Ten hours of data downlinked optical in TBD minutes.
Instrument Engineering Data	0.0001	18000	0.002	1	1.0	2	0.0036	Assume first downlink encounter is missed. Ten hours of data downlinked optical in TBD minutes.

Table 5-7. Science data volume for 2003

Mission: Hyperspectral or SAR or LIDAR Study Name: High Data Rate Instrument 2003

Instrument Processing

Rate Group Table

Science & Engineering Data Collection Time Slots

Subtotal Mass Memory Required (Gbits) 7200

Subsystem Totals 5000.0 90000 7200

Science Instrument or Engineering Interface	Data Rate (Mbps)	Collection Time (seconds or events)	Raw Data Storage (Gbits)	Intelligent Data Extraction Factor	Compression Factor	# of Cycles Before Downlink	Compressed Data Storage (Gbits)	Description/Comments
Instrument channel A	2500	18000	45000	10	2.5	2	3600	Assume first downlink encounter is missed. Ten hours of data downlinked optical in TBD minutes.
Instrument channel B	2500	18000	45000	10	2.5	2	3600	Assume first downlink encounter is missed. Ten hours of data downlinked optical in TBD minutes.
Instrument Engineering Data	0.0001	18000	0.002	1	1.0	2	0.0036	Assume first downlink encounter is missed. Ten hours of data downlinked optical in TBD minutes.

Table 5-8. Science data volume for 2006

Mission: Hyperspectral or SAR or LIDAR Study Name: High Data Rate Instrument 2006

Instrument Processing

Rate Group Table

Science & Engineering Data Collection Time Slots

Subtotal Mass Memory Required (Gbits) 8640

Subsystem Totals 48000.0 864000 8640

Science Instrument or Engineering Interface	Data Rate (Mbps)	Collection Time (seconds or events)	Raw Data Storage (Gbits)	Intelligent Data Extraction Factor	Compression Factor	# of Cycles Before Downlink	Compressed Data Storage (Gbits)	Description/Comments
Instrument channel A	12000	18000	216000	10	20.0	2	2160	Assume first downlink encounter is missed. Ten hours of data downlinked optical in TBD minutes.
Instrument channel B	12000	18000	216000	10	20.0	2	2160	Assume first downlink encounter is missed. Ten hours of data downlinked optical in TBD minutes.
Instrument channel C	12000	18000	216000	10	20.0	2	2160	Assume first downlink encounter is missed. Ten hours of data downlinked optical in TBD minutes.
Instrument channel D	12000	18000	216000	10	20.0	2	2160	Assume first downlink encounter is missed. Ten hours of data downlinked optical in TBD minutes.
Instrument Engineering Data	0.0001	18000	0.002	1	1.0	2	0.0036	Assume first downlink encounter is missed. Ten hours of data downlinked optical in TBD minutes.

5.2.6 Mass Memory Options (See Figures 5-5 through 5-8)

Data from Spectrum Astro suggests the memory density per kg is greater for disk drive technology than for SSRs implemented with FLASH or DRAM memory. Although feature sizes for DRAM and MRAM devices may decrease as various technologies advance (see Figure 5-5). Very high density, low mass, and low power SSR may be available to meet the 2003 and 2006 mission requirements. A desirable disk drive unit may be developed by 2006 with a density factor of 1000 Gbits per kg. A design of this nature would provide 10 Tbits in a 10-kg unit dissipating about 42 watts.

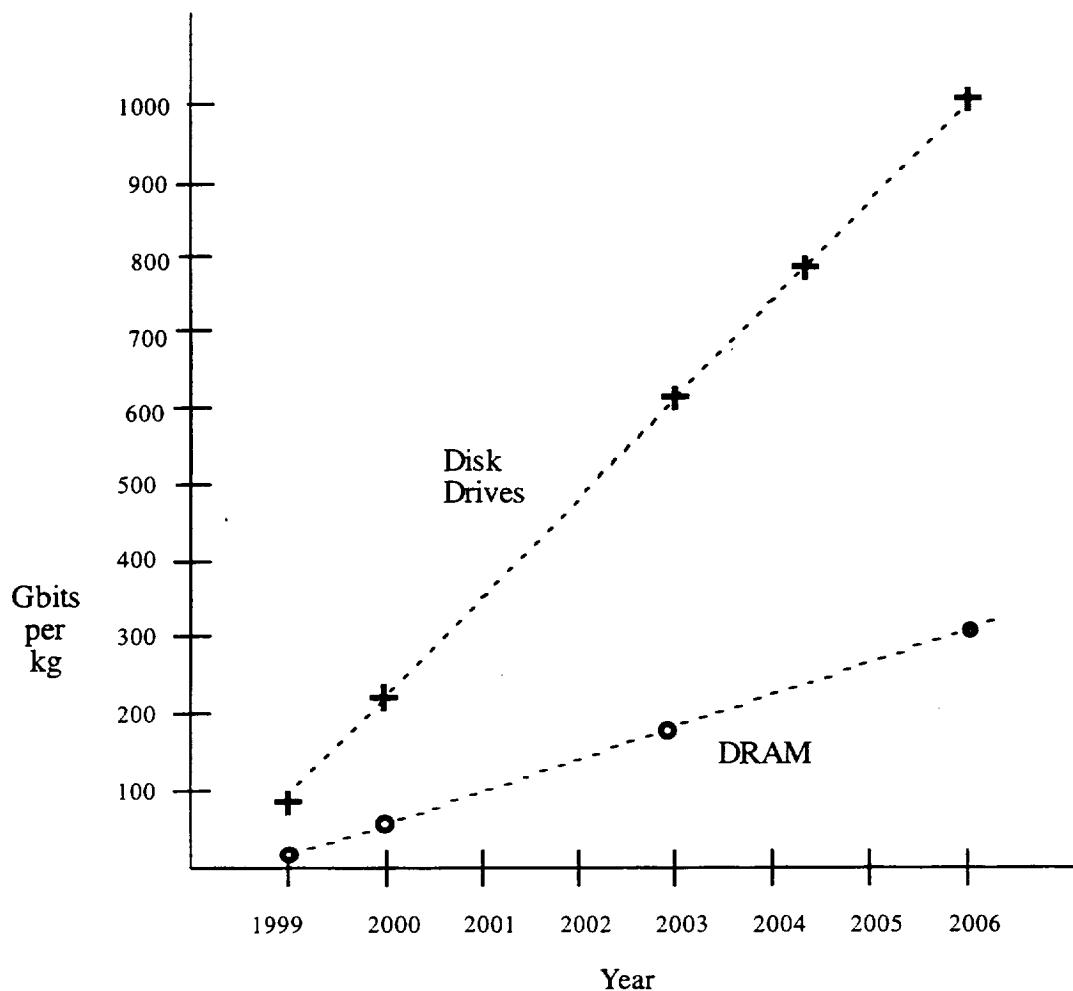


Figure 5-5. Mass memory capacity density vs. time

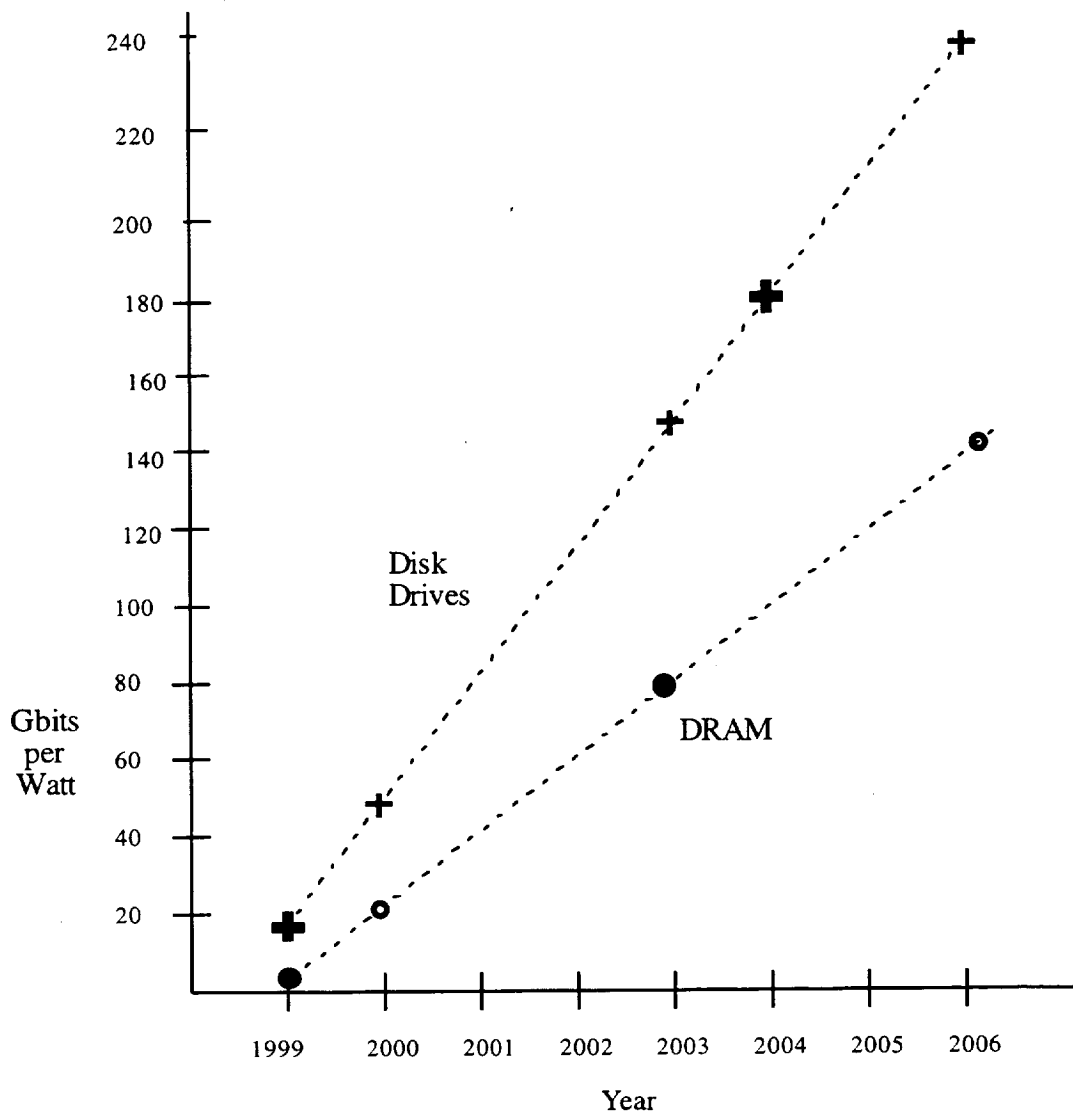


Figure 5-6. Mass memory power dissipation vs. time

5.2.7 Mass Memory Options

A 5000-MIP, 128-node processor array would meet the requirements of the 2000 mission. The design may be about 0.28 m^3 (1 cubic foot) and use considerable power. An advanced technology 4500-MIP, 64-node processor array would meet the requirement for the 2003 mission. It is questionable if a reasonable number (<200) of RISC processors could meet the needs of the 2006 mission requirements.

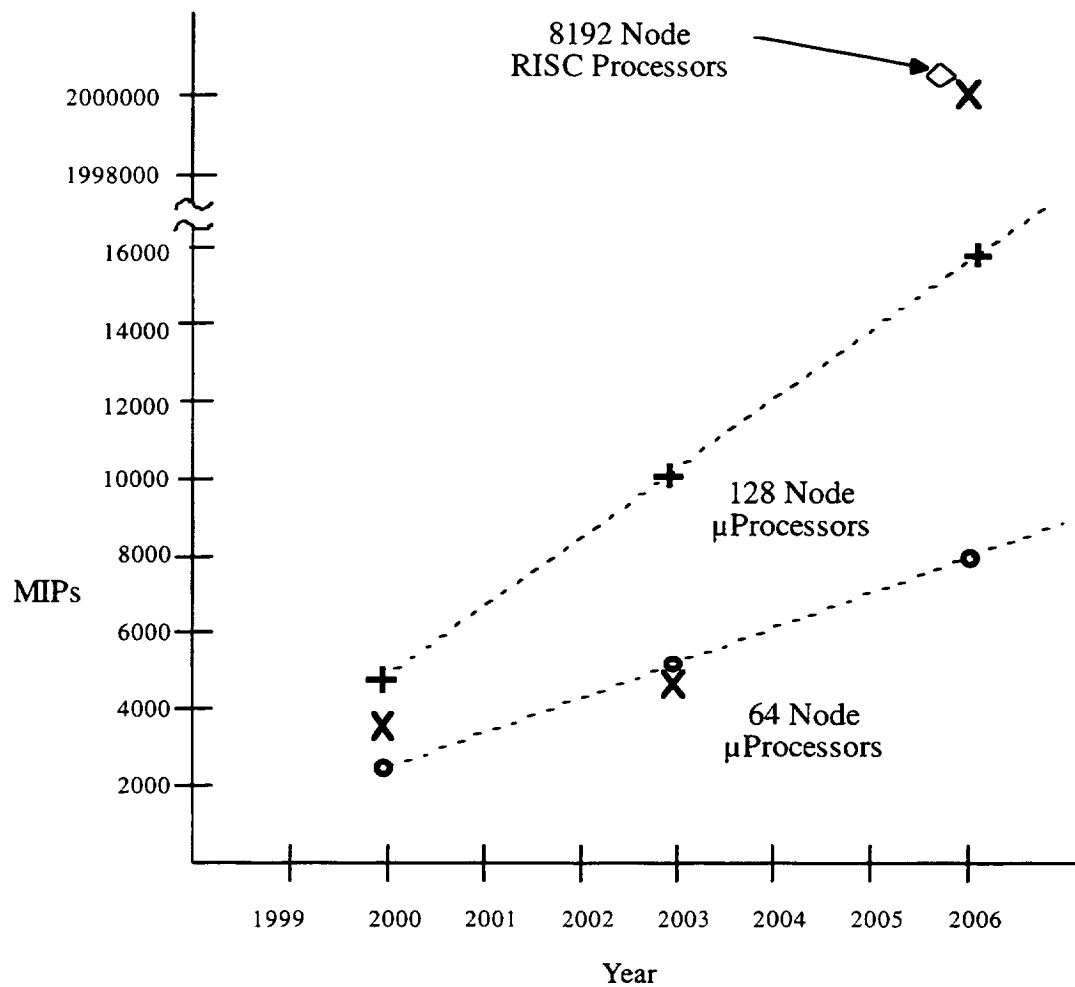


Figure 5-7. CPU MIPs capability vs. time

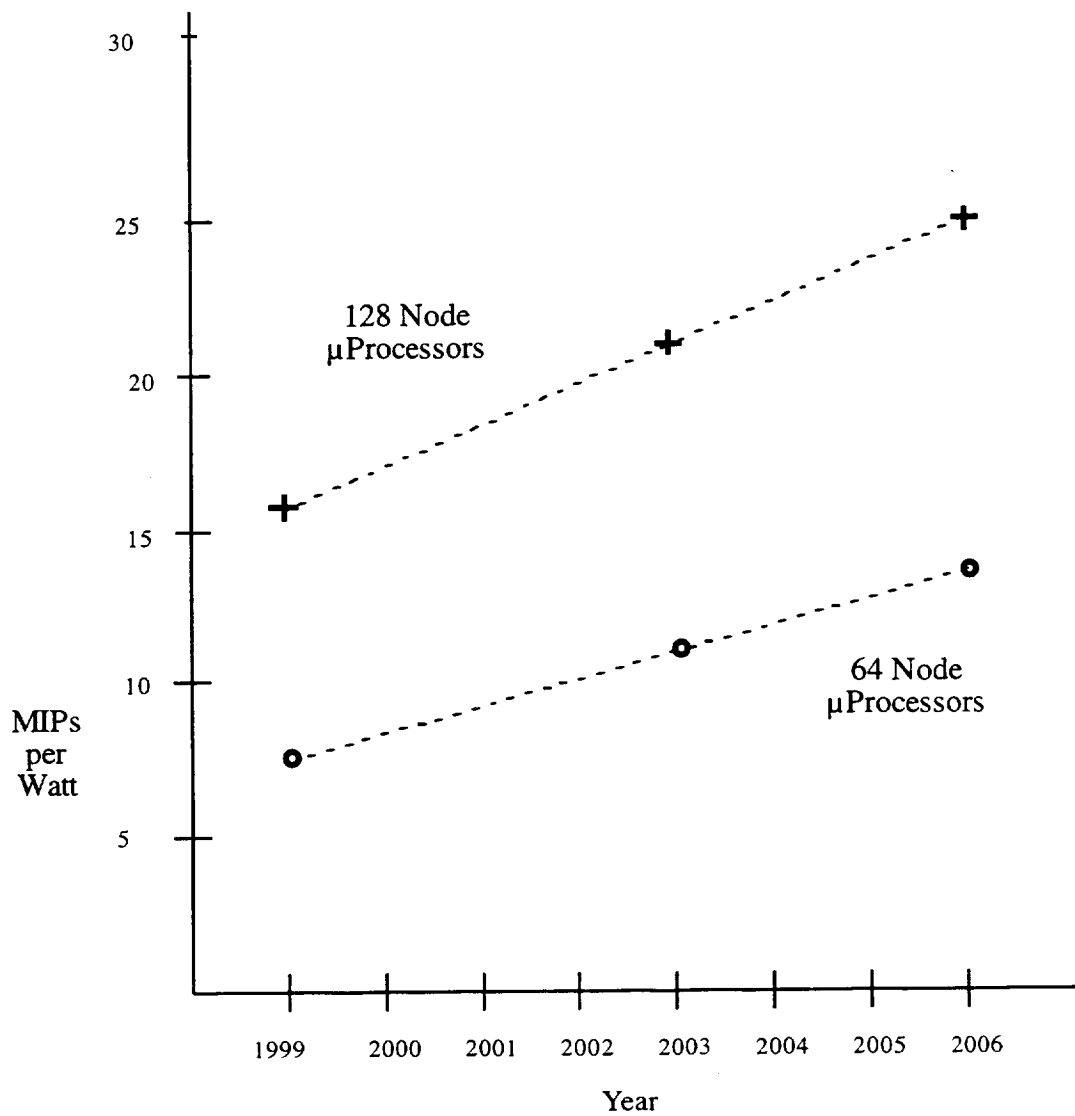
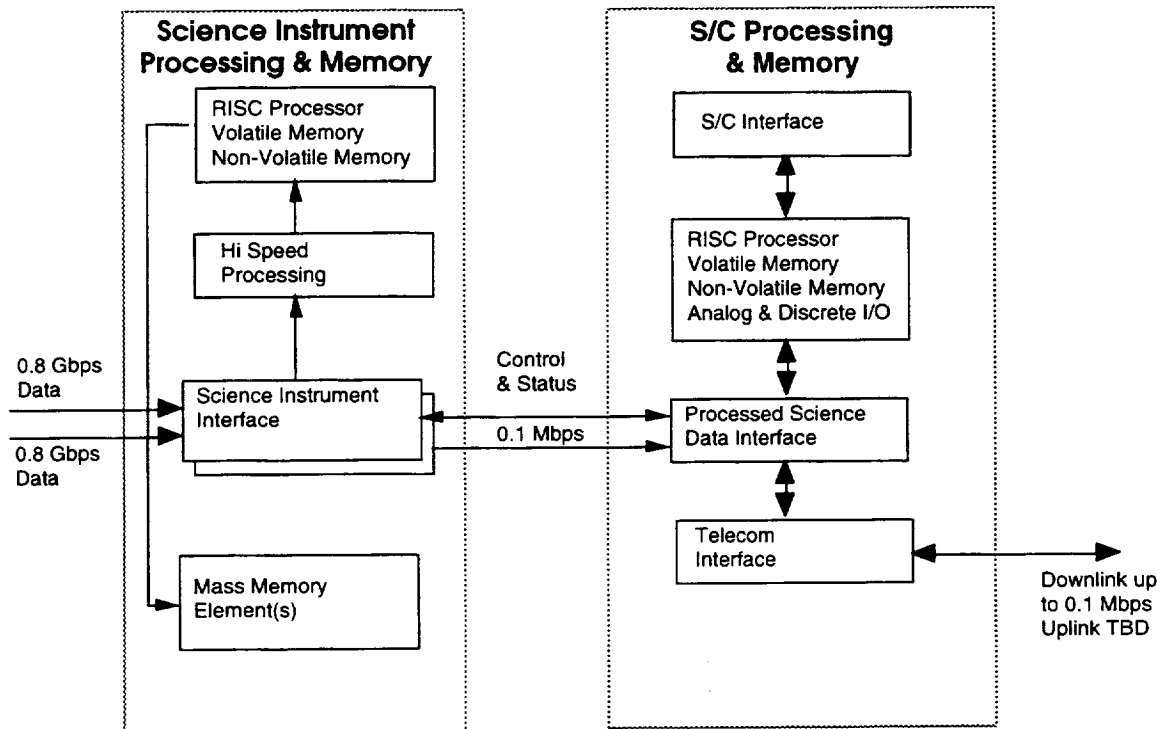


Figure 5-8. CPU power dissipation vs. time

5.2.8 HDR 2000 Architecture (See Figure 5-9)

Real-time science data is collected by high-speed optical or differential transceivers. One option is to use FireWire IEEE 1394.b channels that operate at 0.8 Gbps. A 100-Mbps FireWire IEEE 1394.a channel links the instrument memory interface to the S/C CDS for further processing and formatting before transferring the data to the telecom subsystem.

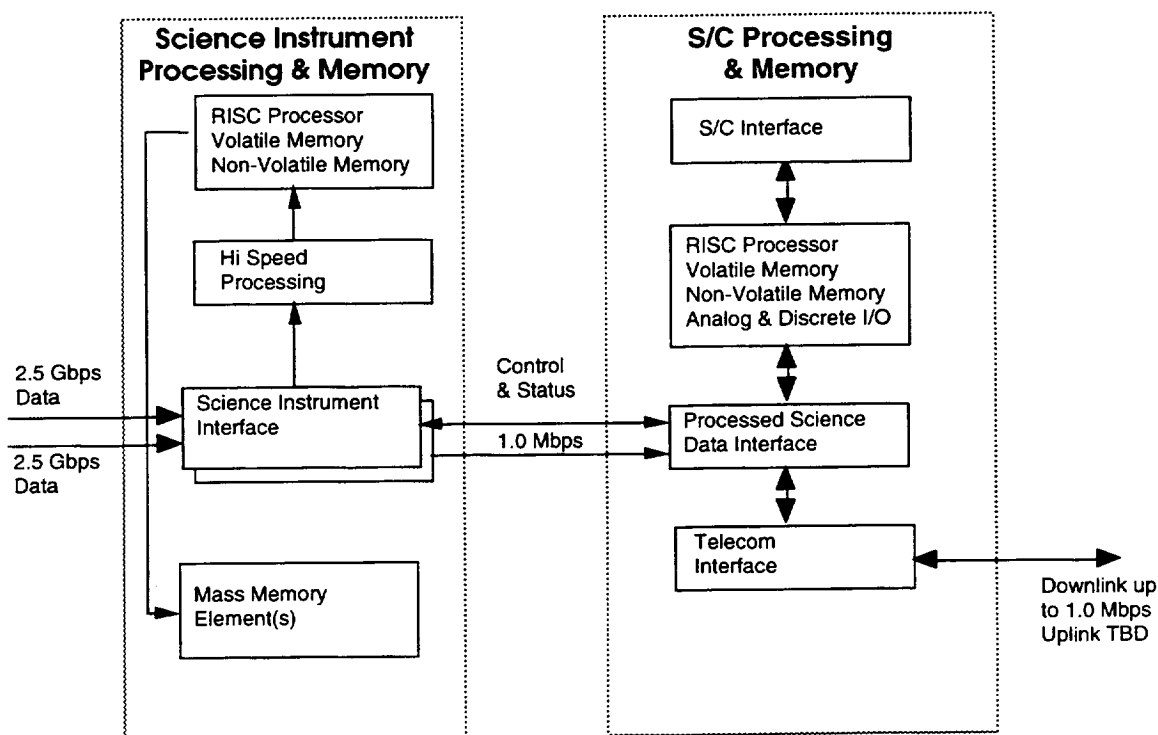


High Data Rate Instrument - 2000

Figure 5-9. High data rate instrument - 2000

5.2.9 HDR 2003 Architecture (See Figure 5-10)

Real time science data is collected by high-speed optical or differential transceivers. One option is to use FireWire IEEE 1394.b channels that operate at 2.5 Gbps. A 1-Gbps interface will link the instrument memory interface to the S/C CDS for further processing and formatting before transferring the data to the telecom subsystem.

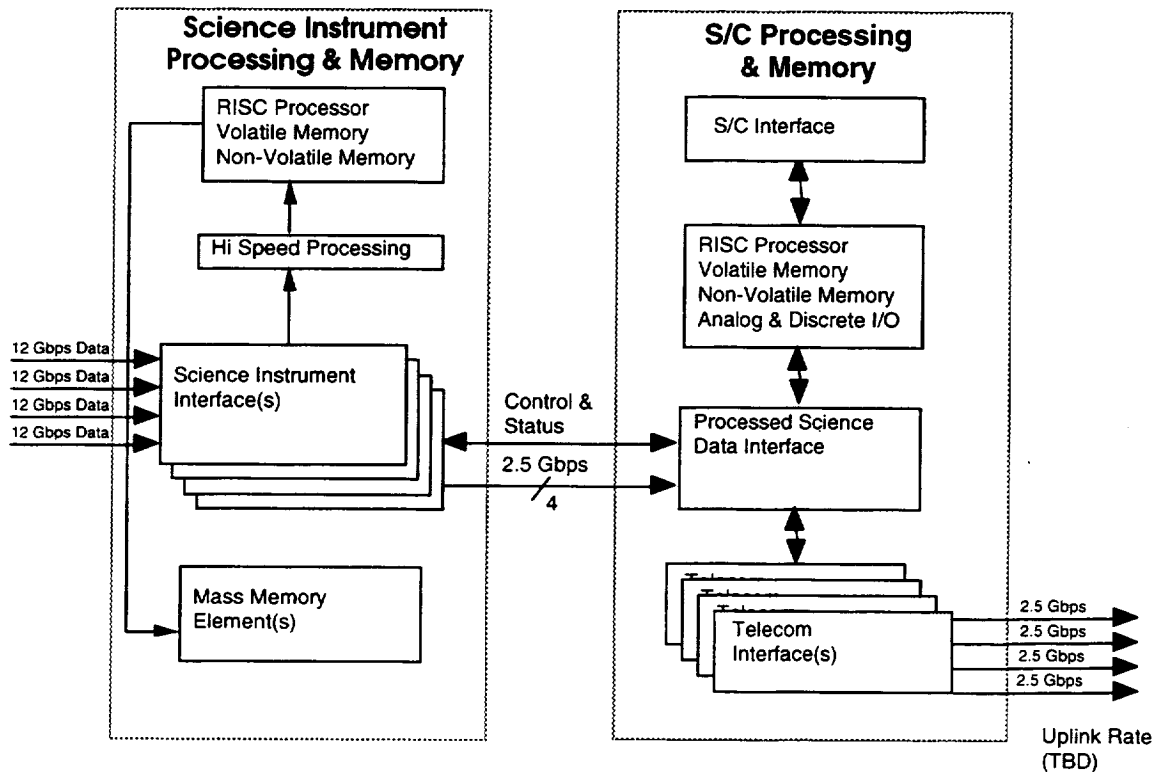


High Data Rate Instrument - 2003

Figure 5-10. High data rate instrument - 2003

5.2.10 HDR 2006 Architecture (See Figure 5-11)

Real time science data is collected by high-speed optical or differential transceivers. Each of the four high-speed channels operates as fast as 12 Gbps. Four high-speed channels transfer data from the science instrument to the S/C CDS. One option is to use four FireWire IEEE 1394.b channels. The S/C CDS will then process and format the data before transferring it to the Telecom subsystem.



High Data Rate Instrument - 2006

Figure 5-11. High data rate instrument - 2006

Each instrument CDS string will have six MCMs weighing 1 kg per string. The 0.15-cm (60-mil) tantalum enclosures will weigh 0.26 kg. The estimated TID environment inside the electronic packages is 10 krads with an RDM of one. We recommend radiation-tolerant electronic parts for this mission. Electronic components should be commercially screened devices. The selected electronic components should have SEL and SEU immunity no less than 75 MeV/mg-cm². The Power Subsystem will provide +/-15 V and +5 V supplies to the instrument CDS strings.

5.2.11 Mass, Power, and Cost Estimate Summary

The mass, power, and flight hardware recurring engineering estimates are shown in Table 5-9. The mass of the dual string instrument CDS architecture is approximately 122 kg including 0.26 kg of shielding. A single CDS string will dissipate 69 watts during science data collection. The recurring hardware cost of the dual string instrument CDS is about \$5 million.

5.2.12 Additional Information Required

In order to refine the design for mass memory, processor type, clock rate, etc., further discussions must be held on the following topics:

- Reliability
- Spacecraft clock accuracy
- Single Event Effects (SEE)

5.2.13 New Technologies Required

This estimate is based on the development of technologies to meet the mass, volume, and power values listed. The list of technologies is shown below:

- Miniaturization of flight electronics
- A flexible architecture that provides for small or no engineering development
- Development of general purpose multi-mission ground support equipment
- Development of flight multi-mission software to allow for a small amount of mission-specific code

References

1. LaBel, K. A., Gates, M. M., Moran A. K., "Commercial Microelectronics Technologies for Applications in the Satellite Radiation Environment," *1996 IEEE Aerospace Applications Conference Proceedings*, Vol. 1, pp. 375-390.
2. Barnes, C., Selva L., "Radiation Effects Review: GaAs MMIC Devices and Circuits," JPL D-13972 pp. 1 through 7, September, 1996.

Table 5-9. Mass and Power Estimates for 2000 Mission

Mission: Hyperspectral

High Data Rate Instrument Study 2000

Referenced from other cell in worksheet

Inputs from Other Subsystems

Inputs Required from You

Database/Calculated

Outputs

Don't Touch

Worksheet	Version: 3.96
Date:	4.27.98
Data Base	File Name: CDSMaster_db
Version:	2.23
Date:	10/12/98

INSTRUMENT PROCESSING WORKSHEET

Estimated by: Vince Randolph

Last Update 10.14.98

Number of CDS Strings 2

Worksheet Status

HW Requiring Cost 9.5 \$M

Estimated Workforce 3.0 \$M

Estimated Total Cost 12.4 \$M

Estimated Volume 1.0 Ltrs

Estimated RAM Req. 9.8 Mbytes

Estimated Mass 122.4 Kg

Processor Performance 250 MIPS

Calculation Function is: ON

Worksheet	Version: 3.96
Date:	4.27.98
Data Base	File Name: CDSMaster_db
Version:	2.23
Date:	10/12/98

Processor Type	Max MIPS	Availability
PowerPC750	250	2000

Technology Cutoff 2000

Unit	Mass [kg]	Power per Unit (W)	Cost (\$K) Recasting	Cost (\$K) Development	Science 1 hr	Xnat 1 hr	Cruise (incl. off) 1 hr	TCM 1 hr	Launch 3 hrs	NASA TRL	Comments	Hardware
2 Processor	122.4	44.0	5,032.0	no entry	88.0	88.0	14.8	14.8	14.8	4		
3 VME Board												
37 MCUs, 1 Gbit DRAM & Proc	0.44	12.00	800.0		5.00	5.00	3.00	3.00	3.00	2	New Slice from X2000 w/128Mbit DRAM, 128M	New Development
4 MCUs, 10 Mbytes FR Code	0.58	10.00	152.0		2.00	2.00	1.00	1.00	1.00	3	TRW DS1 Development, formerly incorrectly si	DS1
2 MCUs												
36 MCUs	0.34	0.80	200.0		0.50	0.50	0.50	0.50	0.50	2	New MCM, I2C has self contained protocol	New Development
41 MCUs, CDS IF	0.50	7.00	200.0		3.50	3.50	0.10	0.10	0.10	2	New bus developed by DSST, One node; IEEE	New Development
39 MCUs, Instrument IF Format	0.12	1.62	40.0		1.00	1.00	0.10	0.10	0.10	9	(Preliminary) 3.3, 2.5 volt, Honeywell, typical P;	New Development
39 MCUs, CDS IF Format	0.12	1.62	40.0		1.00	1.00	0.10	0.10	0.10	9	(Preliminary) 3.3, 2.5 volt, Honeywell, typical P;	New Development
2 MCUs												
2 MCUs												
2 MCUs												
9 On board Disk Memory	120.00	55.00	3,600.0		55.00	55.00	10.00	10.00	10.00	4	\$200k NRE, 1 Gbps ECL read/write interface	EDMM-2
3 Solid State Memory												
3 Remote Engineering Unit												
Shielding (kg)												
10 Krad/s TID behind 60 mils of Aluminum	0.28											

Estimated Subsystem Cost (\$M FY97)

12.4

6 MCUs per CDS String

5.3 Data Compression vs. Raw Data Downlink

Data compression provides increased science return from missions operating over constrained communication channels. The benefits of compression can be enormous when measured in terms of the equivalent power savings in dB to transmit a fixed volume of source data. Compression will be required for most imaging missions in the near future, together with simple screening and windowing methods to select the most relevant data, and with strategies to keep the onboard buffer full of the highest priority data at all times. In the longer range, feature extraction schemes and onboard data analysis methods could provide orders-of-magnitude reduction in downlink rate requirements.

There are always fundamental bottlenecks imposed by the spacecraft's limited onboard storage and communication downlink capabilities. Spaceborne scientific instruments have the capability to collect vastly greater volumes of data than can be transmitted to Earth. There are two fundamental limits that restrict the amount of scientific data that ever reaches Earth: (1) the sustainable downlink data rate and (2) the spacecraft's onboard data storage capacity. Currently, scientists are forced to employ crude strategies to stay within these limits, because there are no tools available for simultaneously optimizing the use of these two scarce resources. For future missions it will be essential to organize and optimize the entire process of collecting, storing, and transmitting scientific data in a way that utilizes these two scarce resources as much as possible.

5.3.1 Possible Compression Techniques:

- 1) "Compression" by Refusing to Collect More Data. One strategy currently used by scientists to stay within the limits of downlink resources is to simply stop collecting data that would exceed the communication capability. However, when scientists employ this strategy, they get only one opportunity to draw the line between data sufficiently valuable for sending to Earth and data not valuable enough to collect. They risk committing their resources to collecting data that may prove to be less valuable than they had expected. Conversely, if the collected data could be held in a buffer while the scientists take a quick look at some of it, they might be able to dynamically adjust their valuation of the residual data not yet transmitted. This opens the possibility of replacing devalued data with new, higher-valued data that would otherwise not be collected.
- 2) Lossless Compression. Lossless compression algorithms allow the source data to be reconstructed perfectly. Thus, lossless compression is acceptable in principle for all science data. A lossless compression ratio of 2:1 has the effect of improving the downlink communication capability by a factor of 2 (3 dB) without sacrificing any data quality.

However, lossless compression also has some serious limitations.

- a) General-purpose lossless compression typically cannot achieve higher compression ratios than 2:1 or 3:1 except for source data with low information density, such as black sky.
- b) Lossless compression ratios are *never precisely predictable in advance*, so there is always a problem with estimating how much source data can be squeezed into the available communication downlink. Guessing too low means that the link is not fully utilized, whereas guessing too high causes some data to be truncated. Either way, the lossless-in-principle algorithm can become a partially lossy algorithm due to this effect.
- c) When lossless compressed data is corrupted by errors due to channel noise, the source data can no longer be reconstructed perfectly, and in fact *errors can propagate* to locations far from the location of the channel errors. This necessitates the introduction

of error-containment strategies, which complicate the overall compression algorithm and detract slightly from the overall compression performance.

- d) There is always a tradeoff between the effectiveness of the algorithm and the *complexity* of its implementation. This is a particularly important consideration for high-speed implementation onboard a spacecraft.

- 3) *Lossy Compression*. To achieve the most significant gains, we must employ so-called “lossy” compression techniques, which allow an intelligent tradeoff between source fidelity and compression ratio. Lossy compression shares features (b), (c) and (d) of lossless compression (see above). However, it allows for significantly higher compression ratios.

Lossy compression offers the greatest potential gains. However, it is necessary to work with scientists in order to arrive at a compression strategy that gives the largest science value return.

Figure 5-12 illustrates a typical simplified scenario in which lossy compression gives substantial gains. The assumptions used in the figure are:

- Europa's radius = 1569 km
- Area = $3 \times 10^{13} \text{ m}^2$
- 100 m resolution
- Full coverage = 3×10^9 (10-bit pixels) = 3000 (1000x1000 images) = 3×10^{10} (bits)

Figure 5-13 shows possible experiments to help determine the value of losslessly compressed images.

Figure 5-14 summarizes the two proposed compression modules: lossless and lossy.

4. *Progressive Compression*. Progressive compression provides a *bridge* between lossy and lossless compression methods. Progressive or hierarchical compression techniques not only compress the data but also partition the compressed data into ordered, hierarchical segments. Each compressed segment, when combined with the previous segments, allows for reconstruction of successively higher fidelity versions of the data. Successive data segments provide diminishing marginal improvements in fidelity as measured according to a distortion metric such as mean squared error. The initial version of the reconstruction is very lossy, whereas the final reconstruction can in principle be lossless or nearly lossless. The scientist end-user can select any amount of desired fidelity between these two extremes, depending on the *marginal science value* of the compressed bits that must be transmitted for each successively improved reconstruction.

A good progressive algorithm compresses and partitions the data into ordered segments with rapidly diminishing marginal value to the scientist. This ensures that the highest-fidelity reconstructions are obtained for any given compressed data volume stored and transmitted.

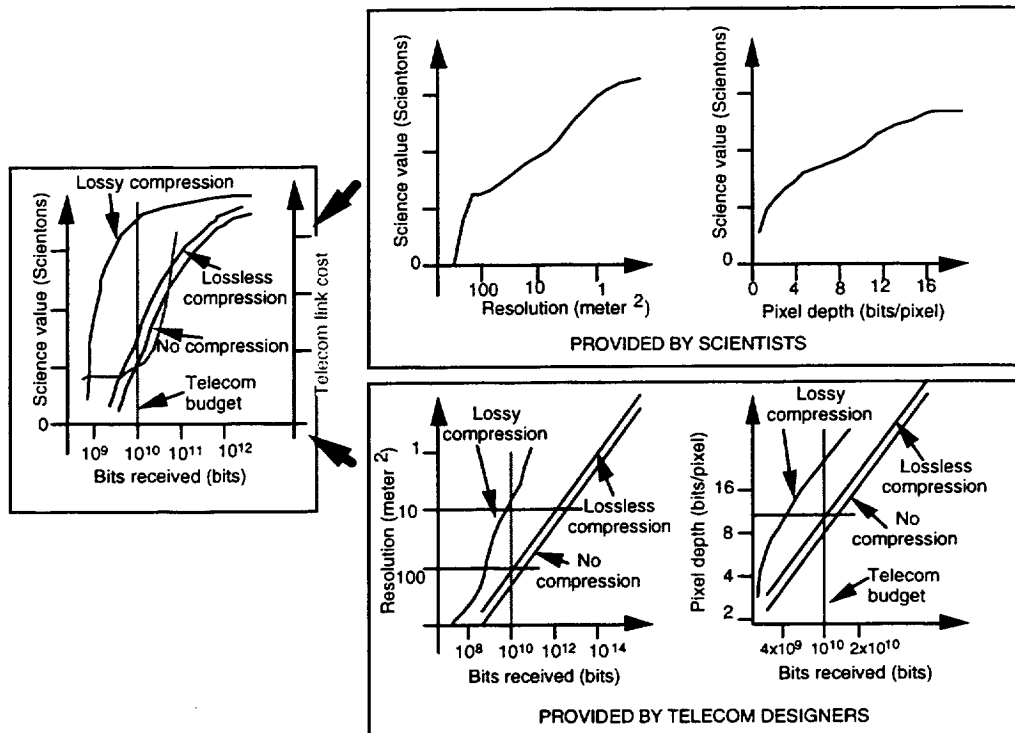


Figure 5-12. Rationale for choosing data compression.

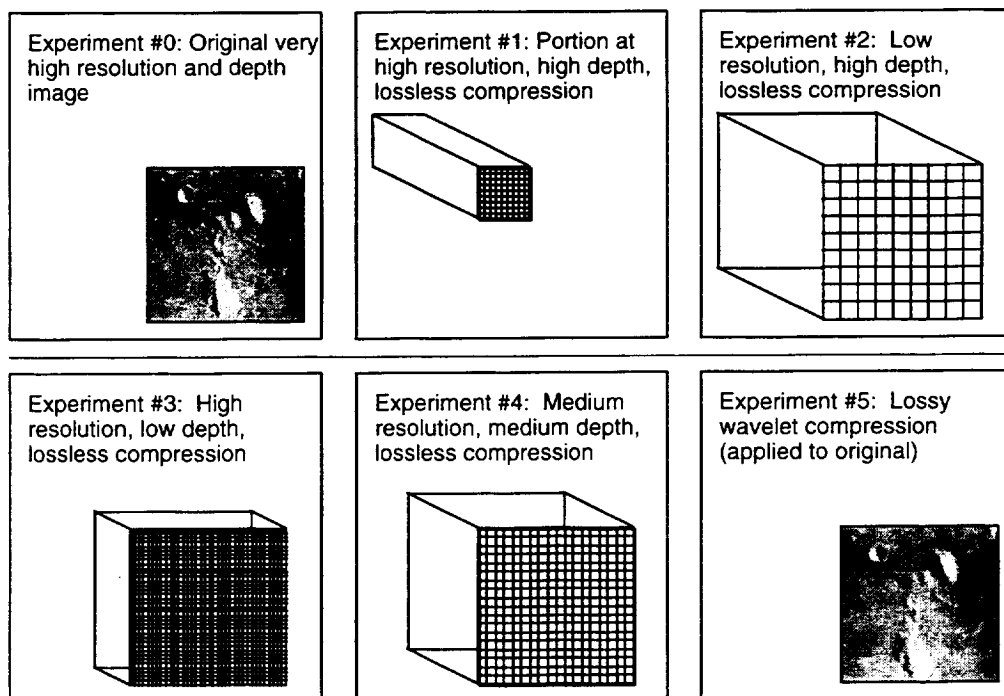


Figure 5-13. Experiments for scientists' evaluation

(a) Lossless Compression

- General-purpose lossless compression typically cannot achieve higher compression ratios than 2:1 or 3:1 except for source data with low information density, such as black sky
- Lossless compression ratios are never precisely predictable in advance, so there is always a problem with estimating how much source data can be squeezed into the available communication downlink.
- When lossless compressed data is corrupted by errors due to channel noise, the source data can no longer be reconstructed perfectly, and in fact errors can propagate to locations far from the location of the channel errors.
- There is always a tradeoff between the effectiveness of the algorithm and the complexity of its implementation. This is a particularly important consideration for high speed implementation onboard a spacecraft.

(b) High Compression Module ("Lossy")

- compression ratios:
 - typically very high quality images at 5:1 or higher
 - higher compression ratios with "acceptable" distortion
 - no upper limit (depends on downlink constraint and amount of original data measured)
- for originally analog data:
 - "no detectable distortion" at the lowest compression ratios
 - achieves much higher compression ratios than "lossless" when required to produce minimal distortion
 - losses similar to data pruning when applied to massively overcollected amounts of data
 - allows scientists to efficiently trade off distortion and pruning considerations when subject to downlink constraints on total data volume
 - requires collaboration between scientists and compression algorithmists to develop, select and apply appropriate algorithms

Figure 5-14. Two proposed compression modules: (a) lossless; (b) Lossy

Progressive compression techniques have been developed for Earthbound applications. The basic principles of these applications are simple: a) store all the data you might ever want to look at; b) retrieve only the data you need currently, to the level of detail and fidelity that you require; and c) use progressive compression to make this process efficient. However, spaceborne applications differ from earthbound applications in one important respect: on Earth there is unlimited archival storage, so valuable data never needs to be thrown away. In contrast, finite spaceborne storage resources will always force scientists to decide what data to keep and what data to throw away (or never collect). Therefore, progressive compression techniques for spaceborne applications must be developed to minimize the scientists' pain when they are confronted with the inevitable buffer overflows. There are also challenges in reducing the complexity of Earthbound progressive compression techniques to make them suitable for implementation onboard a spacecraft.

Figure 5-15 shows the key metrics that should be used in evaluating data compression advantages.

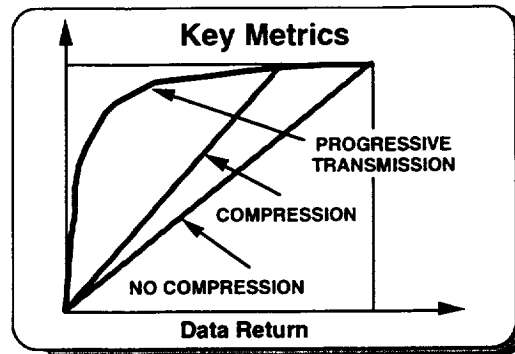


Figure 5-15. Key metrics

5. *Integrated Progressive Compression and Buffer Management.* Progressive data compression methods can make efficient use of a finite onboard buffer and a limited communications downlink by packing and parsing the science data into hierarchical data segments. These hierarchical data segments can be assigned transmission priorities and science values using criteria defined by the end users (i.e., the scientists). Then an integrated data compression and buffer management scheme can ensure that the highest priority data segments are always transmitted first, and only the least valuable data segments are ever discarded. The onboard buffer will be kept constantly full of data that falls between these two extremes; i.e., not important enough to transmit right away but still valuable enough to keep. Data held in this “data limbo” will eventually either be transmitted or discarded, depending on the relative priority and volume of the new data flowing into the buffer.

The strategy for maximizing the finite buffer’s usefulness is to keep it constantly full and overflowing! Newly collected data will always displace older data in the buffer that is either transmitted to Earth or overwritten. Because the downlink data rate is assumed to be the primary bottleneck in the system, the scientists will always face tough choices — either slow down the rate of collecting new data or discard some data already in the buffer. However, by using these compression and buffer-management techniques, the scientists will have maximum flexibility in making these choices. All the data residing in the buffer will be packed and parsed efficiently into multiple segments using progressive compression methods. Each data segment in the buffer (as well as the newly collected data) will be tagged with indicators of its residual science value and its priority for transmission to Earth. As new data arrives, we can apply a simple rule for temporarily creating space in the buffer — always transmit the highest priority data segments and throw away the least valuable data segments.

This scheme would provide the scientists with tools to make wise choices that maximize the overall science value returned to Earth despite the constraints imposed by the spacecraft’s finite storage capacity and limited data rate. All data is compacted and parsed into prioritized data segments using progressive methods. The transmission priorities and science values of the data segments are established by the scientists according to any criteria they desire, and thus the scientists will retain complete control over which data or portions of data are collected, transmitted, or discarded. This scheme enables them to make these decisions without sacrificing substantial portions of the scarce resources to

idleness. Furthermore, the scientists will reap the benefits of efficient data compression throughout the data handling process. This effectively multiplies the limited capacities of both the communication downlink and the onboard storage, and thus yields the best utilization of both scarce resources.

6. *Error Containment.* One of the primary difficulties in using an off-the-shelf compression technique on a spacecraft is that commercial algorithms are intended for computer storage or channels with negligible error rates. In deep space environments, where the error rate is not negligible, a single bit error on a compressed data stream can corrupt all of the subsequent compressed data.

The current use of sync markers, chosen independently of the data, leaves room for improvement. More flexible strategies allow better tradeoff between the degree of error containment and the rate at which data are transmitted.

5.3.2 Current state-of-the-art in high-speed data compression - Examples

- Lossless (Market is driven by compression for storage devices)
 - 30 Mbytes/s - Advanced Hardware Architectures, Inc., single chip CMOS VLSI. Similar speeds can be obtained with the RICE compression chip developed at Goddard
 - 40 Mbytes/s - ALDC1-40S-M IBM Proprietary lossless ALDC Compression Algorithm
 - ⇒ Assuming 2:1 average compression ratio, this can compress a 320 Mbit/s instrument rate to a 160 Mbit/s downlink rate
- Lossy (Market is driven by video compression for digital TV)
 - 10Mbytes/s (input rate) Analog Devices ADV601 Wavelet Video Compression
 - 50 Mbit/s (compressed data rate) IBM 39MPEGS422 PBA17C MPEG2 Video Compression
 - ⇒ Assuming 20:1 compression ratio, this can support a 1Gbit/s instrument rate on a 50 Mbit/s downlink
- For accurate prediction of compression ratios it is necessary to have detailed information on source statistics
- For lossy compression, it is necessary to have user agreement on tolerable distortions
- Data compression needs very low bit error rates on the channel: 10^{-6} or better. This implies the use of channel coding
 - Decoders at 100Mbps or higher are a challenge
 - Only very simple codes can be used
 - High level modulation schemes may be necessary to conserve bandwidth (for RF transmission)
- Conclusions:
 - 100 Mbit/s compression is feasible now for some sources
 - 1Gbit/s compression may be feasible by parallel processing
 - 10 Gbit/s compression is very challenging, even by 2006

6. TELECOMMUNICATIONS

6.1 Introduction

This section of the HDR report describes the telecommunications systems and strategies for delivering instrument data from a 700 km polar orbiting satellite to ground stations at data rates of 0.1 Gbps, 1 Gbps, and 10 Gbps. It includes a description of the RF and optical subsystems that would support these data rates for technology freeze dates of 2000, 2003, and 2006. Recommendations on bandwidth allocation made at the 18th meeting of the Space Frequency Coordination Group (SFCG) in September 1998, Kyoto, Japan, allocated 50 MHz of spectrum at X-band and 1.5 GHz at Ka-band for Earth science missions.

Aggressive 16 QAM bandwidth efficient modulation schemes can support up to 3.2 bits per Hz of allocated X-band spectrum on each polarization state. Thus, the maximum data rate that can be supported by the X-band link is 320 Mbps. (Assuming that this technology is applied to Ka-band with similar efficiency, Ka-band would then support 4.8 Gbps on each polarization. However, this is an aggressive and unproven scheme and is not expected to be material for the earlier phases of the study.) A design for an optical GEO relay satellite is also described. The relay configuration provides a higher instrument data rate throughput for a fewer number of ground stations. In addition, the effects of cloud cover are mitigated. Telecommunications protocols for these high data rates are not covered in this report.

For the 10 Gbps downlink data rates, X-band is not envisioned to be viable, leaving Ka-band and optical communications as the only workable alternatives. At 10 Gbps the data are multiplexed onto four optical carrier wavelengths around 1550 nm, consistent with the standards defined for terrestrial links. Wavelength division multiplexing (WDM) allows high data rates to be achieved with the larger 50-70 micron detectors that mitigate the effects of spot size blurring due to atmosphere-induced aberrations. W-band links were not explored at this time—the technology is not mature compared with X-band and Ka-band links.

Data storage and distribution approaches are also discussed in this section of the report. For continental US (CONUS) based stations, the strategy would be to infuse the metadata with the downlinked data, store it on tape, and distribute it by way of the high speed OC-12 or OC-48 fiber-optic wide area network (WAN). From non-CONUS stations, both the downlinked and infused metadata will be stored on tape and shipped to a central facility for preprocessing and subsequent distribution.

6.1.1 Assumptions

The four key assumptions that were made for the RF and optical telecommunications analysis are italicized below. Assumptions are elaborated on in the paragraphs that follow.

Specified data rates include the required overhead for telecommunications protocols.

- *RF ground stations located at Fairbanks, Alaska and Svalbard, Norway will have the capability to support the high-data-rate links.*

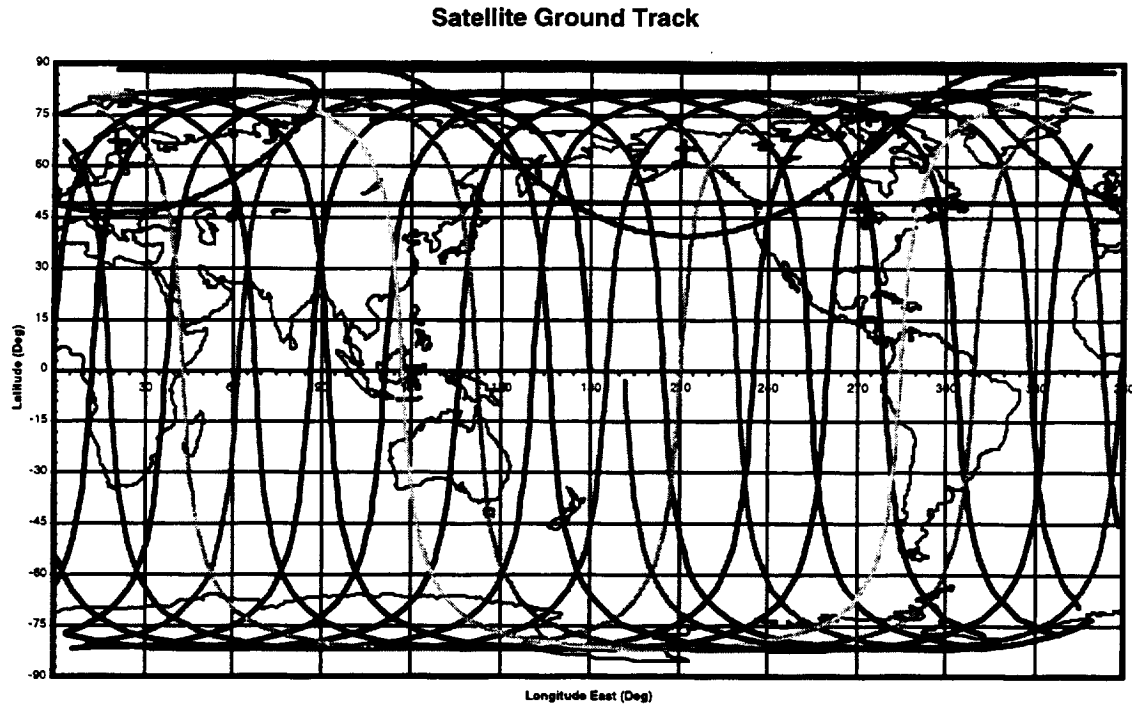


Figure 6-1. Satellite ground track shows that a high latitude RF ground station affords downlink opportunities on every pass

Figure 6-1 shows that existing high latitude locations afford accessibility on every pass. Neither facility currently has K-band capability, however, with the requisite facility upgrades these stations are expected to be able to support Ka-band telecommunications. The link analysis presented here assumes that Ka-band antennas are designed for low loss (5.5 dB). Ka-band ground antenna and receiver costs are not included.

- *A global network of five low-latitude optical ground stations will be available to support the link. Three are primary receivers and are located on US soil. Two others are located in the Canary Islands and at Mt. Stromlo, Australia.*

Although the lower latitude locations resulted in fewer passes per station in any 48-hour period, they typically have less cloud cover than the high latitude locales, and are hence more available to support optical links. The stations and their locations are given in Table 6-1 and also shown in Figure 6-2. Also shown in the table are the locations of two non-US stations that can serve as emergency backup sites for the mission: the Orroral Range in Canberra, Australia, and the European Space Agency's 1-m telescope in the Canary Islands. The Australian Mt. Stromlo facility is baselined as the receiver and replaces the previously proposed, NASA-owned Orroral Range facility that has routinely supported the NASA satellite ranging program. Current NASA and Australian plans call for the Orroral Range to be decommissioned in late 1998.

Two of the US stations are located at sites where existing telescopes can track the satellite. The third station is located at Table Mountain Observatory (TMF) in California, where current plans call for constructing an Optical Communications Telescope Laboratory (OCTL) with a 1-m telescope capable of tracking satellites as low as 250 km in time to support demonstrations in 2001.

Table 6-1. Location, weather availability, and mean pass duration of ground stations with tracking capability to support laser communications experiments in year 2000

Station	Location	Aperture	Weather Availability %	Mean pass Duration 1/2000
NASA/JPL TMF, OCTL	34°N Lat, 117° W Long.	1-m	70	315
Mt. Stromlo Canberra, Aus	35° S Lat, 150° E Long.	0.75-m	60	318
AFRL AMOS Maui, HI	20°N Lat, 156° W Long.	1.2-m & 1.6-m	70	325
ESA Tenirife, Canary Islands	28°N Lat, 18° W Long.	1-m	70	302
MIT Lincoln Labs Firepond	42°N Lat, 71°W Long	1.2-m	40	317

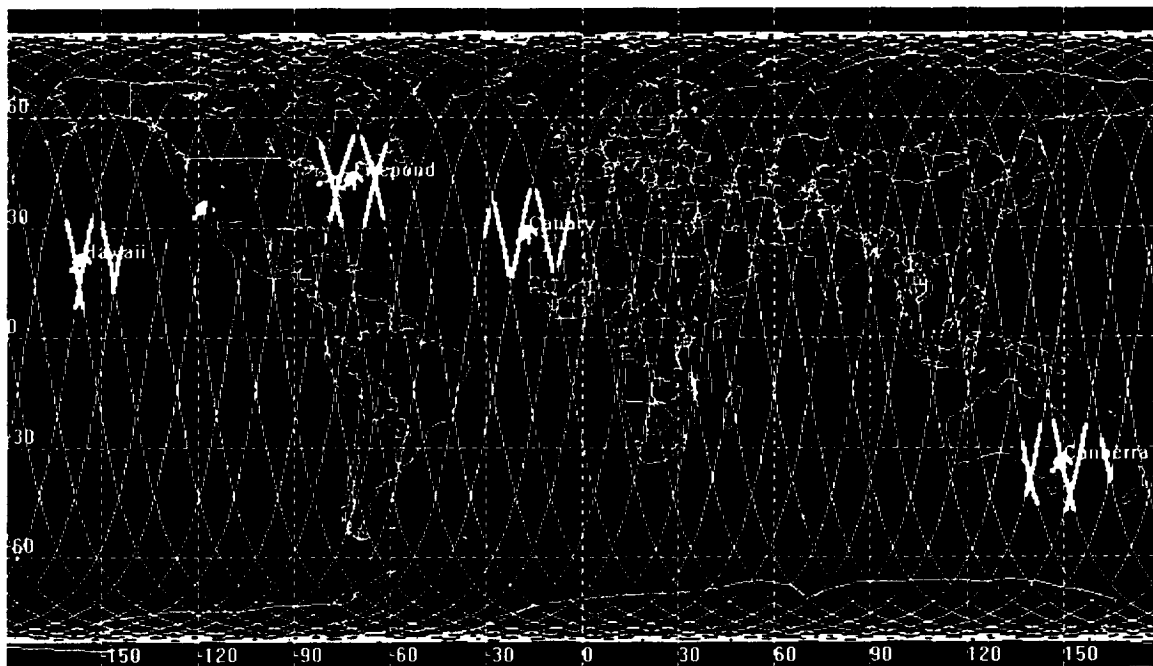


Figure 6-2. Satellite ground track showing the five optical downlink stations. The link between the satellite and the ground station is established between zero and two times per pass

- *The instruments gathered data at the full capacity over land. No data are acquired over the oceans.*

The data are stored on-board and transmitted to the ground stations when they come into view. Figures 6-3 and 6-4 show the data flow through the solid state recorder (SSR) over a 48 hour period for the maximum data rates of the RF and optical communications architectures in year 2000; i.e., 1 Gbps for the RF and 10 Gbps for the optical links. Figure 6-3 shows that a maximum instrument rate of 350 Mbps can be supported without compression or intelligent data extraction using the two RF ground stations. Figure 6-4 shows the downlink to the three US optical stations listed in Table 6-1 will support an instrument data rate of 750 Mbps without compression or intelligent data extraction. For the five stations shown in Table 6-1, the supportable instrument data rate prior to compression and intelligent data extraction is 1.3 Gbps.

1.0 Gb/s D/L, 2 hi-lat sta, 700km alt, 98 deg, All Land Imaged

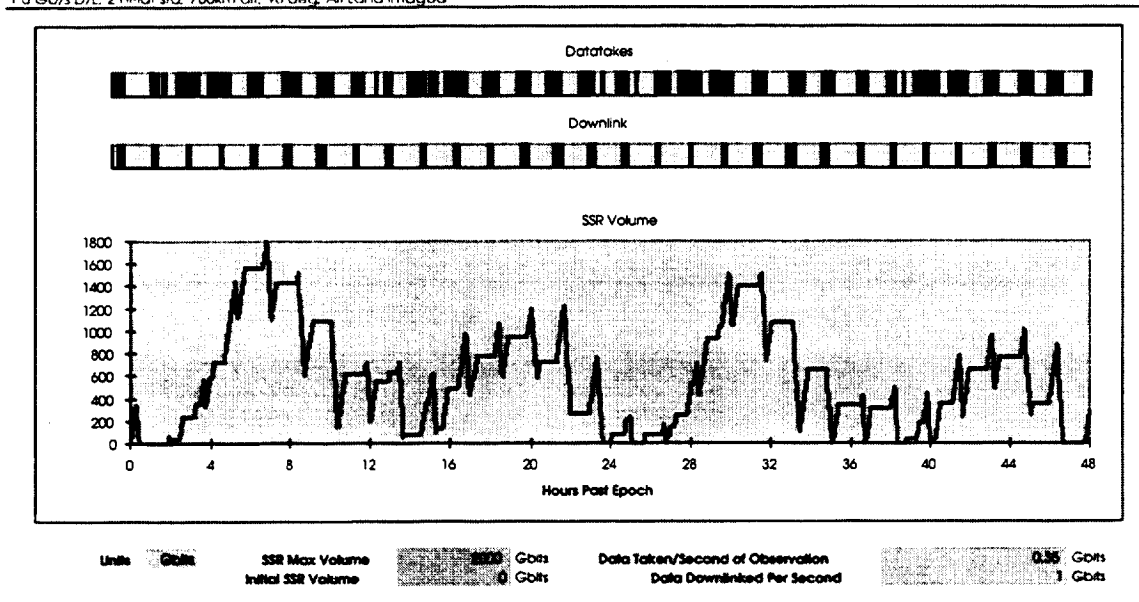


Figure 6-3. SSR data flow over 48 hours for RF downlink at 1 Gbps

The results clearly show that the low number and locations of ground stations preclude taking full advantage of the optical communications capability. There are, however, other laser ground stations, such as the Goddard SLR network, that can potentially provide a solution by year 2003. Goddard's satellite laser ranging (SLR) program has nine laser transceiver stations around the globe in locations such as Peru (25 cm aperture) and Tahiti (75 cm aperture), with plans to expand into South Africa (75 cm aperture) and Argentina (25 cm aperture). Although these systems are fully committed to laser ranging, they do possibly offer a solution to the problem of too few ground stations at the lower latitudes. Goddard is currently designing the new, autonomous operation SLR 2000 stations. These stations will be acquiring and tracking targeted Earth orbiting satellites and recording the data for future retrieval. The Goddard SLR network stations have not been included in this study, although it is recognized that they potentially offer a solution to the need for more optical ground stations.

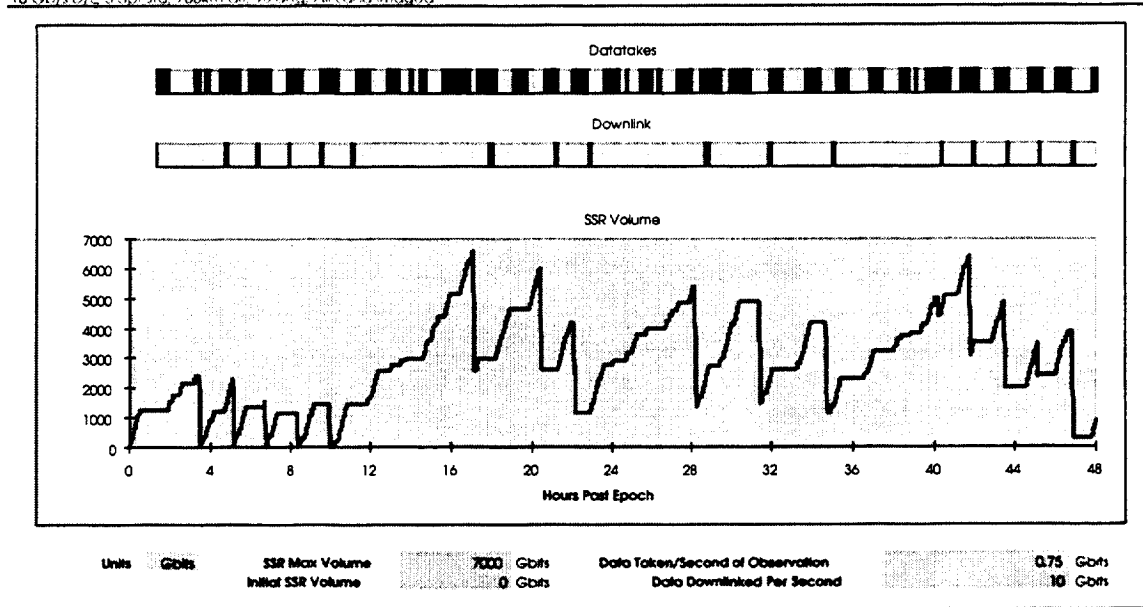


Figure 6-4. Forty-eight hour SSR loading profile for 10 Gbps downlink with three US ground stations

6.2. LEO-to-Ground Downlink

6.2.1 Spacecraft RF Transmitter

The Low Earth Orbiter spacecraft will orbit the Earth at an altitude of 700 km in a circular polar orbit inclined at 98°. The spacecraft will take Radar, Lidar and Hyperspectral data of Earth at various levels of resolution and transmit these data to ground stations. The telecommunications data rates considered were 0.1, 1.0, 10.0 Gbps and are denoted as Case 1, Case 2, and Case 3, respectively. Table 6-2 summarizes the RF telecommunications capabilities needed to meet the required data rates in the study's time frame. As the Table shows, neither X-band nor Ka-band RF telecommunications could support 10 Gbps data rates by years 2000, 2003, 2006. Thus Case 3 was eliminated. In all cases the ground stations were assumed to be the 11.3-m antenna at the Alaska synthetic aperture facility (SAR) and a similar aperture antenna at Svalbard, Norway.

Table 6-2. Summary of X-band and Ka-band capabilities needed to meet required telecommunications data rates in years 2000, 2003, and 2006. The 50 MHz X-band spectrum allocation limits the achievable data rate at this frequency to less than 1 Gbps

RF Telecomm	Year		
	2000	2003	2006
Case 1 - 0.1 Gbps			
X/Ka-bands	Yes	Yes	Yes
Case 2 - 1.0 Gbps			
X-band (limited by spectrum allocation)	No	No	No
Ka-band	Yes	Yes	Yes
Case 3 - 10 Gbps			
X-band	No	No	No
Ka-band	No	No	Yes

Case 1

Case 1 considered two different links. First, the X-band command uplink and the downlink of spacecraft health, and second, the X-band downlink of the stored data. Since the uplink data rate is relatively low, the use of coding would be dictated by the mission's needs. The cases for coding and no coding are given in cases 1.1 and 1.2 below for an omni antenna and in case 1.3 for a phased array. The omni is a low-cost option which, like the phased array, obviates the need to articulate the antenna. The omni option is considered the optimum solution for the low rate links where there is enough RF power available to satisfy the required data and carrier margins.

Case 1.1 No Coding, Omni Antenna

Case 1.1 baselines the Cincinnati Electronics (CE) transmitter, which will be available in 1999 and can be used with an omni antenna (3 dB beam width of 129°) to support up to 160 Mbps. Table 6-3 gives a summary for this X-band link, including losses and gains assumed for the link. The results show that for the baselined minimum margins of 3 dB for data and 6 dB for the carrier, this design can support 100 Mbps. The maximum visibility for this system is about 12 minutes and occurs when the spacecraft passes through the zenith of the ground station. For both stations, the visibility during a 24 hour period is about 150 to 180 minutes, i.e., all the orbits, 15 orbits per day. The transmitted RF power is about 38 W. The CE transmitter will radiate 3 Watts RF. A solid state power amplifier (SSPA) with 35 Watts RF output capability will be needed to support the link.

Case 1.2 Omni Antenna, Viterbi and Reed-Solomon Coding

In this option, the Quickbird X-band transmitter with two channels, capable of supporting up to 160 Mbps per channel for a total transmitted data rate of 320 Msps (mega symbols per second) is baselined (see Figure 6-5). The Quickbird transmitter will be available by 1999, along with an omni antenna. The 3 dB beam width is about 129°. Telecommunications Table 6-3 is the X-

band link budget for this case, with all the assumptions in terms of the losses and gains assumed for the link. The table shows that for the system to support 100 Mbps with coding, (i.e., 229 Msps of data rate after coding) the use of Viterbi coding (rate 1/2 and constraint length of 7) concatenated with Reed-Solomon coding is required. This maximizes the data rate for a given capacity of the transmitting equipment. Also, the choice of an omni-directional antenna on the spacecraft avoids the need for an articulated antenna or antenna-gain shaping, reducing the telecommunications subsystem mass and cost. As in Case 1.1, the maximum visibility time for this system is about 12 minutes when the spacecraft passes through the zenith of the ground stations. Here again the minimum data link margin is 3 dB, and 6 dB for the carrier. The required RF transmitted power is 5.2 W. The Quickbird transmitter will radiate 6 Watts RF, so no additional power amplification is needed.

Table 6-3. This is a summary of link budgets, mass, power consumption, and cost. The satellite is in a 700 km orbit with 98 degree inclination. The maximum slant range for the RF link was 2,389 km. The link analysis below is for the Alaska SAR facility receiving station. The information on X- and Ka-band phased array antennas was provided by GSFC

Maximum Range (km)	700							
Slant Rang (km)	2389							
OrbitInclination (deg)	98							
Ground Station	ASF							
Case				Case 1 (0.1 Gbps)				1 Gbps
				Case 1.1	Case 1.2	Case 1.3		Case 2
S/C Antenna Diameter Type				OMNI	OMNI	XPPA	XPPA	KaPPA
S/C Antenna Efficiency %				55.00	55.00	55.00	55.00	55.00
Ground Station Antenna Diam. (m)				11.30	11.30	11.30	11.30	5.00
Frequency Band				X-Band	X-Band	X-Band	X-Band	Ka-Band
Frequency (MHz)				8450	8450	8450	8450	25000
Space Loss (dB)				178.54	178.54	178.54	178.54	187.96
Non DSN Station Noise Temp (used for Non DSN only) (K)				200.00	200.00	200.00	200.00	200.00
Earth Station Antenna Elevation Angle (Deg)				7.00	7.00	7.00	7.00	7.00
Earth Station antenna G/kT (dB/K)				263.00	263.00	263.00	263.00	265.33
Total Loss in the link (dB)				6.00	6.00	6.00	6.00	6.00
Data Channel 1								
Channel 1 Modulation Index (Peak Radians)				1.54	1.54	1.54	1.54	1.54
Channel 1 Subcarrier (Square = Dir Mod or Sine)				Sq	Sq	Sq	Sq	Sq
Channel 1 Modulation Loss (dB)				0.00	0.00	0.00	0.00	0.00
Channel 1 Bit Rate (kbps)				100,000	100,000	100,000	100,000	1,000,000
Bit Error Rate				1.00E-07	1.00E-07	1.00E-07	1.00E-07	1.00E-07
Coding used (Convolutional and or R/S)			Rate	0.00	0.50	0.50	0.00	0.50
		Constraint Length		0.00	7.00	7.00	0.00	7.00
		R/S (Yes/No)		No	Yes	Yes	No	Yes
		Required Eb/N0 (dB)			2.60	2.60	11.30	2.60
Channel 1 Bit Rate (ksps)				100,000	228,700	228,700	100,000	2,286,996
Desired Channel 1 Data Margin (dB)				3.00	3.00	3.00	3.00	3.00
Carrier Loop Computations								
Carrier Supression Loss (dB)				30.23	30.23	30.23	30.23	30.23
Carrier Loop Expanded BW (Hz)				1000.00	1000.00	1000.00	1000.00	1000.00
Carrier Loop Threshold (dB)				12.00	12.00	12.00	12.00	12.00
Desired Carrier Margin (dB)				6.00	6.00	6.00	6.00	6.00
Required S/C EIRP Calculations								
Required S/C EIRP for the Carrier Margin				-0.22	-0.22	-0.22	-0.22	6.36
Required S/C EIRP for Data Channel 1 Margin				15.90	7.15	7.15	15.90	21.52
Required S/C EIRP for Data Channel 2 Margin				No Tim	No Tim	No Tim	No Tim	No Tim
Required S/C EIRP for Ranging Margin								
S/C Antenna diameter / Power Calculation								
Maximum S/C EIRP Required (dB)				15.90	7.15	7.15	15.90	21.52
S/C Transmitted RF Power (W)				38.50	5.19	0.03	0.22	0.15
S/C Parabolic Dish Antenna Diameter (m)				0.0175	0.0175	0.2000	0.2000	0.2200
S/C Antenna Gain (dBi)				0.00	0.00	22.00	22.00	33.00
S/C Antenna 3 dB Beamwidth, end - to - end (Deg)				129.00	129.00	10.50	10.50	3.21

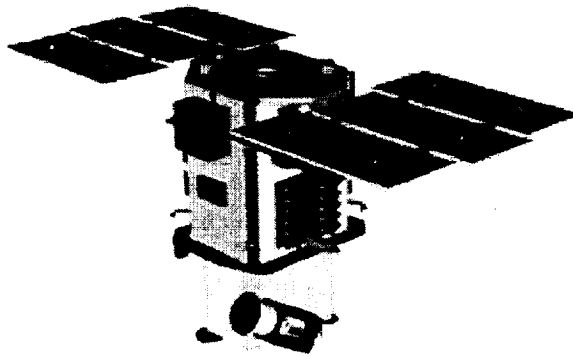


Figure 6-5. Ball Aerospace Quickbird Satellite can transmit up to 320 Mbps

Case 1.3 Phased Array Antenna With and Without Coding

The X-band Phased Array Antenna (XPAA) is composed of a flat grid of radiating elements whose relative phases are appropriately varied to steer the radiated beam pattern in the desired direction. The antenna for the Earth Orbiter-1 (EO-1) mission consists of 64 radiating elements combined with low power, high efficiency solid state amplifiers to achieve the required radio frequency power level. These array antennas are generally mounted on a nadir-pointing spacecraft panel to allow maximum view angle for communications with the ground station. Figure 6-6 is a picture of the phased array antenna that is being developed for GSFC by Boeing Phantom Works in Seattle, WA. This 5.5 kg phased array antenna has an Effective Isotropic Radiated Power (EIRP) of 160 Watts. It can support data transmission up to 105 megabits per second at a bit error rate of $1E^{-7}$.

Table 6-3 gives the link analysis for this antenna. The minimum data and carrier margins are 3 dB and 6 dB, respectively. The link uses the rate 1/2, constraint length 7 convolutional coding concatenated with the Reed-Solomon coding. As in Cases 1.1 and 1.2, the maximum visibility time for this system is about 12 minutes when the spacecraft passes through the zenith of the ground station.

When coding is used to reduce E_b/N_0 , the symbol rate increases to 228 Msps. The X-band phased array antenna with a maximum data rate of 105 Mbps, will not support such a high symbol rate (228 Msps). Hence to achieve the 100 Mbps data rate, we recommend that this phased array antenna be used without coding.

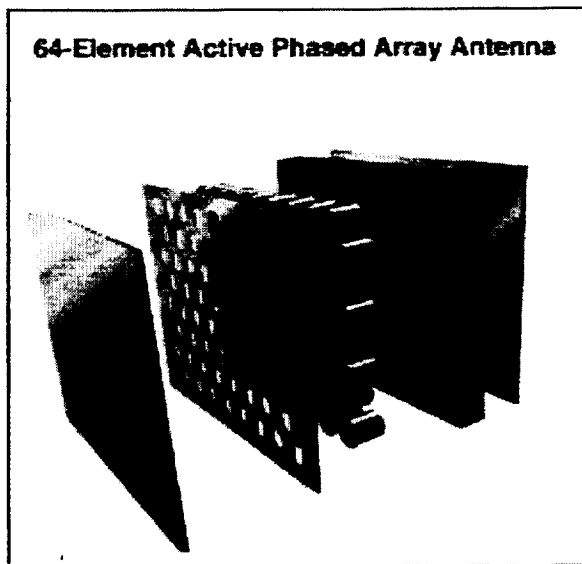


Figure 6-6. Element Active Phased Array Antenna, built by Boeing for GSFC

Case 2 Ka-band Phased Array Antenna

This case assumes a data rate of 1 Gbps and 11.3 m antennas at ASF and at Svalbard, Norway, with the appropriate receiver electronics. For the Ka-band, it is assumed that the antennas are at these locations and that they are appropriately figured for low loss at the higher frequency.

The description of the Ka-band phased array antenna in the paragraphs below is excerpted from the web site (http://msb.gsfc.nasa.gov/technology/Ka_Spec_Rev1.pdf) provided by GSFC personnel. The design shown in Figure 6-7 consists of 256 circularly polarized antenna elements, resulting in an Effective Isotropic Radiated Power (EIRP) of 33 dBW_i at a maximum scan angle of 60 degrees. See Figure 6-8. The antenna has 240 elements nominally active, with 16 spare elements. The elements are fed by 68 4-channel transmit modules, which provide amplification and 3-bit phase control for each channel. The elements are fed in phase quadrature to obtain circular polarization. The modules are under development by AIL Systems, Deer Park, NY under a subcontract to Harris Corp. These devices are state-of-the-art Monolithic Microwave Integrated Circuits (MMICs) using Litton's Solid State 0.25 mm gate length single and double heterojunction PHEMT process and Low Temperature Cofired Ceramic-Metal (LTCC-M) packaging technologies.

Mechanical Concept Provides Simple Interfaces

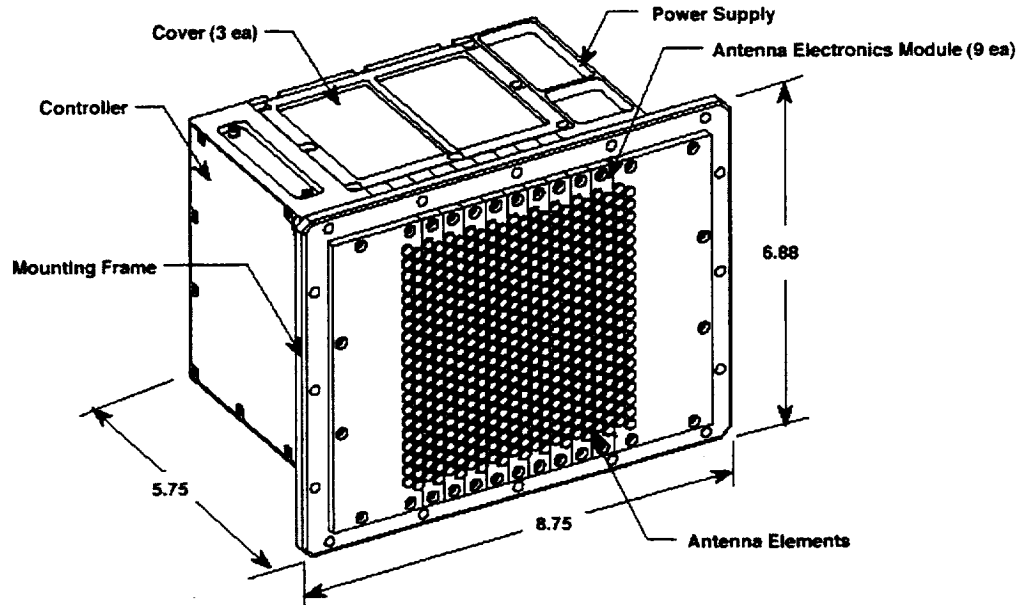


Figure 6-7. Ka-band phased array antenna

Mechanically, the antenna is divided into nine trays, each tray containing four transmit modules per side. Power and control signals are delivered to each module via a printed wiring board from a connector on the side of the tray. The trays are fed with a distribution assembly that holds a dual 9-way power divider and a dual RF driver module. The antenna is controlled by an on-board processor assembly which also contains the Mil-Std-1773 interface with the spacecraft Command & Data Handling Subsystem. It operates from a 28 V dc input into the antenna power supply.

The program will result in an Engineering Model (EM) delivery in June 1999. The EM will undergo a comprehensive environmental test program as part of its acceptance. The antenna has a mass of 4.5 kg and consumes 74 W of electrical power.

The link budget is shown in Table 6-3. The antenna is designed so that its beam can be steered up to 60 degrees off-axis. When mounted on a nadir-facing spacecraft surface, the antenna will communicate with the ground station only down to 20 degrees elevation with this restriction. The antenna has, however, been tested to 62 degrees off-axis, corresponding to an 11 degree horizon mask. At this angle the grating lobe pattern increases by 1.2 dB with only a 0.2 dB increase in the first side lobe. The design has 3 dB data margin and 6 dB carrier margin.

Parameter Trades DC Power vs Scan, EIRP, & PAE

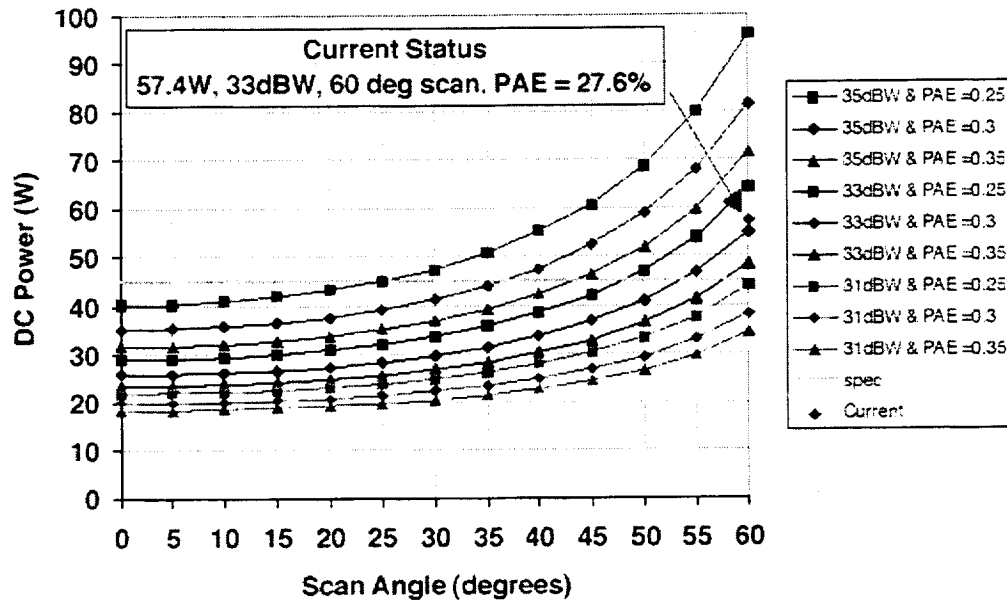


Figure 6-8. Performance of Ka-band phased array antenna as a function of the off-axis beam-pointing angle

Case 3

In the year 2006, the requirements of 10 Gbps make RF communication almost impossible, unless data compression techniques are available to produce better than 2:1 lossless compression ratios. Additionally the SAR data rate is 4.5 Gbps and is usually not compressible, thus posing a major hurdle. Unless some preliminary data processing of the SAR data on-board the spacecraft to produce images occurs first, the intelligent data extraction proposed in Section I cannot be used to reduce the required downlink data rate. Under these conditions the current and near-term projected suite of RF telecommunications will not be able to support the 10 Gbps data rate. However, 16 QAM bandwidth efficient modulation techniques may expand the achievable data rate close to 9.6 Gbps.

Conclusions:

- In case 1, (0.1 Gbps) X-band will be able to support this data rate.
- Ka-band will also be able to support cases 1 and 2, and possibly 3. However the lack of Ka-band ground stations make this solution difficult to achieve.
- The use of an X-band phased array antenna does not show any major advantage over an omni antenna, combined with an advanced transmitter.

- The use of Ka-band frequency does not also show any major advantage over X-band. In fact major cost, about \$3.5 M, will be expended to upgrade the ASF ground station.
- Case 3 (10 Gbps) is out of reach for RF Telecommunications unless major leaps in telecommunications hardware, data compression and intelligent data extraction are achieved

6.2.2 Optical Telecommunications

6.2.2.1 Spacecraft Optical Transmitter

The JPL-designed optical communications demonstrator (OCD) terminal shown in Figure 6-9 is the basis for future JPL optical communications terminal development. It has been adapted for the LEO-to-ground, and GEO-to-ground links discussed in this section. A schematic of the optical train is shown in Figure 6-10. It consists of a telescope with a 10 cm primary mirror and 30% obstruction from the secondary mirror.

The optical source is 1550 nm InGaAsP semiconductor laser diode amplified in an Erbium-doped fiber that emits 150 mW average power. It is based on commercially available, fiber-coupled laser diodes with fiber amplifiers that are designed to support OC-48 terrestrial links. The 10 Gbps links are achieved by WDM of four 2.5 Gbps laser transmitters coupled into the OCT's optical train.

Acquisition and tracking of the ground station by the spacecraft's optical communications terminal (OCT) relies on detection of an uplink beacon beam transmitted from the ground. The acquisition and tracking detector is based on commercially available array detectors that can support the high frame read rates needed to correct for high frequency spacecraft vibrations that cause jitter in the pointing of the downlink beam.

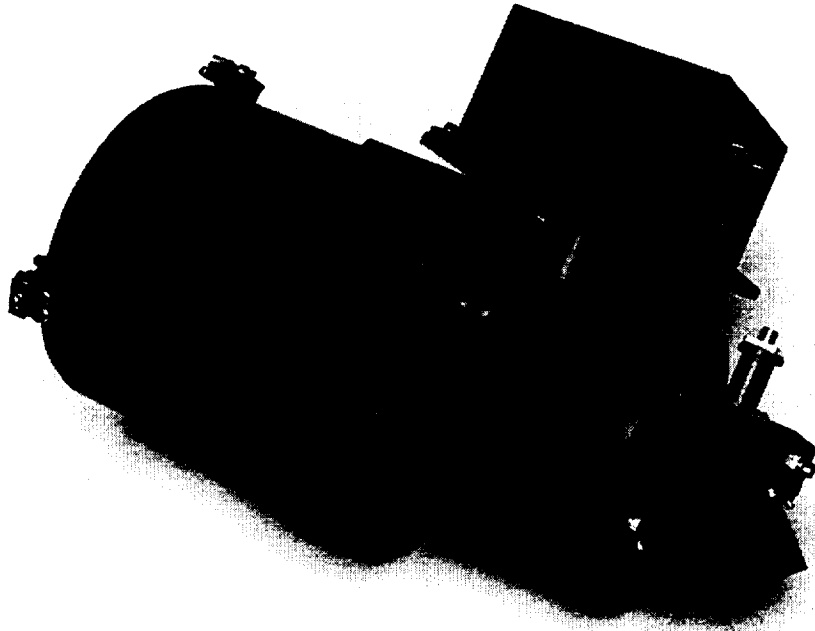


Figure 6-9. JPL's optical communications demonstrator. The fiber output of the modulated laser is coupled through the ferrule at the rear of the device. The ack/trk camera is located in the large box-like section at the top of the picture

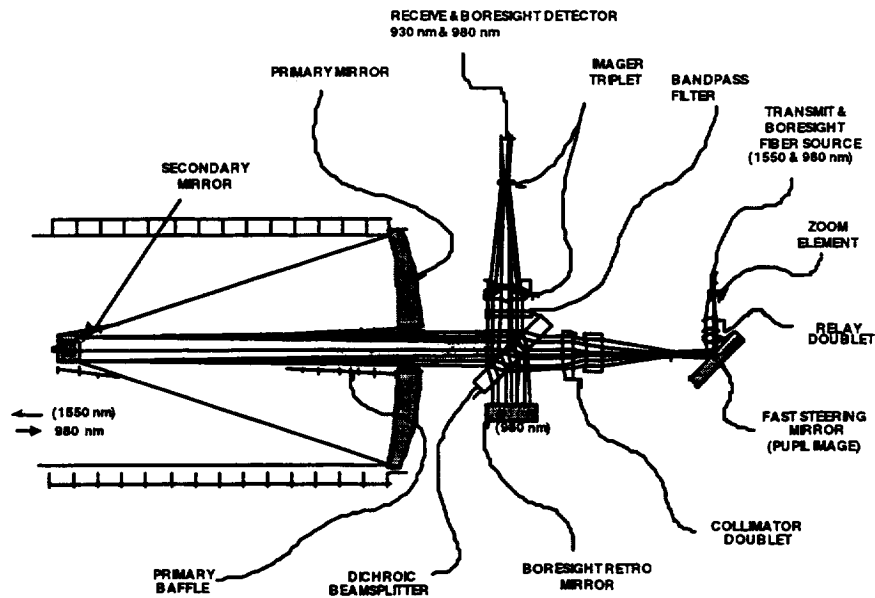


Figure 6-10. Schematic of the basic design of the optical communications terminal

6.2.2.2 Optical Ground Receiving Station

The ground station receives the downlink and provides an uplink beacon for the spacecraft's optical terminal to point to the ground station (see Figure 6-11). Atmospheric scintillation effects on the uplink beacon are mitigated by propagating the uplink through multiple sub-apertures, as was demonstrated during the 1996-1997 GOLD experiment conducted by JPL. The uplink beacon power is less than 5 watts and provides a readily detectable beacon for the satellite. Depending on the data rate, the satellite transmits either a single wavelength or multiplexed wavelengths. The ground receiving station consists of a nominal 1-m receiving aperture with a high bandwidth optical receiver that is composed of an optical detector at the focus of the telescope's optical train and a preamplifier at the detector output. The preamplifier and limiting amplifier conditions the signal prior to clock and data recovery, and data recording and storage. Key segments of the data recovery and storage are discussed in the paragraphs below. The data detector and receiver assembly configurations are unique to optical communications.

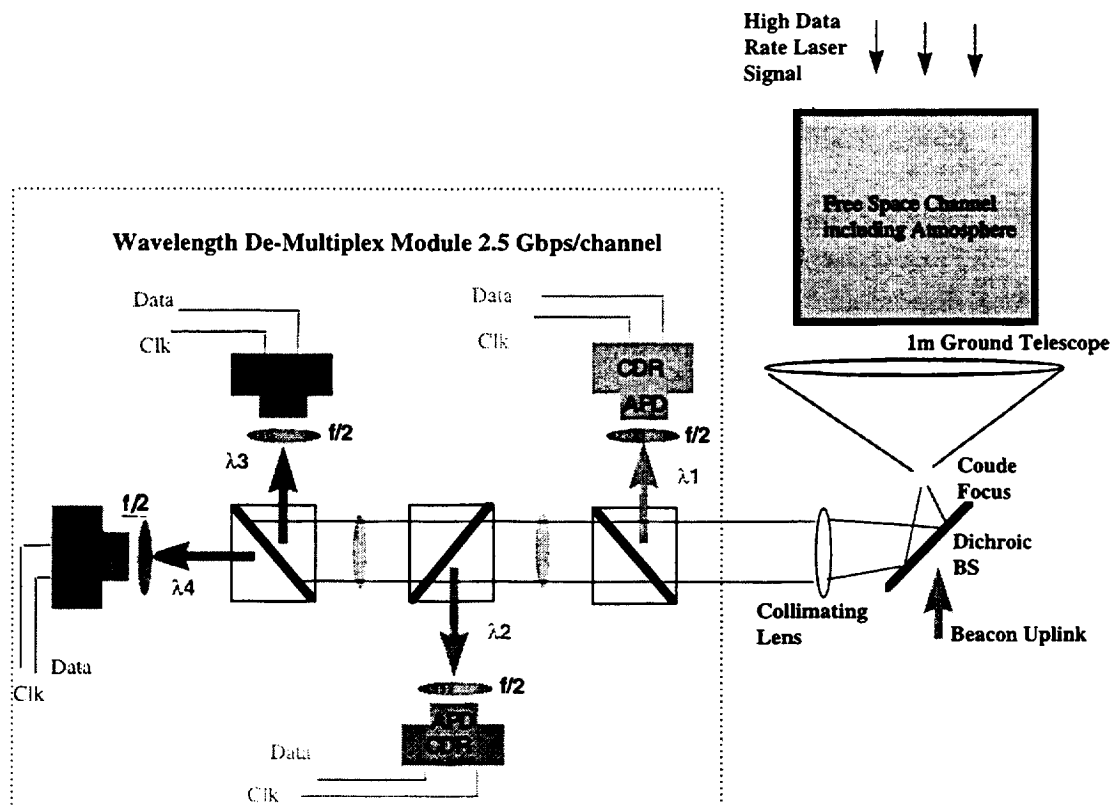


Figure 6-11. Shows a schematic block diagram for the ground station, which de-multiplexes 4 wavelength channels $\lambda_1 < \lambda_2 < \lambda_3 < \lambda_4$. Avalanche photodiode detectors (APD) and clock and data recovery (CDR) electronics are shown for each wavelength.

Data detector/receiver assembly

The schematic of ground data detection/receiving assembly shown in Figure 6-12 is for the 10 Gbps data rate. The 1 Gbps and 0.1 Gbps data rates are supported by using single wavelength transmission and by reducing the modulation rate. The figure shows the de-multiplexing of the four 2.5 Gbps wavelength channels. The downlink signal is collected by the receiver telescope, focused, re-collimated and routed to the wavelength de-multiplexing module. The four wavelengths can be separated using either prisms, gratings or specially designed long-pass filters (see Fig 6-11) that successively pass the longer wavelengths and reflect the shortest wavelength. The separated wavelengths λ_1 , λ_2 , λ_3 and λ_4 are each focused on two avalanche photodiode (APD) detectors. The beacon uplink to the satellite is also shown in Figure 6-12.

The commercially available InGaAs avalanche photodiode (APD) EG&G C30644E meets the optical detector requirements at the ground station. For free space communications, large-area detectors are desirable to collect all of the energy in the atmosphere-blurred focused spot. Typical sizes of APD and PIN detectors for high data rate, free space optical communications shown in Table 6-4 limit data rates to between 2.5 Gbps and 5 Gbps per wavelength channel. The avalanche photodiode detector (APD) has gain, and as the table shows it is approximately 10 dB more sensitive than the PIN. Supporting data rates of 5 Gbps per wavelength channel and above will require the development of high-speed large area devices. There are efforts underway to develop millimeter size detectors with bandwidths as high as 32 GHz.

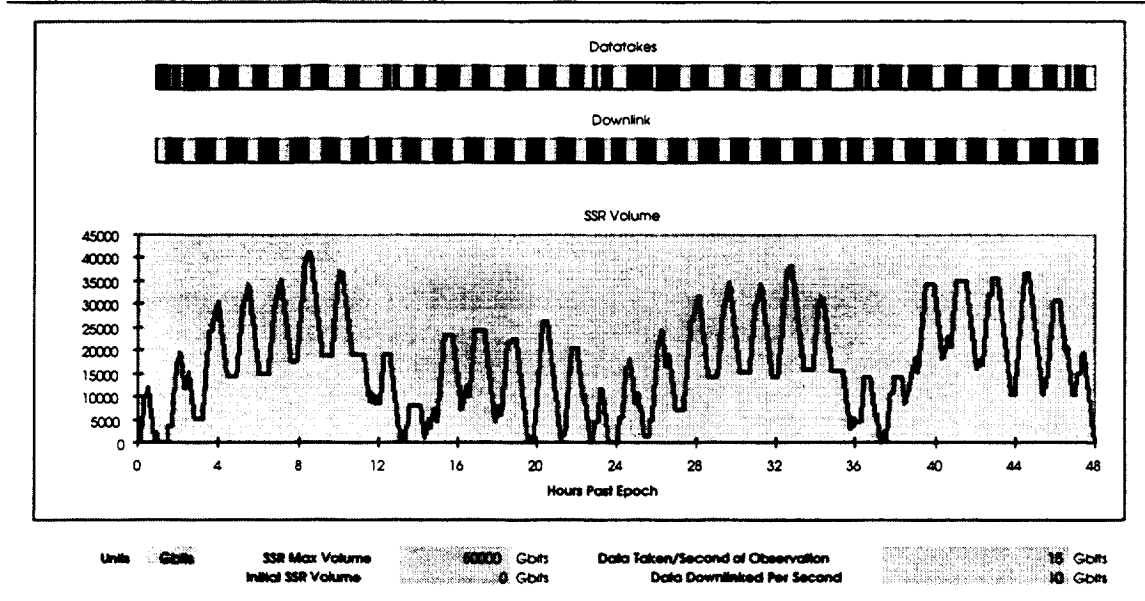


Figure 6-12. Relay satellite with 10 Gbps crosslink with 10 Gbps downlink will support 15 Gbps operational instrument rates at LEO satellite

Table 6-4. Characteristics of InGaAs optical detectors to support the 1550 nm downlink

Detector Type	Active Dia. (μm)	Bandwidth (GHz)	Sensitivity dBm
InGaAs APD	<65	2	-34 @ 2.5 Gbps
InGaAs PIN	100	3.5	-25 @ 2.5 Gbps

6.2.2.3 GEO-Ground and LEO-GEO Links

6.2.2.3.1 GEO-Ground Link

A relay link between LEO and GEO satellites would mitigate the effects of weather on the optical link and allow higher instrument data rates to be supported. The operating scenario would be to transmit the science data to the GEO station during that half of the orbit when the LEO station is in view of the GEO relay. Figure 6-12 shows that, unlike the case of the direct LEO to ground, the relay satellite provides a 1.5 multiplier in supportable data rate. The figure also shows that the relay will support up to 15 Gbps instrument data rates from a LEO satellite.

Although only 6 to 8% efficient, high power Erbium-doped fiber amplifier sources are expected be available in year 2000 to provide the high powers needed to support a 10 Gbps optical crosslink and downlink. IRE-Polus is a supplier of such sources. In future years it is projected that the more efficient (40%) InGaAsP master oscillator power amplifier (MOPA) technology will be available.

The GEO transceiver design differs from that of the LEO-to-Ground system described in Section 2 in certain key areas, viz.:

1. The lightweight 30-cm receiver aperture is baselined on the JPL X-2000 transceiver design (see Figure 6-13). The larger receiver aperture facilitates inter-satellite and ground station acquisition and tracking.
2. The transceiver telescope is fixed to an onboard isolated optical bench and acquisition; coarse tracking is accomplished with the aid of a large gimbaled flat mirror.
3. The unmodulated transmitter serves as the beacon laser for initial acquisition.
4. The GEO platform also has data receive capability.

Other valid design philosophies include putting the burden for the link on the geostationary satellite. In such designs, the geostationary satellite would have a large aperture receiver and high power transmitter, while the LEO terminal would have a small aperture receiver and low power transmitter. These options are not considered here.

The full 30 cm aperture of the space terminal is used for acquisition and tracking of the uplink beacon. A 45 cm beam director on a two-axis gimbal is used to point the downlink to the ground station. The lightweight beryllium beam director allows acquisition and tracking using a low-power, lightweight gimbal.

Wavelength division multiplexing four 2.5 Gbps links, nominally 1 nm apart between 1530 nm and 1540 nm, generates the 10 Gbps data stream. Each channel requires a 3-W average output optical power from the laser sources. Downlink transmission from the space terminal uses a 12-cm sub-aperture of the 30-cm telescope. The sub-aperture transmission allows for a wider beam divergence; in combination with the fine pointing mirrors this relaxes the pointing requirements on the spacecraft.

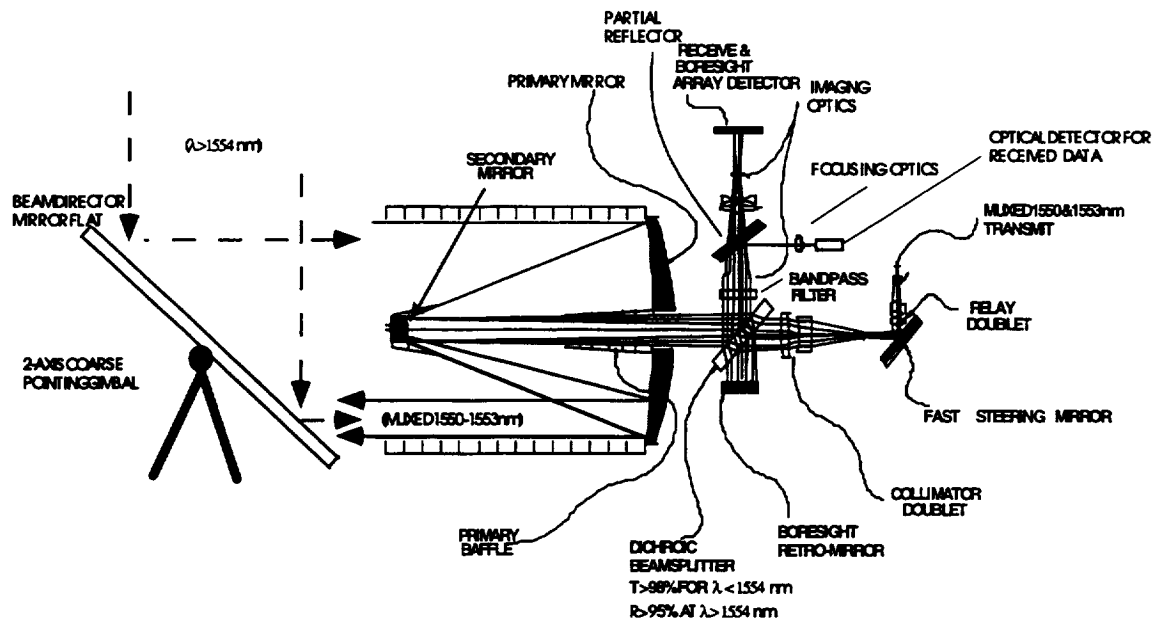


Figure 6-13. Schematic of the transceiver for GEO relay satellite. Unit acquires data recovered from LEO terminal, stores it on-board and retransmits it to ground station. Telescope is body-fixed to satellite and 2-axis coarse pointing gimbal tracks LEO spacecraft during link. Sub-aperture transmitter design allows for larger transmitter beam divergence (22 microradians) and obviates need for separate acquisition beacon

6.2.2.4 Optical Comm Link Analysis

6.2.2.4.1 LEO-Ground

A summary of a typical optical link analysis is given in Table 6-5. The high link margin is characteristic of LEO-to-ground optical links. The 2.5 Gbps example was chosen because it represented the current state of the art and it could be readily multiplexed to achieve the 10 Gbps link. Data rates of 1 Gbps and below are achieved by simply modulating the source at a lower rate and thereby gaining link margin. In this link design, the satellite is at 20-degrees elevation and the divergence of the beam transmitted from the space-borne laser transmitter is expanded to 40 microradians to relax the requirement on the fine-steering mirror pointing control. The link margin in this design increases as the satellite rises. The link assumes 2% pointing offset error and 8% RMS beam jitter.

The ground station inputs to this link were based on the design of the OCTL ground station's optical train. The optical losses of the other ground stations are not known at this time, yet in general they have a larger receiving aperture, i.e., greater receiver gain. Nevertheless, the system was designed with enough margin to accommodate a wide range of variability in receiver optical losses. In addition, the large link margin mitigates the effects of fades caused by atmospheric scintillation and by intermittent thin cloud cover.

Table 6-5. Link analysis for 2.5 Gbps telecommunication data rate

LEO-Ground Link (2.5 Gbps)

Link Summary			
Link Range	1.58E+03 km		
Data rate	2.50E+06 kbps	On-Off Keying	
Coded BER	1.00E-07	No Coding	
Transmit power	0.15 W average	300.00 mW (peak)	24.77 dBm
Transmit losses	47.2 % transmission		-3.19 dB
Transmitter gain	40.5 urad beam width		101.48 dB
Pointing losses			-0.97 dB
Space loss			-262.17 dB
Atmospheric losses	73.5 % transmission		-1.34 dB
Receiver gain	1.00 m aperture diameter		125.73 dB
Receiver optics losses	46.8 % transmission		-3.39 dB
Received signal	1.69E+05 photons/pulse	54.21 uW (peak)	-19.08 dBm
Background signal level	1.09E-01 photons/slot	34.91 pW	
Required signal level	1.05E+03 photons/pulse	0.34 uW (peak)	-35.15 dBm
Link Margin			16.07 dB

6.2.2.4.2 GEO-Ground

A summary of a typical optical link analysis is given in Table 6-6. The ground station is baselined as a 1-meter terminal. It provides enough gain so that the overall link margin is approximately 8.7 dB per wavelength channel using year 2000 detector technology. This margin allows transmission through some cloud cover, thereby reducing the amount of time that the link is affected by adverse weather.

Effects of atmospheric scintillation on the uplink are mitigated by propagating the uplink through multiple sub-apertures as was demonstrated during the 1996-1997 GOLD experiment conducted by JPL. The uplink beacon will be red-shifted (i.e., to the long wavelength side) with respect to the downlink.

Table 6-6. Link summary for GEO-to-Ground link for 10 Gbps data rate with 1-m receiver and 12 cm transmitter using year 2000 technology. Operationally, four 2.5 Gbps channels are multiplexed to achieve the 10 Gbps data rate

GEO-GND-1550 nm, 1-m			
Link Summary			
Link Range	3.61E+0 km		
	4		
Data rate	2.50E+0 kbps	On-Off Keying	
	6		
Coded BER	1.00E-07	No Coding	
Transmit power	2.0 W average	4.0 W (peak)	36.02 dBm
Transmit losses	88.3 % transmission		-0.54 dB
Transmitter gain	22.3 urad beam width		106.4 dB
Pointing losses			-0.97 dB
Space loss			- dB
			289.33
Atmospheric losses at 84° El	89.9 % transmission		-0.46 dB
Receiver gain	1.00 m aperture diameter		125.73 dB
Receiver optics losses	46.8 % transmission		-3.3 dB
Received signal	7.68+03 photons/pulse	2.46 uW (peak)	-26.45 dBm
Background signal level	7.67E-02 photons/slot	24.60 pW	
Required signal level	9.53+02 photons/pulse	0.31 uW (peak)	-35.15 dBm
Link Margin			8.70 dB

6.2.2.4.3 LEO-to-GEO

The LEO-to-GEO system design is similar to that of the LEO-to-ground system described in section 6.2.2.1. Table 6-7 shows that a 6 W average power laser source will be needed to achieve the desired link margin. IRE Polus reports 5 W and 10 W fiber sources with an expected efficiency of 4 to 6%. For reasonable power consumption (<500W), this part of the link is not expected to be attainable with year 2000 technology. We project that by year 2003, MOPA devices with efficiencies on the order of 40% will be developed.

The LEO terminal tracks the beacon beam from the GEO satellite. This beacon is the unmodulated laser source used for the GEO-to-Ground link. All of the power received through the 10 cm LEO terminal aperture (less a 3 dB optical loss) is used for tracking the GEO terminal. This provides in excess of 6 dB tracking margin for a 400 Hz frame rate at the acquisition array detector. The high frame rate allows the LEO terminal's coarse pointing gimbal and fine pointing mirrors to compensate for spacecraft vibrations.

The GEO terminal's acquisition and tracking of the LEO satellite is accomplished using 10% of the optical power received through its 30-cm aperture. The approach calls for completion of the acquisition sequence in less than 5 minutes of the 45-minute link. In this scenario, the LEO satellite initiates the sequence by scanning across the uncertainty in the GEO satellite's relative position as it comes into "view". This is due to the LEO satellite's attitude uncertainty, and to the uncertainty in the LEO satellite's knowledge of its own ephemeris due to atmospheric drag. The

first effect is mitigated by rapidly scanning the laser beam across the attitude uncertainty, and the second by using an onboard global positioning system to improve the satellite's knowledge of its location in inertial space.

Table 6-7. Single wavelength channel LEO-to-GEO link with 30-cm receiver and 10-cm transmitter. Design uses projected year 2003 detector technology with sensitivity 3 dB greater than today's InGaAs APDs

LEO-to-GEO -1550 nm			
Link Summary			
Link Range	3.6E+04 km		
Data rate	2.50E+06 kbps	On-Off Keying	
Coded BER	1.00E-07	No Coding	
Transmit power	6.00 W average	12.00 W (peak)	40.79 dBm
Transmit losses	73.6 % transmission		-1.33 dB
Transmitter gain	26.8 urad beam width		103.47 dB
Pointing losses			-0.97 dB
Space loss			-290.64 dB
Atmospheric losses	100.0 % transmission		0.00 dB
Receiver gain	0.30 m aperture diameter		115.50 dB
Receiver optics losses	64.2 % transmission		-1.93 dB
Received signal	9.62E+02 photons/pulse	0.31 uW (peak)	-35.11 dBm
Background signal level	0.00E+00 photons/slot	0.00 pW	
Required signal level	4.39E+02 photons/pulse	0.14 uW (peak)	-38.51 dBm
Link Margin			3.4 dB

6.3 Ground Station Data Management

6.3.1 Data Storage

Data recording, archiving, and data distribution are common to both optical and RF communications. Current data recording technology can support 1.2 Gbps onto solid state recorder. Projections are that this will double by year 2000 and double every three years subsequently, reaching 10 Gbps by year 2006. For a four-channel multiplexed downlink, the SSR data storage system will support a maximum data rate of 10 Gbps.

Figure 6-14 is a schematic for a single wavelength channel of the WDM receiver channel. After detection by the photodetector and clock and data recovery, the high rate data stream is first recorded on a high-speed solid-state clip-on memory system. The data is then transferred from the memory boards to magnetic tape library or disk drive at a slower rate to make the memory boards available for the next pass. Data transfer rates from the memory modules to magnetic tape recorders is currently 160 Mbps, and reasonable projections are 200, 640 and 800 Mbps for the years 2000, 2003 and 2006, respectively. By year 2000, disk drives are projected to have Terabit storage capacity with input/output rates of 1 Gbps.

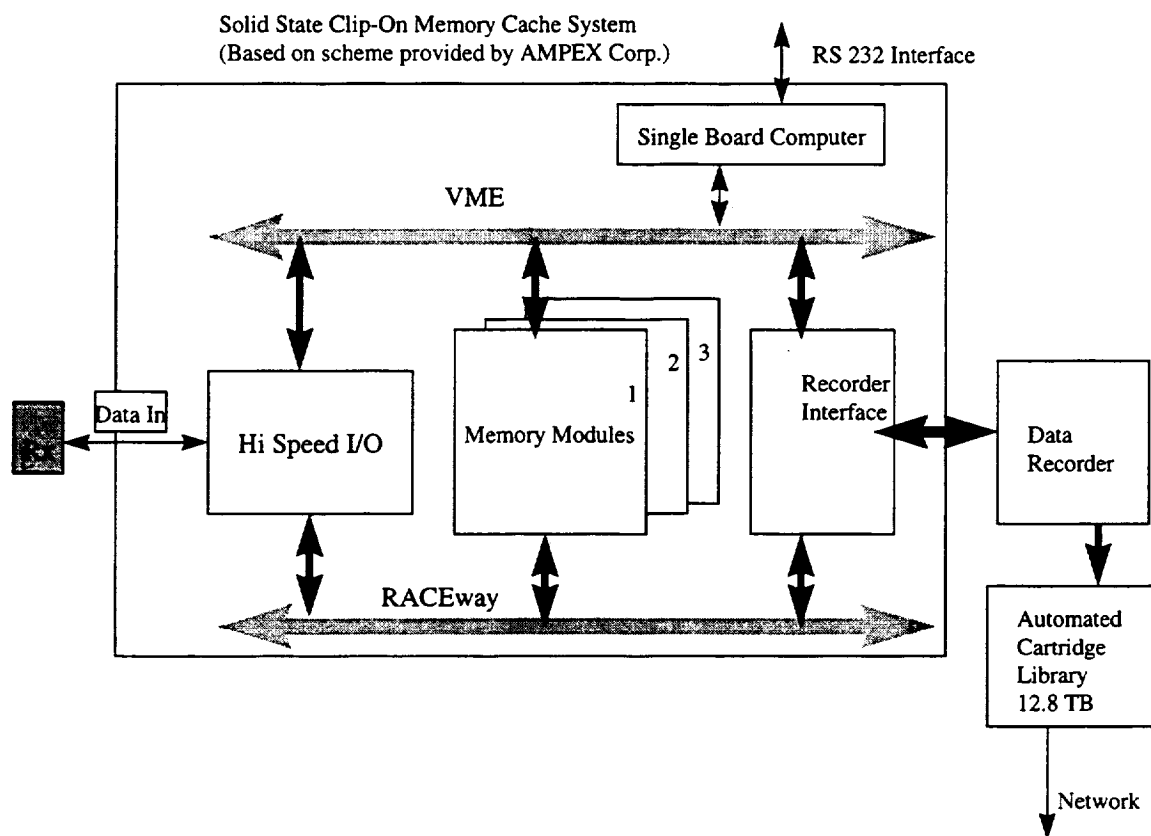


Figure 6-14. Block diagram for transferring high rate data from optical communications receiver to bulk memory. Note that this schematic represents a single channel of data and is based on the schemes discussed in this report as many as 4 such channels may operate in parallel to support the required 10 Gbps downlink

The number of memory modules per clip-on is determined by the expected maximum downlink data rate, and the capacity per board (16 Gbits). For the 1 Gbps downlink, only one clip-on capable of recording up to 2.5 Gbps is needed. For elevation greater than 20 degrees, the duration of LEO pass at the five ground stations is approximately 315 seconds. The total expected transmitted data-volume would be 315 Gigabits, requiring approximately 20 memory boards at 16 Gbit storage per board. At transfer rates between the SSR and the tape recorder of 200 Mbps, the data can be stored in less than 30 minutes. Table 6-8 gives the data transfer time in minutes based on the projected technology growth of data storage using high-speed tape. The results show that at the 10 Gbps data rate the data can be transferred to the storage medium for future distribution in just over an hour using year 2000 technology. This reduces to about 40 minutes as technology developments support higher transfer speeds between the SSR and the tape drive.

6.3.2 Data Distribution

Data downlinked from the spacecraft will be distributed over the network where that infrastructure exists. Figure 6-15 is a schematic showing the distribution of the data from the ground station across the high speed WAN to a central distribution facility or to the principal

investigator. Within CONUS, we expect the projected development of high speed WANs with access nodes that will support the rapid distribution of data from these facilities to occur.

Table 6-8. Memory boards and number of high-speed SSR clip-ons needed to support data rates. Time to transfer data calculated using 0.2 Gbps, 0.64 Gbps and 0.8 Gbps data transfer rates in 2000, 2003 and 2006, respectively

	Year 2000	Year 2003	Year 2006
Recorder	2.5 Gbps	5 Gbps	10 Gbps
SSR to tape drive transfer rate, (Mbps)	200	640	800
0.1 Gbps			
Number of clip-ons	1	1	1
Memory boards per clip-on	2	2	2
Time to transfer data to recorder, min.	2.6	0.8	0.7
1 Gbps			
Number of clip-ons	1	1	1
Memory boards per clip-on	20	20	20
Time to transfer data to recorder, min.	26	8	7
10 Gbps			
Multiplexing	4 channels x 2.5	2 channels x 5	2 channel x 5
Number of clip-ons	4	2	2
Memory Boards per clip-on	50	100	100
Time to transfer data to recorder, min.	66	41	41

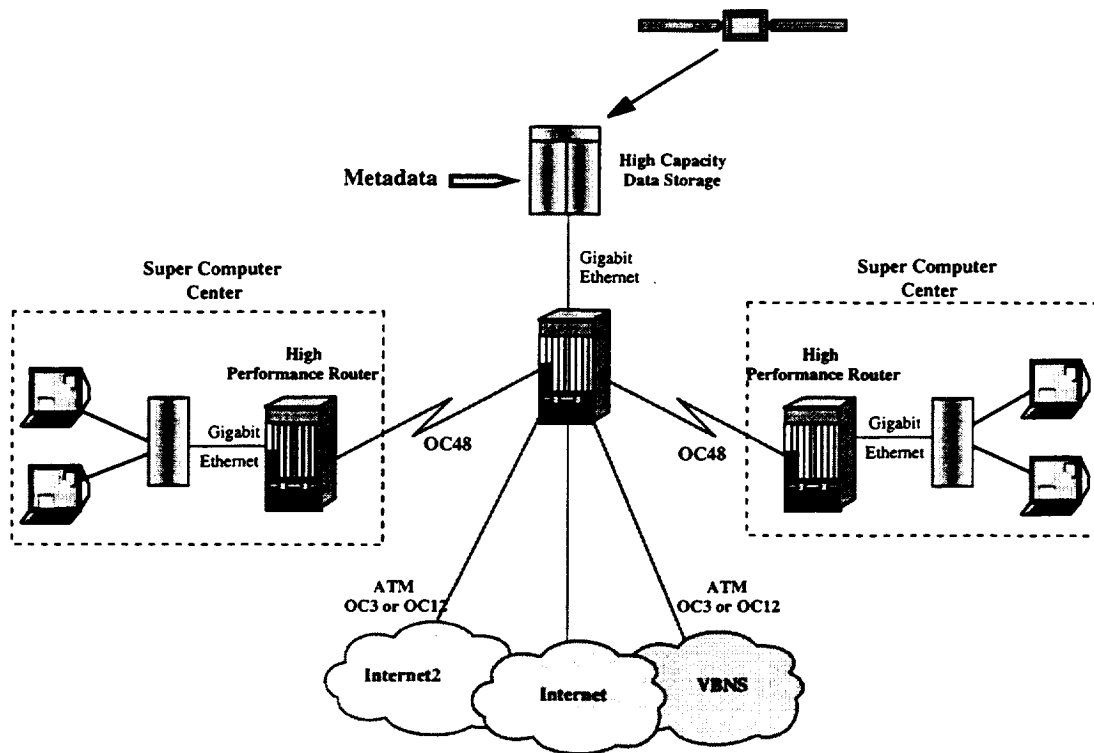


Figure 6-15. High-speed data distribution network for stations with direct connectivity to the high speed WAN. Metadata are stored at the facility along with the downlink data stream prior to transfer to the central facility or to the PI. Data are distributed via the Internet, Internet 2 or MCI's Backbone Network Service (vBNS). Figure is compliments of James Lawson, Juniper Corp

These networks provide high-speed user access to a limited community of users that have intermittent need for the full bandwidth. The high-speed backbone shown in Figure 6-16 connects 14 major US cities, including Los Angeles and Boston (locations of interest for Table Mountain and Firepond receiving stations), is at OC-12, capable of transmitting 622 Mbps. Branch connections from the backbone use 274 Mbps (DS3) and 155 Mbps (OC-3) to a number of universities and some National Laboratories (e.g., NASA Ames). Trials are underway during the current calendar year (from San Francisco to Los Angeles) to upgrade the backbone to OC-48 which will allow the backbone to be 2.448 Gbps, and OC-192 (10 Gbps) in the near future. The branch lines from these higher rates will also be upgraded and a reasonable projection of user speeds will be 622 Mbps - 1.2 Gbps. At locations where network access is unavailable, the data are re-recorded on tape or magnetic disk and shipped by courier service.

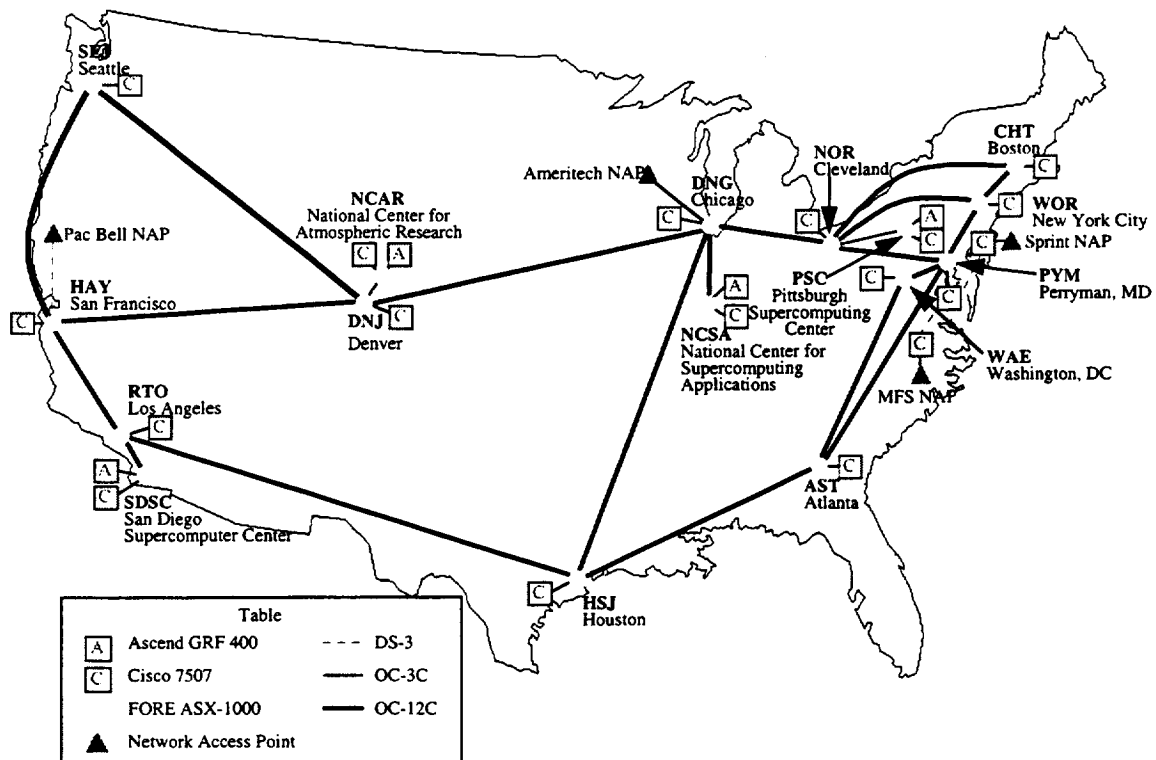


Figure 6-16. High-speed WAN connectivity across CONUS. This figure is compliments of Scott Huddle, MCI

6.4 Mass, Power and Cost

6.4.1 RF Transceiver

Table 6-9 gives estimates of the mass power-consumption and cost for the different RF cases presented.

Table 6-9. RF system mass power consumption and cost

Hardware Mass, Power Consumption, and Cost						
		Case	Case 1 (0.1 Gbps)			
# Of Units	Hardware components	Case 1.1	Case 1.2	Case 1.3	Case 2.2	
1	High Gain Antenna Mass (kg)					10 ⁽²⁾
	Medium Gain Antenna Mass (kg)					
2	Low Gain Antenna (Omni) Mass (kg)	0.5	0.5			
1	Transmitter Mass (kg)	3.6	3.0	10.0	5.0	
	Transmitter DC Power Consumption (W)	30.0	35.0	110.0	55.0	190 ⁽²⁾
1	Receiver Mass (kg)	0.8	0.8			
	Receiver DC Power Consumption (W)	12.0	12.0			
1	Power Amplifiers (TWTA/SSPA) Mass (kg)	2.8				
	Power Amplifiers (TWTA/SSPA) DC Power (W)	70.0				
1	Gimball					
1	Microwave Components Mass (kg)	4.0	4.0	3.0	3.0	3.0
Total Mass Of the redundant System (kg)		11.7	8.3	13.0	7.0	13.0
Total DC Power Consumption (W)		112.0	47.0	110.0	55.0	190.0
Non-Recurring Engineering (\$M) Cost		3.1	2.9	2.1	2.1	5.0
Recurring Engineering (\$M) Cost		6.4	4.8	7.1	6.0	13.6
Cost of a Redundant System with One Set of Spares (\$M)		9.5	7.7	9.2	8.1	18.6
(1): Four Transmitters on Simultaneously						
(2): Ka-Bnad Phased array on Simultaneously						

6.4.2 Optical Transceiver

The mass and power estimates for the GEO terminal, the LEO terminal for LEO-to-ground, and the LEO terminal for the LEO-to-GEO systems are given in Tables 6-10 through 6-12. The relay system is seen as viable only after year 2003 because the technology to support the LEO-to-GEO link is not as developed as that for the GEO-to-ground link. Table 6-12 gives the estimates for the LEO terminal of the LEO-to-GEO link, assuming a year 2003 technology cutoff projecting the development of high efficiency (40%) high power (>5 W) 1550 nm MOPAs. A 10% mass and power overhead is assumed for the Power and Thermal Conditioning unit. With MOPA technology the GEO system in Table 6-10 will have a mass of 40 Kg and a power consumption of 78 W.

Table 6-10. Estimated mass and power of GEO system for 10 Gbps GEO-to-Ground multiplexed optical communications transceiver subsystem, year 2000 fiber technology. Mass and power consumption are reduced to 40 kg and 85 W using projected 2003 MOPA technology

Subsystem	Mass, kg	Power, W
Telescope Optical Assembly	11	-
Coarse Tracking Assembly	12	29
Laser Transmitter Assembly (4 X 2W assemblies 6% laser efficiency)	12	133
Receiver Assembly	3	10
Ack/Trk detector and FPM assembly	6	10
Electronics Assembly	2	10
Power & Thermal Conditioning Unit	5	18
Total	51	210

The optical communications terminal consists of the subsystems below. Mass and power consumption estimates for a 2.5 Gbps fiber amplifier system are given in Table 6-11. This design is based on year 2000 technology.

Table 6-11. Estimated mass and power estimates for LEO terminal sub-systems for 10 Gbps LEO-to-ground link based on year 2000 technology

Subsystem	Mass, kg	Power, W
Telescope Optical Assembly	6	-
Laser Transmitter Assembly	10	10
Ack/Trk detector and FPM assembly	6	10
Coarse Pointing Mechanism	10	80
Control Electronics	10	37
Power & Thermal Conditioning Unit	4	14
Total	46	151

Table 6-12. Estimated mass and power for 10 Gbps LEO system for multiplexed optical communications transceiver subsystem. This is projected to year 2003 technology and projects 40% efficiency high power MOPAs development

LEO System	Mass, kg	Power, W
Telescope Optical Assembly	11	-
Laser Transmitter Assembly (4 X 6W assemblies 40% laser efficiency)	10	60
Ack/Trk detector and FPM assembly	6	10
Coarse Tracking Gimbal Assembly	10	80
Control Electronics Assembly	10	37
Power & Thermal Conditioning Unit	5	18
Total	52	205

Certain key technologies need to be developed by year 2003 to reduce the power consumption, and mass of the space transceiver. These are as follows:

1. InGaAsP MOPA laser diodes with 40% electrical to optical efficiency and capable of emitting in excess of 4 - 6 W peak power at 1550 nm with 50% duty cycle.
2. High power MOPAs will be able to be modulated to greater than 2.5 Gbps data rates while maintaining 20 dB extinction ratio.
3. Modulated diodes must maintain 1 nm bandwidth under high speed modulation.
4. Low power consumption, low noise arrays 1550 nm sensors for acquisition and tracking. A possible candidate is InGaAs active pixel sensors which are reported to have ~80% quantum efficiency.
5. High quantum efficiency (0.85), low noise, large diameter (>200 microns) high-speed detectors with performance comparable to silicon at 800 nm will be available at 1550 nm that can provide an additional 3 dB sensitivity.

Table 6-13 shows the incremental growth in mass and power consumption as more lasers and electronics are added to implement WDM. The costs assume that any major identified risks have been retired by the JPL Proto-flight Optical Communications Terminal development.

Table 6-13. OCT mass, power, and costs for the different terminals and data rates

LEO- Ground System	Mass, kg	Power, W	Cost, \$M
0.1 Gbps (00)	27	130	5
1 Gbps (00)	30	135	5
10 Gbps (00)	46	151	6
GEO-Ground System			
10 Gbps (00)	51	210	12
LEO System for LEO-GEO link			
10 Gbps (03)	52	205	10

6.4.3 Ground Data Storage and WAN Distribution

The use of WDM to increase the data rate is clearly the most cost-effective solution for data recovery on the ground (see Table 6-14). Receivers supporting up to 2.5 Gbps data rates are 1998 technology and prices already low can only be expected to drop in the out years. The development of large area high-speed optical detectors is a good technology development path in the out years. Such development will eliminate losses caused by overfilling the optical detector, and allow systems with lower margins to be flown. The cost assumptions here are that the cost of the receiver system will remain constant, and that large area detectors will be developed by the terrestrial network community as the data rates in terrestrial links increase. Already, Corning is marketing large effective area single mode fiber (LEAF) for the higher capacity links.

Table 6-14. Ground receiver, data storage system and distribution system costs

Receiver & Storage			
Cost per 2.5 Gbps WDM channel	Cost \$ Year 2000 (M)	Cost \$ Year 2003 (M)	Cost \$ Year 2006 (M)
Detector/Receiver (2.5 Gbps)	0.02	0.01	0.05
* Solid State Memory 17 K/board ('00)	0.884	0.442	0.221
Clip-On Hardware Interface Costs	0.03	0.03	0.03
Data recorder	0.12	0.12	0.12
Tape Library	0.04	0.04	0.04
Subtotal	1.09	0.642	0.461
Cost of 10 Gbps Storage	4.4	2.56	1.8
Distribution			
WAN connection cost per CONUS station	0.202	-	-

* Assumes cost of \$0.50 per megabit in '00 decreasing a factor of two every three years

Installation costs for data delivery on the WAN is \$202K. These costs are unique to CONUS stations and are not necessarily applicable to Hawaii, the Canary Islands or Australia. Of this cost, \$55 K is for the base system installed at the ground station, \$80K is for the OC-48 single mode fiber interface to the central facility and \$35K is for the gigabit Ethernet interface. The OC-12 ATM or Packet over SONET interface is \$32K.

6.5. Conclusions and Recommendations

6.5.1 Conclusions

Retrieval of on-board science data from LEO satellites can be accomplished using RF and optical high data rate links. The 50 MHz bandwidth allocation at X-band limits the data rate supportable by this carrier frequency to 0.3 Gbps, which is when an aggressive bandwidth

efficient modulation 16 QAM scheme is used. The Ka-band link can support up to 1 Gbps data rates in the 1.5 GHz bandwidth using conservative modulation schemes. With two ground stations at Svalbard, Norway and ASF Alaska, the 1Gbps data rate will support a 350 Mbps instrument data rate. However, if the same aggressive modulation scheme that is being adopted for X-band is achievable with similar efficiencies at Ka-band, then Ka-band would be able to support data rates of approximately 10 Gbps on two orthogonal polarizations. This would correspond to approximately a 3.5 Gbps instrument data rate. The 16 QAM modulation scheme is currently being studied at JPL for the ARISE project.

Optical communications can support all three data rates, but because of the existing RF infrastructure may only be cost effective for the 1 Gbps and 10 Gbps links, where there is a need to develop the RF ground station infrastructure (similar to optical frequencies). Because of its susceptibility to weather, optical communications requires ground stations located at the mid-latitudes. Three such stations in the US will support a 750 Mbps instrument data rate with a 10 Gbps downlink data rate. Five stations located globally at ground sites with appropriate telescope facilities will support data at an effective instrument data rate of 1.3 Gbps.

We have investigated an alternative approach to the direct LEO-to-ground link, which is to use a relay satellite at GEO. With a GEO relay, the optical link will support an equivalent instrument data rate of 15 Gbps for a 10 Gbps downlink data rate. The relay satellite also obviates the need for a global network, and would use US-based ground stations located in Hawaii, California, and Arizona. Together these stations would provide 97% weather availability.

High-speed data recording on the ground is achievable at rates up to 1.2 Gbps per channel. The optimum configuration for a high-speed RF link would be two 4.8 Gbps orthogonally polarized channels. For the optical, this would be four 2.5 Gbps WDM channels. The data recording speeds will need to be increased to support these high-data-rate links.

The high-speed WAN being developed for CONUS will allow the ready distribution of data to principal investigators. For stations with no access to the high-speed network, the data will be stored on tape and shipped.

6.5.2 RF Communications Recommendations for Future Work

From the RF analyses and trades, RF communications needs major technological advances to be able to support future Low Earth Orbiter missions, with large data rates. Below are some recommendations on the key technologies that need to be supported to realize high data rate RF telecommunications.

- High Rate Transmitters
 - Explore issues involved in improving transmitter efficiency
 - Explore issues involved in reducing mass, size and cost
 - Explore issues involved in achieving increased data rates at Ka-band frequencies
 - Explore bandwidth efficient modulation schemes (16 QAM) for LEO-to-ground links
 - Explore the use of higher frequencies such as V- and W-bands

- Antenna Technologies
 - Explore new technological concepts in antenna design, such as, inflatables, deployables, and configurables
 - Explore issues involved in improving antenna efficiency
 - Explore issues involved in reducing mass, size and cost of spacecraft antenna
- Ground Stations
 - Determine cost to upgrade ground station receivers and antenna to support high data rates at higher frequencies, in particular at Ka-band
 - Explore feasibility of expanding ground network to other station locations on CONUS that could provide access to the WAN.
 - Explore other mission scenarios that could amortize the development costs of ground station upgrades for high data rate
 - Determine the cost of operations and explore issues involved in reducing these costs

6.5.3 Optical Communications Recommendations for Future Work

- Receivers
 - Explore issues in developing high sensitivity, large-area avalanche photodiode detectors operating in the 1550 nm wavelength region. Such development will reduce the number of wavelengths needed to support the 10 Gbps links.
 - Explore issues in developing high-speed clock and data recovery electronics
- Transmitters
 - Explore issues in development of high power, high efficiency direct modulation semiconductor MOPAs that will reduce the required onboard power consumption.
- Ground Stations
 - Make cost vs. performance trade of a relay satellite with that of a ground station network that will provide equivalent availability.
 - Explore the feasibility of deploying the Goddard SLR2000 ground stations as optical comm receiver terminals.
 - Investigate possible development paths and strategies to aid in the development of high-speed data storage.
- Systems
 - Support current plans for system-level and space-flight demonstrations of high data rate technologies.

References

1. F. Lansing and A. Kantak, Team-X Database
2. F. Lansing and A. Kantak, Telecom Calculator
3. <http://msb.gsfc.nasa.gov/technology/kaband.htm>
4. <http://eo1.gsfc.nasa.gov/NUwww/Technology/xpaa.htm>
5. J. Bosworth, GSFC, verbal communications on the status of the Orroral Range and the SLR 2000 transceivers,(10/26/98).
6. F. Pellerano, GSFC, verbal communications on Ka-band phased array antenna and cost, (10/28/98).
7. K. Perko, GSFC, verbal communications on X-band phased array antenna, (10/30/98).
8. W. Miller, GSFC, discussions on modulation and on related GSFC programs (11/2/98).
9. B. Younes, GSFC, verbal communications on bandwidth allocation for X-band (50 MHz) and Ka-band (1.5 GHz) (11/6/98).
10. W. A. Whyte, LeRC, email communication that the Space Frequency Coordination Group recommendation that bandwidth requirements exceeding 50 MHz be accommodated in the Ka-band and not in X-band (11/12/98).
11. T. Yan et al., "Preliminary Downlink Design and Performance Assessment for Advanced Radio Interfeometry Between Space and Earth (ARISE), *The Telecommunications and Mission operations Progress Report 42-136*, February, 1999.
12. K. E. Wilson, J. R. Lesh, K. Araki and Y. Arimoto, "Overview of the Ground-to-orbit Lasercom Demonstration", Invited Paper, *SPIE Free-Space Laser Communication Technologies Proceedings* February 1997, San Jose.

7. GENERAL CONCLUSIONS AND RECOMMENDATIONS FOR FUTURE WORK

7.1 General Conclusions

The demands for improved monitoring of the Earth's resources and dynamic processes will drive scientists to require high spatial and spectral resolution from Earth-orbiting satellite. We have reviewed the instruments needed to support this increasing demand, and have identified hyperspectral imaging, synthetic aperture radar, and lidar as key areas of rapidly expanding scientific interest. In reviewing the demands from year 2000 to 2006, we have found that the hyperspectral and SAR imagers demands for higher spectral and spatial resolution will drive the instrument data rates from 1.8 Gbps in year 2000 to 4.5 Gbps in 2003 and 45 Gbps by 2006. To meet these demands, we have reviewed several emerging technologies and propose a solution space that combines several of these key technology areas. A summary of the results from the various sections of the report is given below, followed by our conclusions.

Telecommunications

- The 50 MHz bandwidth allocated to X-band transmission limits the achievable data rate to 0.3 Gbps. The existing infrastructure at X-band frequencies makes this transmission most suited and most cost effective for the lowest data rate links.
- The phased array Ka-band antenna recently developed by Goddard can support up to 1 Gbps. To support a 10 Gbps link within the allocated 1.5 Gbps bandwidth will require some type of bandwidth efficient modulation schemes such as 16 QAM. This technology is not currently available at these data rates. However, we anticipate that it would be by year 2006. Assuming ground stations at Svalbard, Norway and Alaska SAR facility the 10 Gbps downlink data rate will support an effective instrument data rate of 3.5 Gbps
 - RF ground stations cannot currently support these high Ka-Band data rates and receiver technology will have to be developed in conjunction with spacecraft transmitter technology to support these rates.
- Four WDM 2.5 Gbps optical channels will support 10 Gbps data rates in year 2000.
 - With five ground stations globally located at low latitude telescope facilities, the 10 Gbps optical communications will support an equivalent instrument data rate of 1.5 Gbps from the LEO satellite.
 - A relay satellite at GEO with the 10 Gbps optical link will support an equivalent instrument data rate of 15 Gbps from the LEO satellite, to one of three 1-m class optical ground stations located in the southwestern US and Hawaii.

Results show that the high rate communications approaches investigated support a maximum instrument data rate of 15 Gbps. None of the approaches support the 45 Gbps instrument rate of year 2006 without the use of some type of data reduction scheme.

On Board Data Management

There are two options to reduce the data from instruments operating at these high data rates. These are: (i) data compression (lossy and lossless), and (ii) on board data processing and intelligent data extraction.

Currently, lossless (2:1) data compression devices support input data rates of about 240 - 320 Mbps. These rates are much lower than the lowest output rates from the hyperspectral-imaging instrument, and data compression is therefore not a viable approach for this data type. The input rates however do support the data rate for the SAR instrument in year 2000, only. Yet, level-zero processing of the SAR data will be required prior to compression. Lossy compression (20:1) using parallel processing techniques will support up to 1 Gbps input data rates. The loss of information content at these high compression ratios was not acceptable to the scientists, and was therefore not pursued here.

Intelligent data extraction can reduce the data volume for transmission by an order of 10 to 100. Processors for $O(10)$ to $O(100)$ reduction in hyperspectral imaging data volume consume less than 100 W of spacecraft prime power. Processors to reduce the year 2006 data volumes by $O(1000)$ will consume kilowatts of power and the approach is not considered a viable option here.

In intelligent data extraction, the data from each pixel is projected onto principal components (eigenspace), thereby reducing the original size of the spectrum to the size of eigenspace. The eigenspaces are derived from the multiple examples of each class and their principal axes point in the direction of maximum variance of the data. The size of the eigenspace can be chosen by scientists or dictated by system requirements to achieve the $O(10)$ reduction. $O(100)$ reduction, or mid-level information extraction is achieved by using spatial and spectral information to cluster low-level features into regions. The descriptors of these regions constitute the reduced data stream that is transmitted to Earth.

Although it is accepted that hyperspectral data could be processed onboard the satellite, there is still some uncertainty whether or not SAR data could be. Table 7-1 below gives the effective instrument data rate for both assumptions along with what we see as the most appropriate choice of telecommunications frequency. The table shows that among the downlink options considered in this study, only the optical relay link can support the most demanding data rates of year 2006 after $O(10)$ reduction of hyperspectral data. To support this data rate with direct to ground RF or optical links will require a greater number of RF and/or optical ground stations than has been considered here. The table also shows that RF is the most appropriate link if $O(100)$ reduction in data volume is implemented.

Table 7-1. Effective instrument data rate in Gbps for raw, uncompressed SAR and compressed hyperspectral imaging, and compressed hyperspectral imaging SAR imaging.

Year	2000		2003		2006	
Raw Data (Gbps)	1.8		4.5		45	
Frequency Band	Ka/Opt		Relay-Ka/Opt		N/A	
Extraction Ratio	10:1	100:1	10:1	100:1	10:1	100:1
Uncomp SAR & Comp Hyperspectral (Gbps)	0.34	0.2	1.62	1.33	8.8	5.2
Frequency Band	X	X	Ka/Opt	Ka/Opt	Relay Ka/Opt	Relay Ka/Opt
Comp SAR & Comp Hyperspectral (Gbps)	0.20	0.018	0.45	0.045	4.5	0.45
Frequency Band	X	X	Ka	X	Relay Ka/Opt	Ka

Optical communications is susceptible to inclement weather, and we have sized the onboard storage requirements of the optical design to support ten hours of data collection. There is a maximum period of five hours between opportunities to downlink data to optical ground stations. This storage capacity hence allows for the loss of one such downlink opportunity with O(10) reduction in the instrument data rate. Under this scenario, and assuming no data compression, the storage requirements are 5.8 Tbits in year 2000, 7.2 Tbits in year 2003, and 8.6 Tbits in year 2006 with a lossy data compression of 20:1, to transfer the data to the ground.

For a GEO optical relay link the required LEO spacecraft data storage is 50 Tbits. This requirement is further reduced to 5 Tbits if we assume O(10) reduction in instrument data volumes as above.

The data downlinked from the spacecraft is stored using a high-speed solid state recorder. For CONUS-based stations the data would be distributed on the high-speed fiber-optic WAN. Data downlinked at non-CONUS is recorded on magnetic tape for future delivery.

In conclusion, we have reviewed the onboard storage requirements needed to support the large volumes of data generated by these high rate instruments and have balanced these with a combination of onboard data processing and high data rate transmission to retrieve these data. We have considered technologies ranging from high data rate RF and optical telecommunications to intelligent data extraction and onboard processing, and image compression. The results show that by using onboard processing to achieve an order of ten reduction of the hyperspectral imager instrument rate, Ka-band and optical technologies support the instrument data rates to year 2003. X-band would support these instrument rates only if the SAR instrument data were also compressed on board. The results also show that a relay satellite could support the highest data rate links in year 2006. This is applicable for both the optical frequencies and Ka-band,

assuming that bandwidth-efficient modulation is used to support a 10 Gbps link. The alternative is to deploy a greater number of RF and/or optical ground stations than was considered here. The relay satellite configuration has an added advantage of allowing distribution of the data on the high-speed WAN network currently under construction by terrestrial fiber communications providers.

7.2 Recommendations for Future Work

Intelligent Data Extraction

Listed below is a description of the proposed tasks for future work on autonomous scientific data extraction.

Use the EOS hyperspectral data set as a test case and have the scientists label some of the images that will compose the training set for the algorithm and ground truth used in evaluation of results. Then perform the following tasks:

Task 1.

Prepare the data set and label portion of the images for algorithm training and ground truth.

Task 2.

- 1) Apply the combination of proposed in the study algorithms: Principal Component Extraction and Iterative Conditional Modes to new data sets of hyperspectral (224 spectral bands) imagery of Earth ground cover. Experimentally determine optimal interaction between two algorithms and modes of operation.
- 2) Investigate the affects of parameter settings on algorithm performance and obtain the optimal parameter setting. Make necessary modifications and further developments to existing algorithms to accommodate new data.

Task 3.

- 1) Conduct experiments to understand the structure of the data, and select most appropriate model for data representation and feature extraction. Concentrate on extracting most scientifically meaningful features from the data for pixel representation.
- 2) Run algorithms from Task 2 on new data features. Add necessary modifications and developments to existing algorithms to accommodate new data.

Task 4.

- 1) Search for new data classes through applications and developments of different clustering techniques.

Task 5.

- 1) Propose parallel architecture for best technique, and implement this technique on parallel platform.

RF Telecommunications

- High Rate Transmitters
 - Explore issues involved in:
 - Improving transmitter efficiency
 - Reducing mass, size and cost
 - Achieving increased data rates Ka-band frequencies
 - Implementing bandwidth efficient modulation schemes (16-QAM) for LEO-to-ground links
 - The use of higher frequencies such as V and W-Bands
- Antenna Technologies
 - Explore:
 - New technological concepts in antenna design, such as, inflatables, deployables, and configurables
 - Approaches to improving antenna efficiency
 - Approaches to reducing mass, size and cost of spacecraft antenna
- Ground Stations
 - Determine cost to upgrade ground station receivers and antenna to support high data rates at higher frequencies, in particular at Ka-band
 - Explore feasibility of expanding ground network to other station locations on CONUS that could provide access to the WAN.
 - Explore other mission scenarios that could amortize the development costs of ground station upgrades for high data rate
 - Determine the cost of operations and explore issues involved in reducing these costs
 - Investigate the Ka-band RF relay option
 - Make cost vs. performance trade of a relay satellite with that of a ground station network that will provide equivalent availability.

Optical Telecommunications

- Receivers
 - Explore issues in developing:
 - High sensitivity large-area avalanche photodiode detectors operating in the 1550 nm wavelength region. Such development will reduce the number of wavelengths needed to support the 10 Gbps links.
 - High-speed clock and data recovery electronics
- Transmitters
 - Explore development of high power, high efficiency direct modulation semiconductor MOPAs that will reduce the required onboard power consumption.
- Ground Stations
 - Do cost vs. performance trade of a relay satellite with that of a ground station network that will provide equivalent availability.
 - Investigate possible development paths and strategies to aid in the development of high-speed data storage
 - Explore the feasibility of deploying the Goddard SLR 2000 ground stations with optical comm receiver terminals.
- Systems

- Support current plans for system level and space flight demonstrations of high data rate technologies
- Explore protocols for high data rate communications

APPENDIX A.

BREAKTHROUGH TECHNOLOGY – INTELLIGENT DATA EXTRACTION

Motivation

Recent developments in technology have been continuously increasing the gap between the ability of the instruments to collect the data, and the capacity of data downlink. Currently, we are capable of collecting much more data than we are capable of sending to Earth. Moreover, the rates at which scientists analyze data is significantly slower than data acquisition. These two gaps can be reduced if the scientifically important information content per bit of data is maximized.

To achieve this, the scientists will have to specify the goals or data of scientific interest. For example, the scientist might prefer to receive a composite of the scientifically interesting image fragments collected from thousands of images of a terrain rather than 100 raw consecutive images. Or the scientist might prefer to obtain 3 images of geologically active region and disregard 10 images of desert. While the scientist specifies the task, the computer system will perform the selection process. Current machine learning technologies allow the translation of such tasks into computer programs, which installed on-board of the spacecraft will serve the role of data selectors and data analyzers for the scientific goals specified. Scientific requests and reasoning behind scientific data analysis will be coded and computer programs will be interpreting the data in the ways defined by scientists. As a result, not only the required downlink bandwidth would go down tremendously, but also the work with the acquired data will take on a different format, allowing scientists to spend much less time on extracting scientifically interesting information from large image data sets, and much more time analyzing and studying scientifically relevant information, selected by the on-board computer.

Study Definition

This study will identify appropriate algorithms for extracting scientifically interesting information from image collected by Earth-orbiting instruments in order to reduce bandwidth of the downlink while preserving scientifically-interesting content of the image. Approach will be hierarchical, achieving different levels of data reduction and scientifically driven. The study will be conducted for three different data reduction rates: $O(10)$, $O(100)$ and $O(1000)$ and for two different instruments: hyperspectral and SAR.

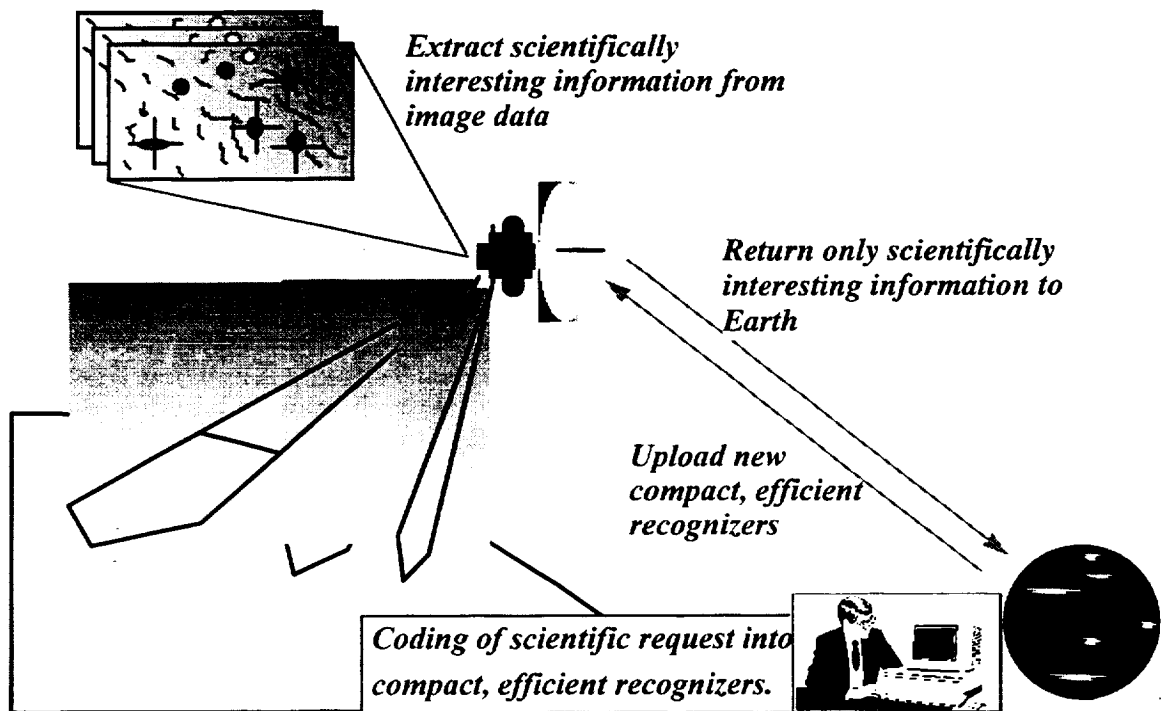
Coding Scientific Goals Into Computational Tasks

The primary scientific goal of specified mission is to classify existing ground cover into groups interesting to the scientists. They might be interested in Earth resources (various minerals), types of crops, presence of crop diseases, ocean contamination levels, various types of vegetation or amount of snow cover.

Science driven on-board feature extraction procedure will automate the loop between scientific request and data delivery, while significantly minimizing downlink bandwidth. To generate the request, the scientist might wish to point on examples of data types of interest. These examples will be automatically extracted from images and fed through machine learning software, which will code scientific requests into compact, efficient

recognizers and upload them to spacecraft (See Figure 0). On-board computational process will extract features of scientific interest from image data and downlink them to Earth.

Depending on available bandwidth, different levels of information extraction will be applied in order to preserve as much detail as possible for direct scientific analysis. Low-level ($O(10)$ data reduction), mid-level ($O(100)$ data reduction) and high-level ($O(1000)$ data reduction) features can be extracted from data and reported according to bandwidth availability.

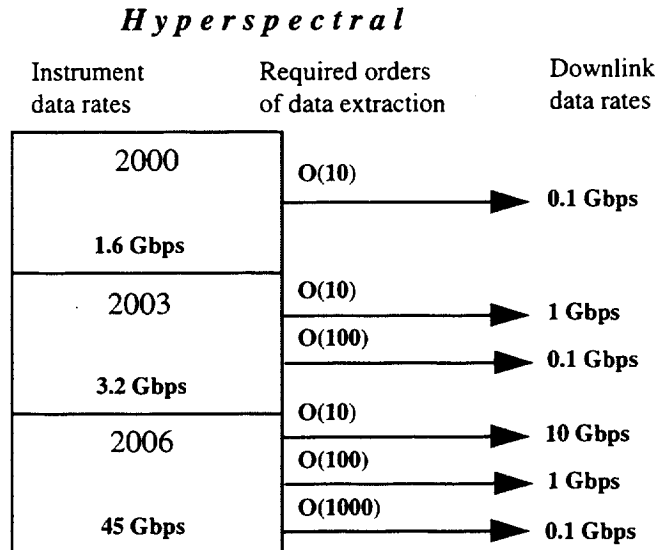


Intelligent coding of scientific requests results in reduced downlink size.

Machine learning algorithms will be employed to achieve this goal. The typical machine learning problem can be divided into two parts: training or learning the model for interesting classes, and given the model, new data classification. In this study we will mainly evaluate the cases when model is learned from class examples provided by scientists (such examples can be easily obtained for Earth-observing missions). We will also address the case, when no examples are present and the model has to be learned concurrently with data acquisition and classification.

A.1 Hyperspectral Imaging Instrument

This instrument combines imager with spectrometer, producing a 2048 x 2048 image for each of 224 spectral channels. Spectral information is encoded in 12-bit numbers and the frame time is 8.68 seconds. Therefore, the raw data rate is 1.3E+9 bits/second. Three data rates are projected for this instrument for years 2000, 2003 and 2006. Three data reduction rates: O(10), O(100), and O(1000) have to be achieved for this instrument, as shown in the following diagram.



A.1.1 O(10) Data Reduction Rate

A.1.1.1 Algorithm Description

O(10) data reduction can be obtained by replacing 224 spectral channels with information concisely describing scientifically important spectral content. The spectral bands typically exhibit high interband correlations so that some redundancy exists between the spectral images. These correlations, coupled with the large quantities of data, lead to the consideration of efficient methods of information extraction (or feature extraction) for science-analysis purposes.

If the goal is to eliminate redundant information (information which does not uniquely describe the type of Earth resource) and preserve all the class-unique signatures, the principal component analysis method provides the necessary solution.

This method allows transformation of 224 spectral channels into a significantly smaller number of components, which capture the most variance in the data. This is done by projecting the data into eigenspace, the orthogonal space where the axis (principal components) points in the direction of maximum variance of the data. The amount of variance (distinct signatures) preserved in new principal components is known from

eigenvalues (coordinates of data along eigenvectors). Such transformation contains an energy-packing property that manifests itself as a significant increase in variance (contrast) in the first principal components, with monotonically-decreasing variance in higher-order principal components. Since the amount of computation in pattern recognition problems depends on the dimensionality of feature vector (224 originally), the usual procedure is to choose a smaller subset of the elements of this vector for processing. The principal component method is optimal in the sense that, for each value of K, the first K principal components contain more class-separability information than any group of K original spectral channels. This indicates the methodology for the feature extraction O(10) method.

One of the goals of this study is to determine execution time and storage requirements of the algorithm. The approach is to specify analytically the formulas for execution time and storage requirements of the algorithm, then to determine experimentally the actual time for processing data with some fixed parameter setting and, using formulas, interpolate the execution time for any other parameter setting. The space required can be determined analytically only.

The algorithm consists of two steps as shown in Figure A-1. First, the principal components are extracted from the covariance matrix of training data. Such data can be either data available on Earth (from previous missions or from the earlier cycle of the same mission) or data available only on board and collected periodically for the specific purpose of training. For consideration of the worst case scenario, it will be assumed that training is done on board and all collected data are used for training. Therefore, this first step can be regarded as training for data extraction. The principal components, extracted from the data, will constitute a new basis designed to maximize class separability while minimizing the length of spectral signature. Such principal components can be obtained through singular value decomposition (SVD) techniques.

The SVD method first constructs the covariance matrix from the training data, then the eigenvectors (principal components) and eigenvalues are extracted from the covariance matrix. Calculation of the covariance matrix is proportional to $I \cdot P^2$, where I is the number of training examples (or data samples) and P is the original dimensionality of training data (224). The calculation of eigenvectors and eigenvalues is proportional to P^3 .

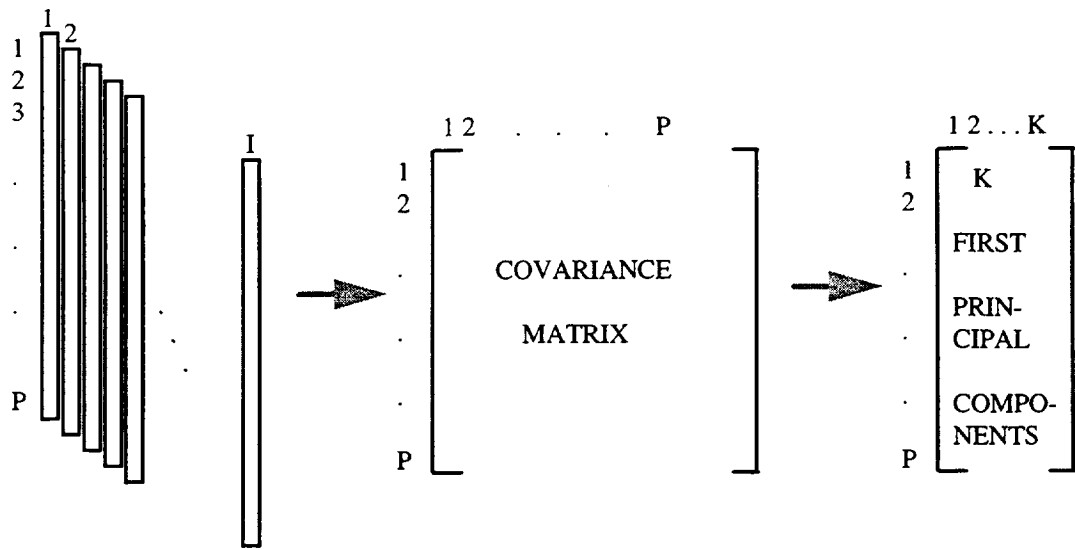


Figure A-1. Principal component extraction.

In the second step (commonly referred to as production), the demeaned spectrum for each collected pixel is projected on first K principal components, where K is the required reduced number of signature components. In this manner, the P -dimensional initial feature vector (raw spectrum signature) is reduced to K -dimensional feature vector, producing a P/K data reduction rate, while preserving the maximum possible class separability. The number of operations required for this step is proportional to $K \cdot P$ and this process is described in Figure A-2.

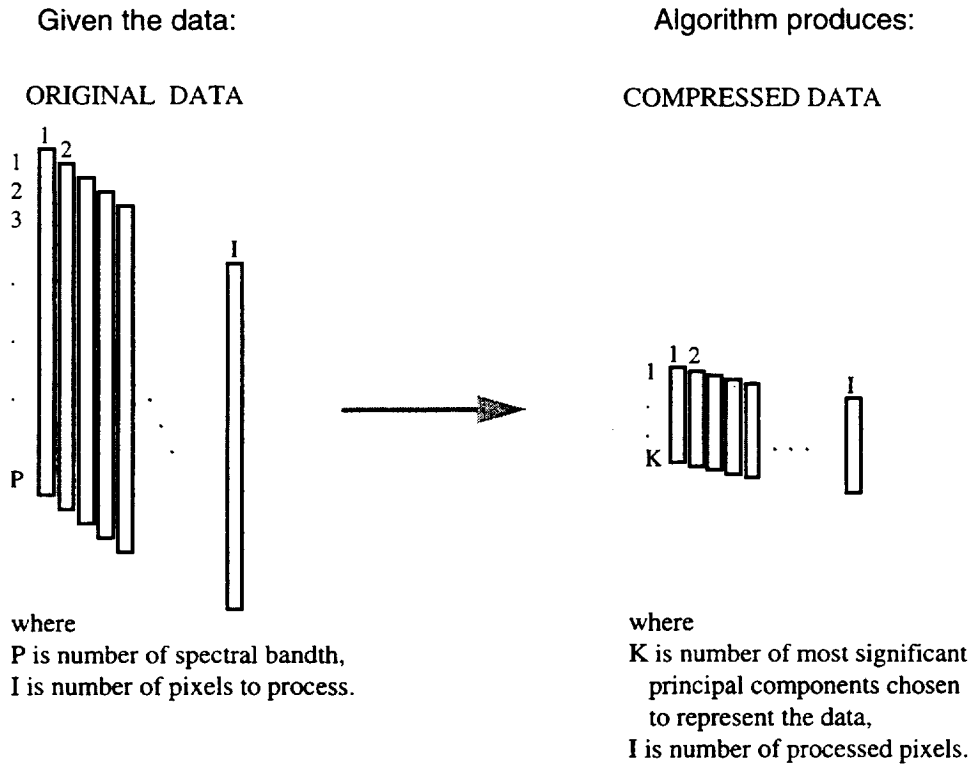


Figure A-2. O(10) data reduction process.

A.1.1.2 Computational Complexity

Let:

MOPS be	# of Mega Operations per second,
Bytes be	# of bytes required by algorithm processing,
Training be	# of FLOPS necessary for training,
Production be	# of FLOPS necessary for production,
P be	# of bands in spectrum,
I be	# of training examples (pixels),
K be	# of components in compressed feature vector,
M be	height of image block,
N be	width of image block.

Then:

$$\begin{aligned}
 \text{MOPS} &= f(I, P, K) \\
 &= \text{Training} + \text{Production} \\
 &= I * P^2 + P^3 + K * P \\
 \text{Bytes} &= \text{Img Block} + \text{Principal components} + \text{Compressed data} \\
 &= M * N * P + K * P + M * N * K.
 \end{aligned}$$

Assume the worst-case scenario when all the collected data are used for training and then projected on principal components for data reduction, then $I = M*N$ and:

$$\text{MOPS} = M*N * P^2 + P^3 + K*P.$$

Since the number of bands P and the number of elements in the compressed feature vector K are significantly smaller than $M*N$, MOPS can be approximated as:

$$\text{MOPS} = M*N*P^2.$$

Similarly, since $K*P$ is significantly smaller than other terms in the sum for # of bytes required for processing, it can be approximated as:

$$\text{Bytes} = M*N*(P+K).$$

For onboard implementation, the data will have to be divided in blocks and compressed blocks will have to be transmitted to Earth with their corresponding basis (the basis is necessary for data reconstruction).

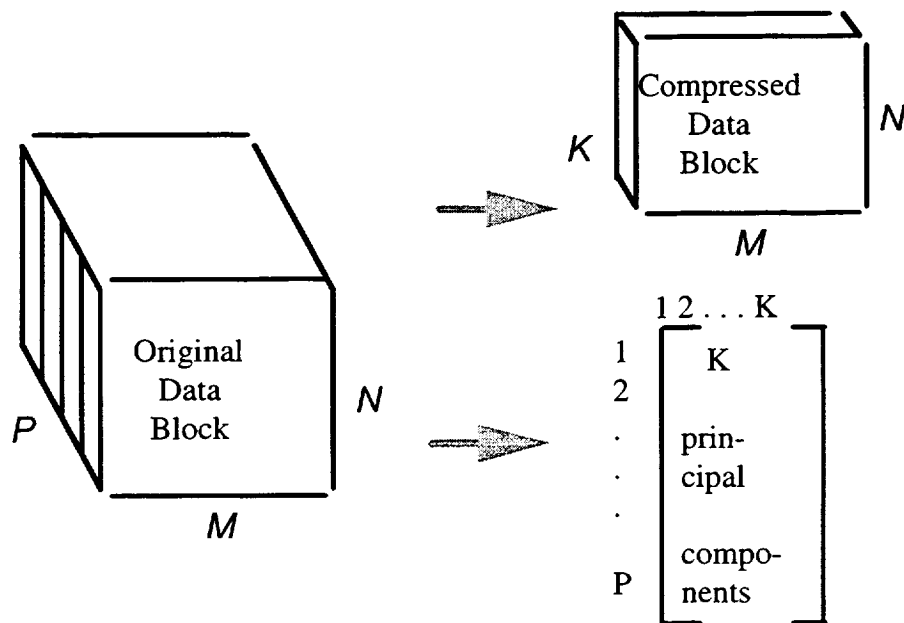


Figure A-3. Intelligent compression of data block.

Both formulas (for MOPS and for Bytes) are easily scaleable; that is, given MOPS and Bytes for some fixed M, N, P, K MOPS and Bytes for any other setting of M, N, P, K can be calculated.

For example, if $M_{\text{new}} = kM * M$, $\text{MOPS}_{\text{new}} = kM * \text{MOPS}$
or
if $(P+K)_{\text{new}} = k(P+K)*(P+K)$, $\text{Bytes}_{\text{new}} = k(P+K)*\text{Bytes}$,

where kM is the coefficient by which the number of rows of data has changed relative to the nominal number of rows of data; and $k(P+K)$ is the coefficient by which the sum of bands in the original spectrum has changed from nominal. The nominal case has been chosen and executed. For this case:

$M = 250$
 $N = 250$
 $P = 10$
 $k = 2$

The number of floating point operations (MOPS) has been measured:

MOPS = 12.5 or

OPS = 12.5 M.

The number of Bytes needed to store data can be calculated.

Assuming two bytes per datum:

Bytes = $M \cdot N \cdot (P+K) \cdot 2 = 1.5M$

The graphs of execution times and space required vrs. parameters are depicted in Figure A-4.

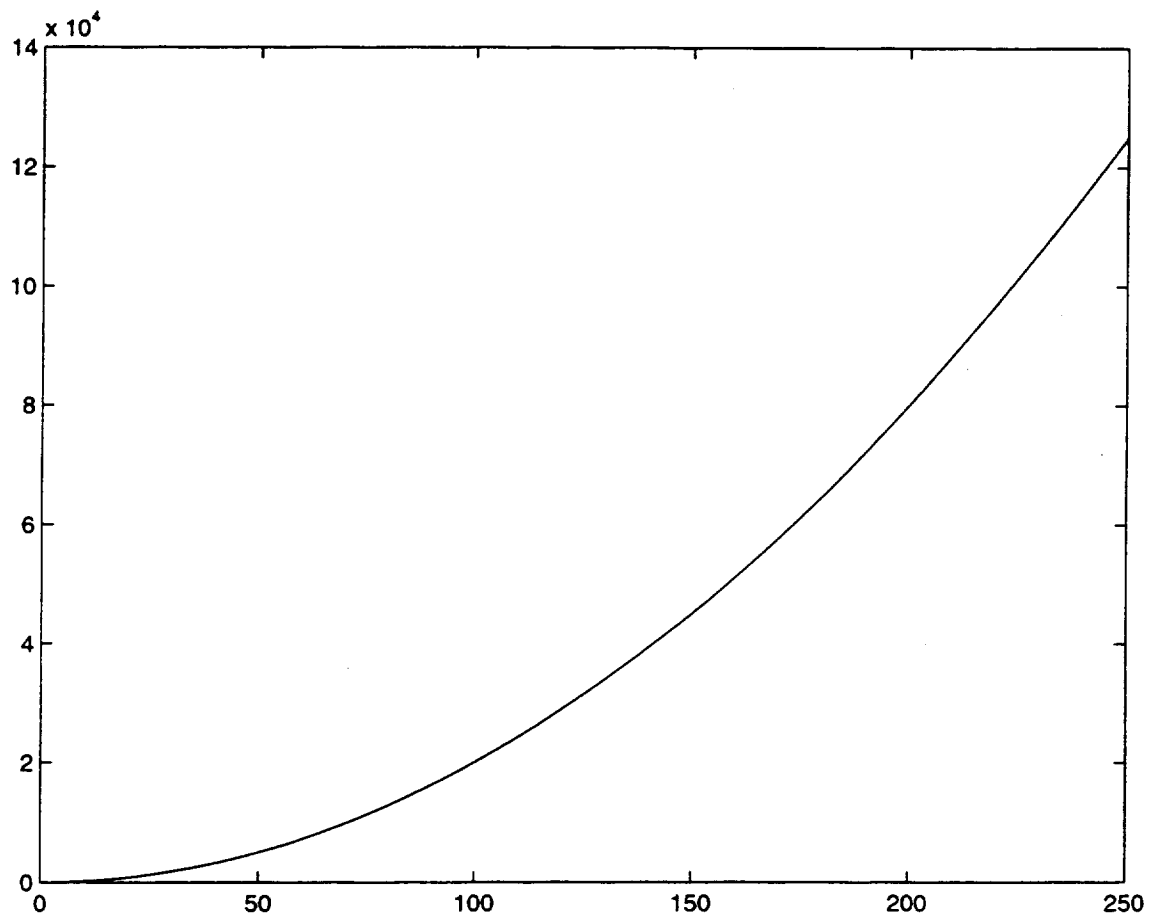


Figure A-4A. MOPS vrs P.
 $P = 1 \dots 250$, $M = 1000$, $N = 1000$, $MOPS = 2 \cdot P^2$.

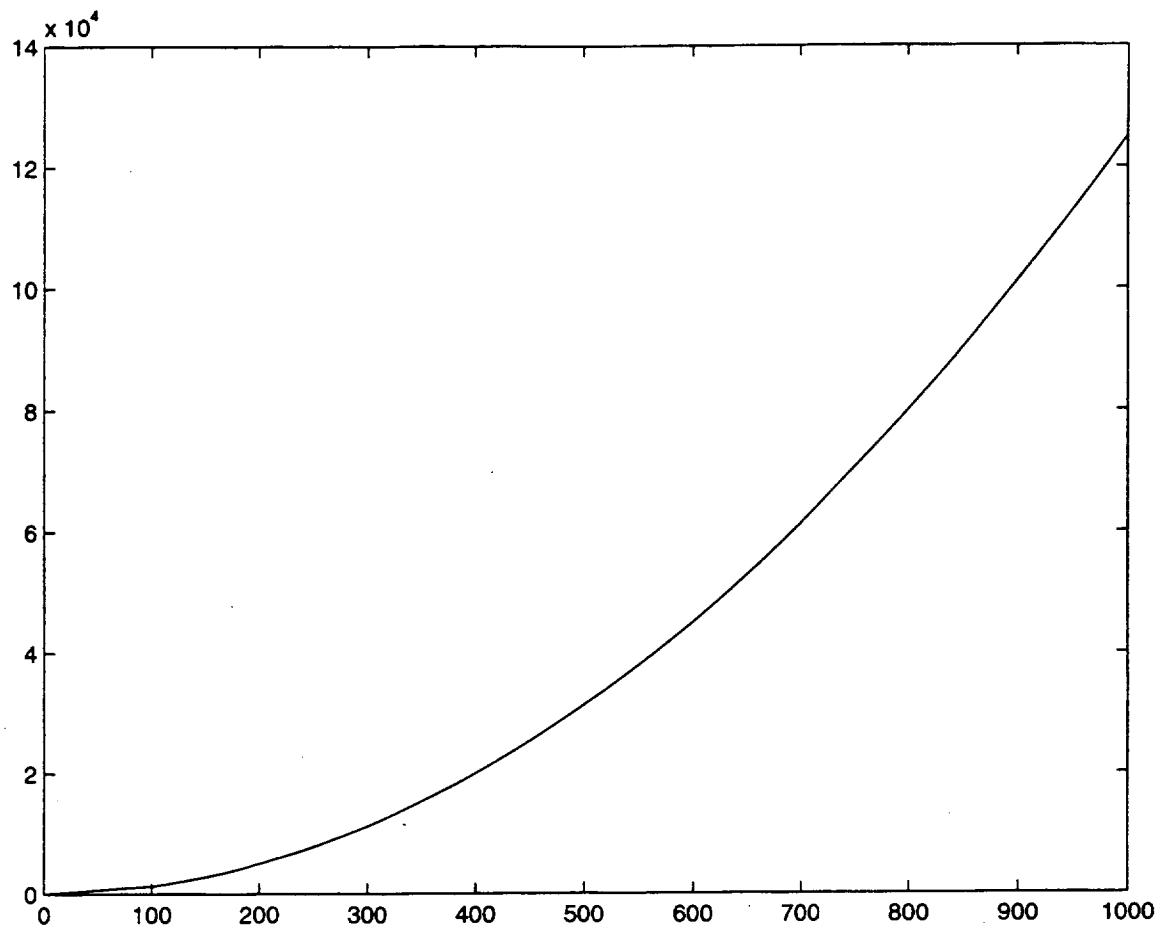


Figure A-4B. MOPS vrs M and N.
 $M = N = 1 \dots 1000$, $P = 250$,
 $MOPS = 0.125 \cdot M \cdot N$.

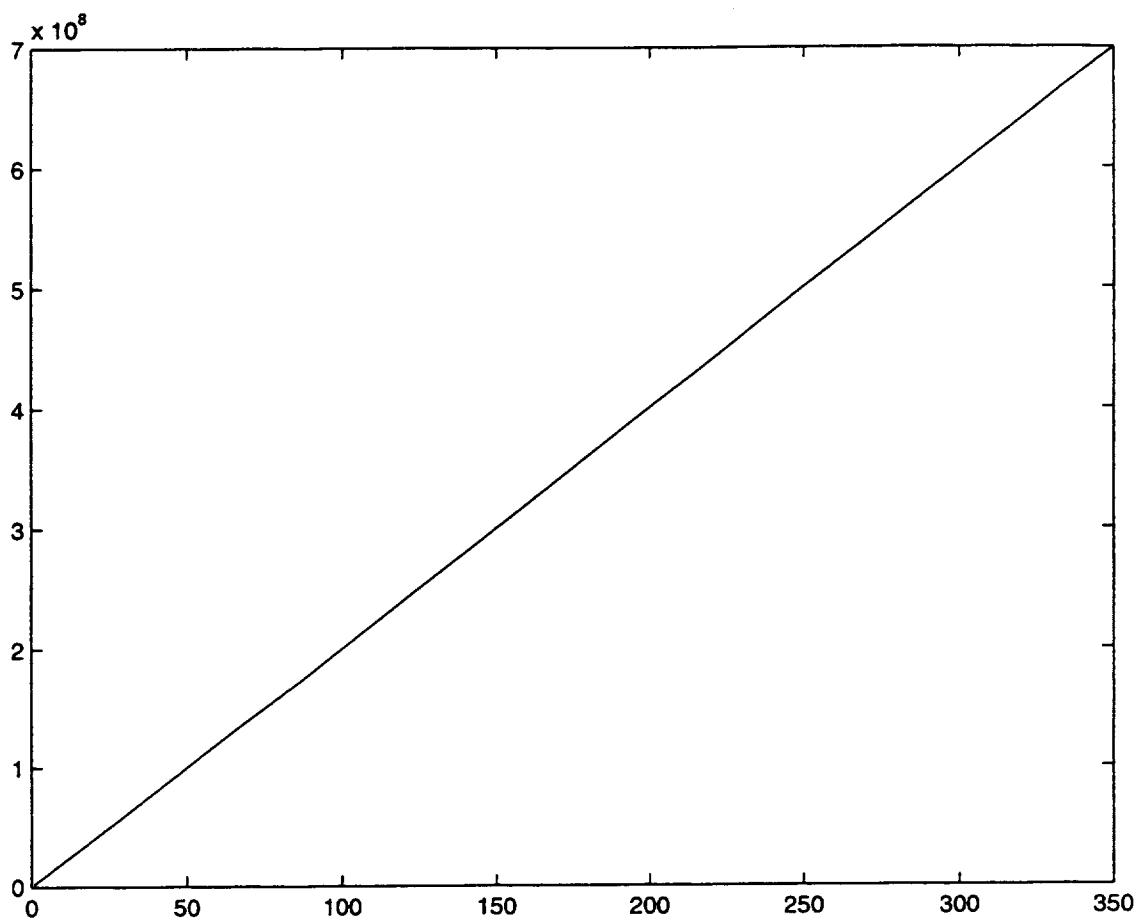


Figure A-4C. Bytes vrs $(P+K)$.
 $(P+K) = 1 \dots 350$, $M = 1000$, $N = 1000$,
 $\text{Bytes} = 2000000 * (P+K)$.

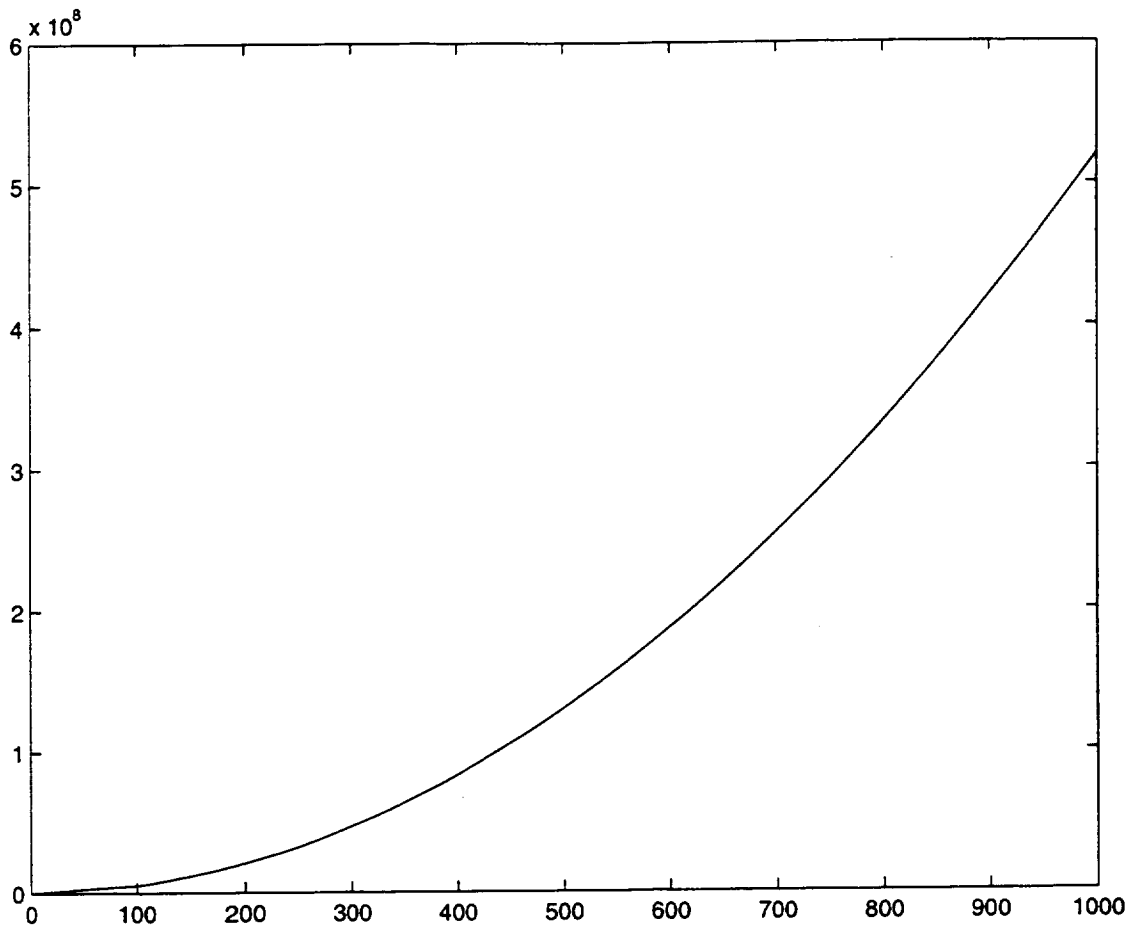


Figure A-4D. Bytes vrs M and N.
 $M = N = 1 \dots 1000$, $(P+K) = 260$,
 $\text{Bytes} = M \cdot N \cdot 520$.

The feasibility of achieving processing requirements and storage requirements, given the computational requirements described in Figure A-4, is addressed in the next section.

A.1.1.3 Feasibility

One of the most obvious limitations for space applications is computer processing power available on board. The remote exploration and experimentation (REE) project (626-30) is used in this study for an estimation of computational resources on board the spacecraft in future years. Therefore, the graph in Figure A-4A indicates that, by 1999, it will be possible to compress $1000 \times 1000 \times 100$ blocks per second, or (from Figure 5-8-b) $400 \times 400 \times 250$ blocks per second. Also, by the year 2002, the capability of processing blocks of size $1000 \times 1000 \times 220$ (from Figure A-4A) or blocks of size $890 \times 890 \times 250$ (from Figure A-4B) will be within reach and will be demonstrated for REE applications.

Current REE applications will be implemented on a scaleable parallel computer spanning from 4 to 64 nodes. The principal component application will require a maximum of 200 Mbytes of storage in 1999 and the 2002 system will require a maximum of 450 Mbytes of storage (from Figures A-4C and A-4D). On the other hand, REE will demonstrate 25-node architecture with 128 MBytes per node by 1999, and 64-node architecture with 256 Mbytes per node by 2002. If 25-node architecture is also used for principal component analysis in 1999, and 64-node architecture is used for principal component analysis in 2002, the maximum local storage required in both 1999 and 2002 would be 8 Mbytes per node, which is significantly less than the maximum storage required by REE application and, therefore, presents no challenge.

A.1.2 O(100) Data Reduction Rate

A.1.2.1 Algorithm Description

O(100) or mid-level information extraction algorithms will cluster low-level features into regions or other descriptive shapes using spatial information and spectral signature information for each pixel. Then, region descriptors will be extracted from and reported to Earth. This process will enable condensed representation of the image further increasing data rates by one - two orders of magnitude. For example, mid-level data compression may be achieved by replacing the spectrum for each pixel with one number, representing the class of ground cover. Then, spatially-contiguous groups of pixels from the same class can be encoded as regions and only coordinates of region edges and region type can be saved. This especially makes sense for large regions.

The proposed method is a statistical method and requires training data; that is, examples of regions for each scientifically-interesting type of ground cover. Statistical models (mixtures of Gaussians) characterizing the properties of the ground cover types are extracted from such expert examples. Once model parameters are fixed, the inference procedure maximizes the probability of image-labeling given the observed data. This allows objective and automated classification of a large set of images.

The current science data processing algorithm is based on fitting a mixture of Gaussian distributions into existing data and predicting the class of the data according to the maximum likelihood criterion. The response of the data in each spectral interval and the spatial location of the data relative to its neighbors is considered during data classification.

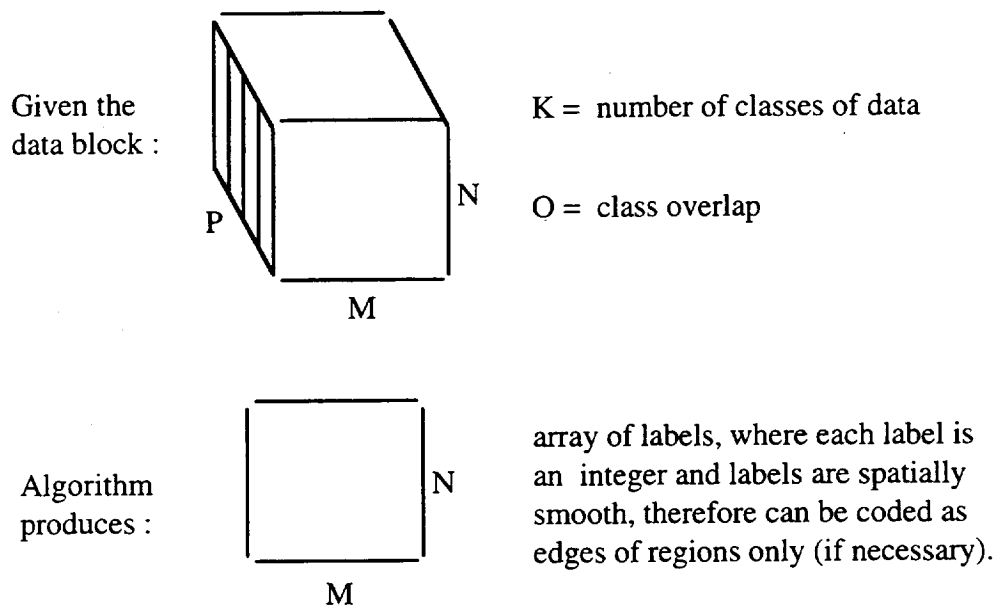


Figure A-5. Mid-level data compression process.

The goal is to determine current and future execution times of the algorithm, its space requirements and compression rates.

The approach is to specify analytically the formulas for execution time and storage requirements of the algorithm, then to determine experimentally the actual time for processing data with some fixed parameter setting and, using formulas, interpolate the execution time for any other parameter setting. The space required can be determined analytically only.

The algorithm consists of two steps. First, it converts the $M*N*P$ image block into probability block where, instead of data responses at different spectral intervals (P intervals are given), the probabilities of the data, given specific class (likelihood (data(M,N) | class(k),) are calculated and stored.

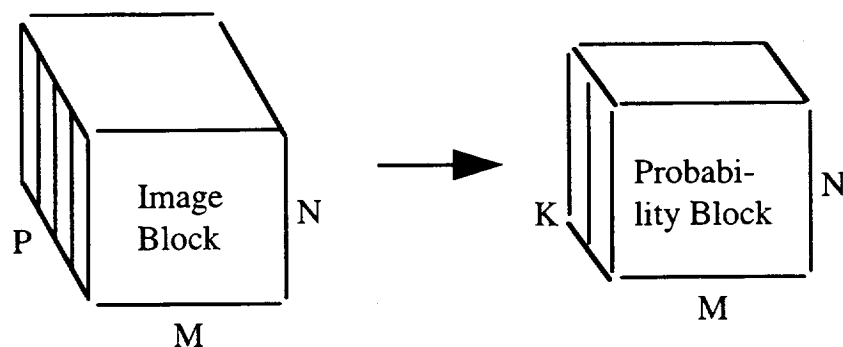


Figure A-6. Conversion of spectral information to class-probability information.

Subsequently, classes are assigned to probabilities by choosing the class for data(M,N) that maximizes log-likelihood of class, given data, + smoothness term. The smoothness term is a function of the number of data neighbors having the same class as data(M,N). This process is iterative and the number of iterations (iter) is a function of data. It depends on how separable the classes are in p-dimensional space or, in other words, how much overlap between classes exist. In general, $\text{iter} = O(20)$, but the exact number of iterations cannot be predicted based on M,N,P, and K. For the purpose of this study, it is safe to assume that $\text{iter} = 100$. For the purpose of real time application, iter can be bounded and class overlap can be measured. If the number of iterations will reach the bound or class overlap will be too high, the current process can be stopped and the bad quality of results or the presence of an unknown class in given data can be reported.

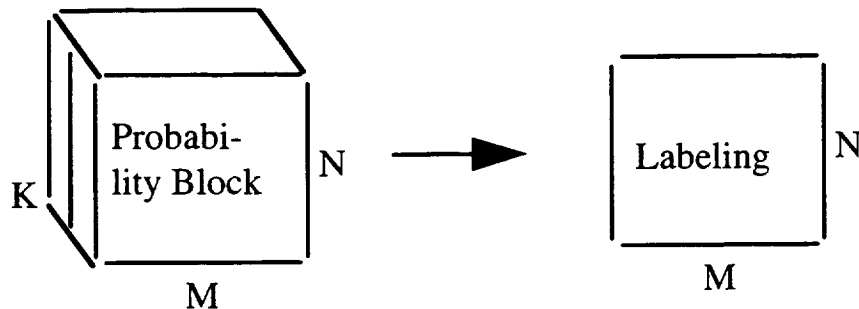


Figure A-7. Unique label assignment.

To determine which Gaussian mixture-model given data belongs to, the model itself has to be stored. The model is represented by the sum of Gaussians for each class. For the sake of simplicity, let us assume that each sum has only one Gaussian in it and let us increase the number of classes to account for each Gaussian in the sum. For example, without loss of generality relative to execution speeds and data storage, we can assume that instead of having one class represented by a mixture of 3 Gaussians, we will have three classes represented by one Gaussian per class. To store the Gaussian model, only the mean ($1 \times P$) and covariance ($P \times P$) matrices for each Gaussian (class) need to be stored. Furthermore, the full covariance matrix can be transformed to a matrix where only diagonal-elements are non-zero, therefore reducing the number of significant values per/covariance matrix to P.

A.1.2.2 Computational Complexity

Let:

MOPS be	# of Mega Operations per second,
Bytes be	# of bytes required by processing,
Model be	# of bytes required to store Probabilistic Model,
Image Block be	# of bytes required to store image Block,
Probability Block be	# of bytes required to store probability block,
Labeling be	# of bytes required to store image labels (worst case)

iter # of iterations needed for algorithm
convergence (bound at
iter = 100)

Then:

$$\begin{aligned} \text{MOPS} &= f(M, N, P, K, O) \\ &= M * N * P * K + \text{iter} * M * N * K \\ &= M * N * K * (P + \text{iter}) \\ \text{Bytes} &= \text{Model} + \text{ImageBlock} + \text{Probability Block} + \text{Labeling} \\ &= (k * (P + K)) + (M * N * P) + (M * N * K) + (M * N). \end{aligned}$$

Ignoring first and fourth terms (which are significantly smaller than second and third terms):

$$\text{Bytes} = (M * N * P) + (M * N * K) = M * N * (P + K)$$

Both formulas (for MOPS and for Bytes) are easily scaleable; that is, given MOPS and Bytes for some fixed M, N, P, K, MOPS and Bytes for any other setting of M, N, P, K can be calculated.

For example,

$$\begin{aligned} &\text{if } M_{\text{new}} = kM * M, & \text{MOPS}_{\text{new}} &= kM * \text{MOPS} \\ &\text{or} \\ &\text{if } (P + K)_{\text{new}} = k(P + K) * (P + K), & \text{Bytes}_{\text{new}} &= k(P + K) * \text{Bytes}, \end{aligned}$$

where kM is the coefficient by which the number of rows of data has changed relative to nominal number of rows of data; and $k(P + K)$ is the coefficient by which the sum of number of classes and number of spectral intervals has changed from nominal. The nominal case has been chosen and executed. For this case,

$$\begin{aligned} M &= 1000 \\ N &= 1000 \\ P &= 1 \\ k &= 4 \\ \text{iter} &= 100. \end{aligned}$$

The number of floating point operations (OPS) has been measured.

$$\text{MOPS} = 6000$$

The number of Bytes needed to store data can be calculated. Assuming two bytes per number:

$$\text{Bytes} = (M * N * (P + K)) * 2 = 1000 * 1000 * 5 * 2 = 10M$$

From the nominal value of MOPS and the above formulas, the time and space required for processing can be easily calculated.

Previous calculations indicate that requirements on algorithm parameters are strictly imposed by processing speed available and memory available on board the spacecraft. At the end of this study, a graph will be produced depicting the dependency of algorithm parameters on computer resources. Presently, the separate issue of limitations imposed by algorithms have to be addressed. Even though such limitations are directly

influenced by computer resources, assuming infinite computer power still does not guarantee robust performance of the algorithm. Robustness of the algorithm is mainly influenced by three factors:

- 1) quality of data (that is, how descriptive (unique)) the signatures for each class are, the amount of training scientifically-interesting classes and the class-separability of the new, unanticipated classes of data.
- 2) Number of spectral intervals p .
- 3) Number of data classes k .

The first factor, quality of data, is hard to assess theoretically. It depends on instruments, scientific goals, and many other factors which are not controlled by the algorithms. The worst the quality of the data is the longer it will take for the algorithm iterate to converge to stable solution (the larger is iter). For real time purposes, the bound will be placed on number of iter. The second and third factors are easily assessable from an algorithm performance point of view. Current process can support from 10 to 100 orthogonal spectral intervals and classify approximately 10 classes. With time, the number of spectral intervals p and classes k that we will be able to process will grow, requiring more time and storage for algorithm execution.

The projection is made for years 2002 and 2006, and the results are summarized in the table below. It is important to note that TWO algorithms are addressed separately. The first algorithm, supervised learning (parameters subscribed with s), learns the classes of data from examples provided by scientists, builds a model from these examples, and then processes observables through the model to classify them. The second algorithm, unsupervised learning (parameters subscribed with u), fits the model into existing data, resulting in assignment of classes to data. Both algorithms have very similar computer resources requirements (the same formula can be used to calculate the requirements for both algorithms) and the results for both algorithm are summarized in the table below. Image size ($M \times N$) and the number of iterations are kept constant (at 1000×1000 pixels² and 100 respectively) since these variables are not expected to change with time. Also, the worst case estimates are given (the number of spectral intervals usually can be reduced significantly through principal component analysis).

Table A-1. Worst-case time and space estimates required by maximum setting of algorithm parameters.

	1998	2002	2006
Ps	10 - 100	100 - 1000	500 - 2000
Ks	10	20 - 50	40 - 100
Pu	10 - 20	20 - 50	---
Ku	10	20 - 40	---
max TIMEs	30000 MOPS	816750 MOPS	3118812 MOPS
max SPACEs	220 MBytes	2100 MBytes	4200 MBytes
max TIMEu	17822 MOPS	89109 MOPS	----
max SPACEu	60 MBytes	180 MBytes	----

A.1.2.3 Feasibility

Next, Tables A-1 and A-2 will be used to show that limitations on algorithm parameters are not dictated by algorithm performance and stability, but by available hardware speed. Table A-1 summarizes the worst case execution time and space estimates that would allow maximum utilization of available algorithms. Table A-2 summarizes hardware capabilities demonstrated by REE applications in 1999 and 2002. It is obvious from these two tables that boundaries of algorithm parameters cannot be achieved on board the spacecraft. For example, by 2002 scientific algorithms will be able to handle 1000 spectral bands and 50 classes, but it will require 816750 MOPS to perform such processing. On the other hand, REE will demonstrate the capability of 100000 MOPS (given 100 Watt for processing) or 57600 MOPS (given 64-node architecture), which is not enough to push algorithmic capabilities to the limits on board the spacecraft. Therefore, scientific algorithm parameters are not bounded by algorithm performance and stability but by hardware speed available. In addition, Tables A-1 and A-2 show that available memory will be sufficient to support any possible parameter setting (memory available in reconfigurable REE hardware is significantly larger than memory required for full algorithm utilization), indicating once more that the only limitation on the setting of scientific parameters is the processing speed of hardware.

Assuming the power, demonstrated by REE in 1999 (200 MOPS) and 2002 (1000MOPS) and assuming 100 Watt for processing, Figures A-8A and A-8B suggest the following parameter settings. If spectral signature is 10 values long, then 13 classes can be processed in 1999 and 63 classes can be processed in 2002 (from Figure A-8A), and if we need classification of data into 30 classes, we can use spectral signatures of 125 values long in 2002 (from Figure A-8B). For many scientific applications such parameter settings will be sufficient.

For applications which require processing of longer spectral signatures, previously described principal component algorithms can always be used not only as data compressor, but as extractor of principal (most variable) information from spectrum, therefore representing spectral signatures in condensed form. For applications, which require classification of data into a larger number of classes various methods

(depending on the mission) can be employed. For example, one can reconfigure hardware so that more nodes are used (then demonstrated by REE application), therefore increasing the hardware processing speed. Also, it is important to remember that, so far, only real-time processing was assumed, meaning that a 1000x1000x224 image block is processed approximately at the same rate as it is received. It is possible to buffer some of the data and process them later during the mission (when data are not being collected and CPU is not occupied by other processes). This will allow implementation of classification into higher number of classes (if necessary). And, finally, in some missions it will be possible to reduce the number of principal components to just a few, therefore allowing classification into a higher number of classes.

Table A-2. Demonstrated by REE hardware capabilities.

YEAR	1999	2002
# OF NODES	25	64
MEMORY (in Bytes / node)	128M	256M
SPEED (in OPS / Watt / sec)	200M	1000M
SPEED (in OPS / Node / sec)	900M	900M

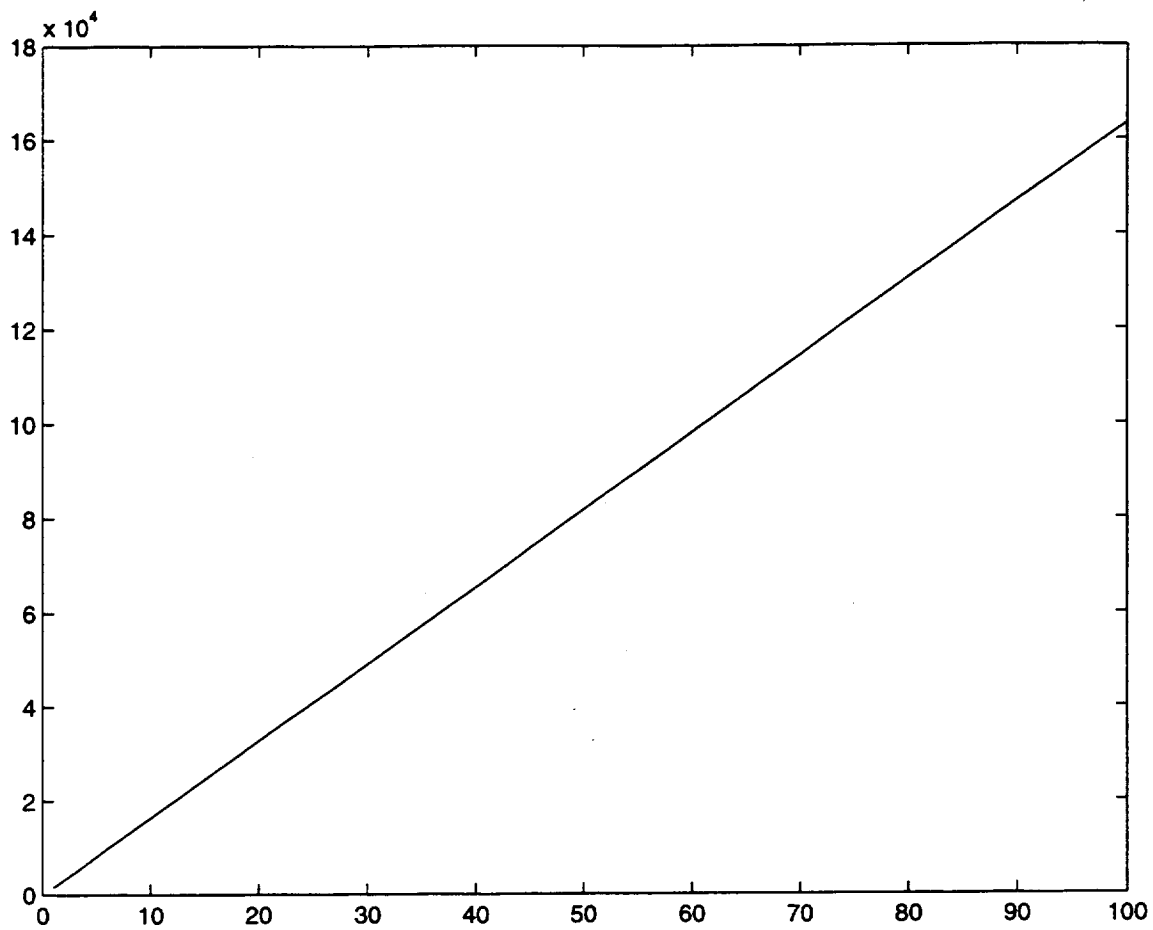


Figure A-8A. MOPS vrs k (number of classes).
 $MOPS = 6534.7 * (k/4)$
 $k = 1 \dots 100, M=N=1000, p=10.$

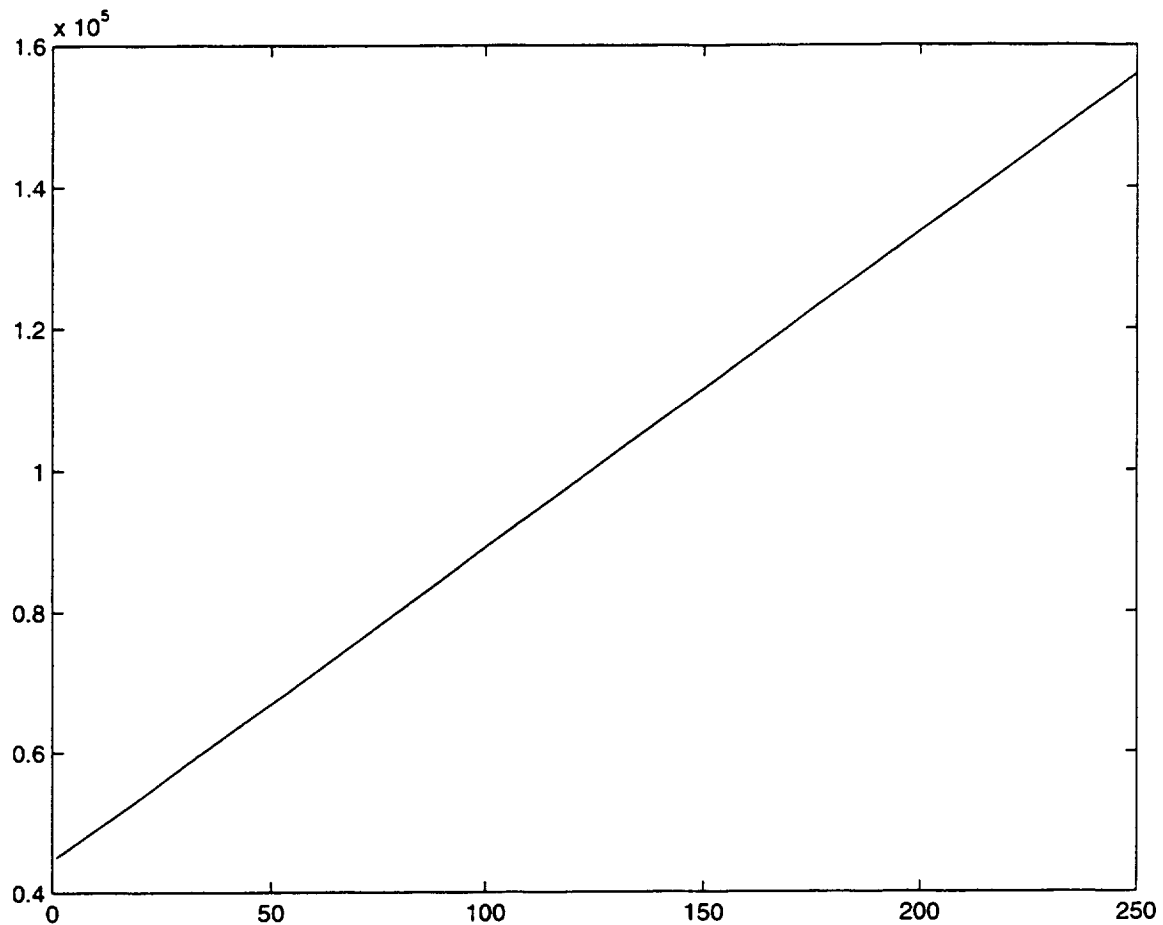


Figure A-8B. MOPS vrs p (number of spectral bands).

$$\text{MOPS} = 45000 * (p+100)/(1+100)$$

$$p = 1..250, M=N=1000, k = 30.$$

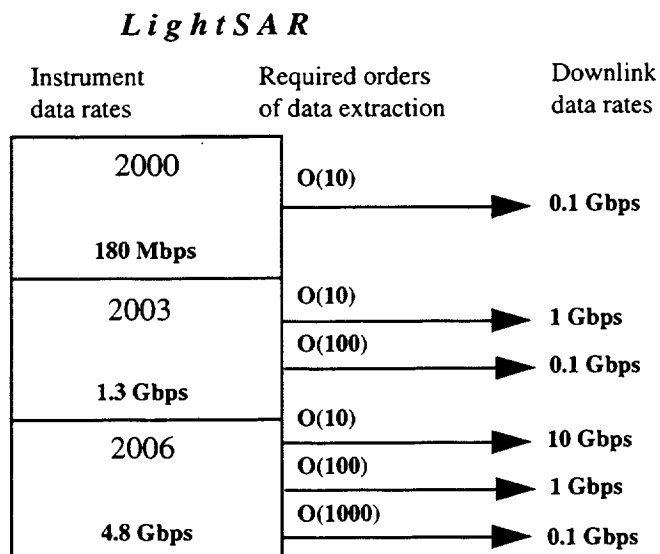
A.1.3 O(1000) Data Reduction Rate

O(1000) or high-level information extraction algorithms will report only statistical information relevant to the scientist. For example, the percentage of specified ground-covers and centroid of corresponding ground cover locations can be reported for each image. If an interesting ground cover is present, its statistical aspects and other attributes can be calculated on board and reported to scientists. It is possible to schedule data transmission in such a way that regions of higher interest are reported with higher precision, and regions with lower scientific interest are reported with lower precision. For example, for moderately interesting ground cover, only statistical information will be reported, and for ground cover of high interest, the low-level feature map can be reported.

Statistical and attribute calculations can be added to low-level and mid-level information extraction algorithms at practically no extra costs related to memory, execution time or power. Obviously, there will be information loss that will have to be minimized by omitting only information of lesser interest to the scientists.

A.2 Light SAR Imaging Instrument

Three data rates are projected for this instrument for years 2000, 2003 and 2006. Three data reduction rates: $O(10)$, $O(100)$, and $O(1000)$ have to be achieved for this instrument, as shown below.



The raw data produced by LIGHT SAR imaging instrument is not an image and, therefore, can not be readily comprehended by image processing codes. Once raw data has been converted to the image, the resulting image is just a two-dimensional array of pixels with multiple values per pixel, each corresponding to different SAR polarizations. Therefore, the resulting image is similar to hyperspectral image where each pixel has a polarization signature associated with it, rather than spectrogram, as in a hyperspectral imaging device. Therefore, information extraction processing will be the same for both images: hyperspectral or SAR, with the exception that for hyperspectral images, P is the number of bands in raw spectral signature, and for SAR images P will be number of SAR polarizations. Therefore, the same feasibility study can be applied to both, once the raw SAR data has been converted into image.

Therefore, the only remaining question is: can the conversion of raw radar data to images be done autonomously on board the spacecraft? The software that does such radar data conversion already exists and it is composed of such operations as Fourier transforms, resampling and averaging. The number of operations required to process $1000 \times 1000 \times 8$ image block is on the order of 1000 MOPS and the amount of memory necessary for processing is on the order of 100 Mbytes. These numbers will change depending on required output resolution. Since the reason for converting radar data onboard is for science-driven interesting data recognition and extraction, the need for high resolution is not anticipated for most data. The data processing rates of 1000MOPS/Watt will be available for onboard processing at 2002, while storage requirements are not limiting in any way. This means that, given a processing power of 1000MOPS/Watt, only a few extra Watts will be necessary for SAR-to-image data conversion. The same data processing as for hyperspectral imaging device can be applied for SAR device as shown in Figure 5-4 (see Section 5.1).

APPENDIX B. ACRONYM LIST

AACS	Attitude and Articulation Control System.
AC	Alternating current.
ACS	Attitude Control Subsystem.
ADACS	Attitude Determination and Control System.
ADC	Analog-to-digital converter.
ADCS	Attitude Determination and Control System.
ADS	Attitude Determination System.
AFE	Avionics Flight Experiment.
AMMOS	Advanced Multimission Operations System.
AO	Announcement of opportunity.
AOS	Acquisition of signal.
APDT	Advanced Projects Design Team.
APL	Applied Physics Laboratory (Johns Hopkins).
arcsec	arcsecond.
ASC	Advanced stellar compass.
ASF	Alaskan SAR Facility.
ATLO	Assembly, test, and launch operations.
ATP	Authority to proceed.
AU	Astronomical unit ($\sim 1.496 \times 10^8$ km).
AZ	Azimuth.
BOL	Beginning of life.
BOT	Beginning of track (DSN).
bps	Bits per second (baud rate).
BWG	Beam waveguide.
c	Speed of light ($\sim 2.998 \times 10^5$ km/s).
°C	Degrees Celsius.
CCD	Charge-coupled device.
C&DH	Command and Data Handling (subsystem).
CCS	Computer command subsystem.
CCSDS	Consultative Committee for Space Data Systems.
CDR	Critical design review.
CDS	Command and Data Subsystem.
CDU	Command detector unit.
CEM	Concurrent engineering methodology.
CEM	Cost estimating model (the TeamX linked spreadsheets).
CMC	Complex Monitor and Control (subsystem).
CMD	Command.
CNES	Centre National d'Etudes Spatiales (France).
COTS	Commercial off-the-shelf.
CPV	Common pressure vessel.
CRT	Cathode ray tube.
DC	Direct current.
dB	Decibel.
DEC	Declination.
deg	degrees (of arc).
deg/hr	degrees per hour.
deg/s	degrees per second.
DNP	Develop New Products.
DoD	Department of Defense.

DOD	Depth of discharge.
DSCC	Deep Space Communications Complex.
DSN	Deep Space Network.
DSS	Deep Space Station.
EDL	Entry, descent, and landing.
EDR	Experiment Data Record.
EEIS	End-to-end information system.
EIRP	Effective isotropically radiated power.
EL	Elevation.
ELV	Expendable launch vehicle.
EM	Electromagnetic.
EM	Engineering model.
EOL	End of Life.
EOT	End of track.
ERT	Earth-received time.
ESA	European Space Agency.
ESSP	Earth System Science Pathfinders.
ET	Ephemeris time.
EUV	Extreme ultraviolet.
FDS	Flight Data Subsystem.
FE	Far-encounter (phase).
FFRDC	Federally funded research and development center
FM	Frequency modulation.
FOG	fiber-optic gyroscope.
FOV	Field of view.
FPGA	Field-programmable gate array.
FST	Flight System Testbed.
FSW	Flight software.
FY	Fiscal year.
Gb	Gigabits (billion, 10^9).
GCF	Ground communications facilities.
GCMS	Gas chromatograph/mass spectrometer.
GCR	Galactic cosmic ray.
GDS	Ground Data System.
GEO	Geosynchronous Earth orbit.
GHz	Gigahertz (10^9 Hz).
GLL	Galileo (spacecraft/mission).
GMT	Greenwich Mean Time.
GPS	Global Positioning System.
GRS	Gamma-ray spectrometer.
GSSR	Goldstone Solar System Radar.
GTL	Geotail.
GTO	Geostationary (or geosynchronous) transfer orbit.
HA	Hour angle.
HAN	Hydroxy-ammonium nitrate.
HEDS	Human Exploration and Development of Space.
HEP	High-energy particles.
HGA	High-gain antenna.
hr	Hour.
HRG	Hemispherically resonating gyroscopes.
h/w	Hardware.
Hz	Hertz.

ICE	International Cometary Explorer (spacecraft).
IEEE	Institute of Electrical and Electronics Engineers.
I/F	Interface.
IFOV	Instantaneous FOV (size of one pixel).
IMU	Inertial measurement unit.
INS	Inertial navigation system.
I/O	Input/output.
IPC	Information Processing Center.
IPDT	Integrated product design team.
IPV	Individual pressure vessel.
IR	Infrared.
IRAS	Infrared Astronomical Satellite.
IRU	Inertial reference unit.
ISOE	Integrated sequence of events.
I&T	Integration and test.
IUS	Inertial upper stage.
JGR	Journal Of Geophysical Research.
JPL	Jet Propulsion Laboratory.
K	Kelvins.
\$K	Thousand dollars.
kb	Kilobits—thousand (actually 1024 or 2^{10}) bits.
kbps	Kilobits per second.
kHz	Kilohertz—thousand Hertz.
krad	Thousand rads.
KSC	Kennedy Space Center.
kW	Kilowords—thousand (actually 1024 or 2^{10}) 16-bit words
KWF	Keyword file.
L	Liters.
LAN	Local area network.
LECP	Low-energy charged-particle (detector).
LEO	Low equatorial orbit.
LGA	Low-gain antenna.
LMA	Lockheed Martin Astronautics.
LMC	Link Monitor and Control (subsystem).
LOI	Lunar orbital insertion.
LOS	Loss of signal.
LOX	Liquid oxygen.
LPSB	Low-power serial bus (architecture).
LVA	Launch vehicle adapter.
LVF	Launch vehicle fairing.
LVLH	Local vertical, local horizontal.
LZ	Level zero.
\$M	Million dollars.
Mb	Megabits—million (actually 1,048,576 or 2^{20}) bits.
MCM	Multi-chip module.
MCT	Mission Control Team.
MDL	Micro-Devices Laboratory.
MFS	Multifunctional structure.
MGA	Medium-gain antenna.
MGDS	Multimission Ground Data System.
MGN	Magellan (spacecraft).
MGS	Mars Global Surveyor.

MGSO	Multimission Ground Systems Office.
MHz	Megahertz—million Hertz.
MIPS	Million instructions per second.
MIPS	Multimission Image-Processing System.
MISR	Multi-angle imaging spectro-radiometer.
MLI	Multi-layer insulation.
MMH	Monomethyl hydrazine.
MO	Mars Observer.
MOS	Mission operations system.
mr	milliradian.
mr	microradian.
MSR	Mars sample return.
MW	Megaword—million (actually 1,048,576 or 2^{20}) 16-bit words.
NA	Narrow-angle (camera).
NASA	National Aeronautics and Space Administration.
NAV	Navigation.
NDE	Non-destructive evaluation.
NE	Near-encounter (phase).
NFR	net-flux radiometer.
NIMS	Near-infrared mapping spectrometer.
NTO	Nitrogen tetroxide.
NV	Non-volatile (memory).
OB	Observatory (phase).
O/F	Oxidizer/fuel (ratio).
OPCT	Operations Planning and Control Team.
OPS	Operations.
OPSCON	Operations Planning and Control (team).
OSR	Optical solar reflector.
OSSA	Office Of Space Science and Applications.
OTM	Orbital trim maneuver.
OWLT	One-way light time.
PAM	Payload-assist module.
PASM	Power-activated switch module.
PCA	Pressurant control subassembly.
PDC	Project Design Center.
PDE	Propulsion-drive electronics.
PDF	Probability density function.
PDS	Planetary Data System.
PDT	Pacific Daylight Time.
PE	Post-encounter (phase).
PF	Proto-flight.
PFR	Problem and failure report.
PI	Principal investigator.
PIA	Propellant isolation subassembly.
PIO	Public Information Office.
P/L	payload.
PLL	Phase-lock loop (circuitry).
PMAD	Power management and distribution.
PN10	Pioneer 10 (spacecraft).
PN11	Pioneer 11 (spacecraft).
PPS	Power/Pyro Subsystem.
PST	Pacific Standard Time.

PSU	Pyrotechnic switching unit.
PWB	Printed wiring board.
QA	Quality assurance.
QA&R	Quality assurance and reliability.
QML	Qualified manufacturers list.
RA	Right ascension.
rad	Radiation absorbed dose.
RAM	Random-access memory .
RDM	Radiation design margin.
RF	Radio frequency.
RFI	Radio frequency interference.
RFI	Request for interest.
RFP	Request for proposals.
RFS	Radio Frequency Subsystem.
RHU	Radioisotope heating unit.
RLG	Ring-laser gyroscope.
RLV	Reusable launch vehicle.
ROM	Read-only memory .
RPIF	Regional Planetary Imaging Data Facilities.
RPS	Radioactive power source.
RTG	Radioisotope thermoelectric generator.
RTLT	Round-trip light time.
s	Seconds (time) .
SA	Solar array.
SAF	Spacecraft Assembly Facility.
SAR	Synthetic aperture radar.
s/c	Spacecraft.
SCET	Spacecraft event time.
SCLK	Spacecraft clock (time).
SDST	Small deep-space transponder.
SE	Support equipment.
SEB	Source-evaluation Board.
sec	Seconds (of arc).
SECDED	Single-error correction, double-error detection.
SEE	Single-event effects.
SEE	Standard error of estimate.
SEU	Single-event upsets.
SGM	Second generation micro-spacecraft.
SIRTF	Space Infrared Telescope Facility.
SOE	Sequence of events.
SOH	State of health.
SNR	Signal-to-noise ratio.
SPC	Signal Processing Center.
SRAM	Static random access memory.
SSA	Solid-state amplifier.
SSE	Solar System Exploration (initiative).
SSI	Solid-State Imaging (subsystem).
SSI	Space Services, Inc.
STD	Standard.
STS	Space Transportation System (space shuttle).
SWG	Science working group.
TAP	Technology and Applications Program.

TAU	Thousand AU (mission).
TAXI	Transparent asynchronous trans(X)mitter/receiver interface.
TCM	Trajectory correction maneuver.
TDM	Time-division multiplexing.
TDST	Tiny deep-space transponder.
TID	Total ionizing dose.
TMOD	Telecommunications and Mission Operations Directorate.
TOS	Transfer orbit stage.
TRC	Teacher resource centers (NASA).
TRL	Technology readiness level.
TRM	Transmission (time).
TWNC	Two-way non-coherent (uplink mode).
TWT	Traveling-wave tube.
TWTA	Traveling-wave tube amplifier.
ULS	Ulysses (spacecraft).
USO	Ultra-stable oscillator.
UTC	Universal time, coordinated.
UV	Ultraviolet (radiation).
V	Volts.
VDE	Valve-drive electronics.
VGR1	Voyager 1 (spacecraft).
VGR2	Voyager 2 (spacecraft).
VIMS	Visible and infrared mapping spectrometer.
VIS	Visible-light imaging subsystem.
VLBI	Very-long baseline interferometry.
VME	Versa Module Eurocard.
VNIR	Very-near infrared.
VNIR	Visible and near infrared.
VTOC	Vacuum tube on a chip.
W	Watts.
WA	Wide-angle (camera).
WBS	Work-breakdown structure.
XMIT	Transmit.
XRFS	X-ray fluorescence spectrometer.
yr	Year.

